Lithium transport in crown ether polymers

Collie, Luke E.

Lithium Transport

in

Crown Ether Polymers

by

Luke E. Collie BSc. (Hons.)

University of Durham

Department of Chemistry

A Thesis submitted for the degree of Doctor of Philosophy

October 1995

Statement of Copyright

Declaration

The work described in this thesis was carried out in the Department of Chemistry at the University of Durham between October 1989 and June 1992. All the work is my own, unless stated to the contrary and it has not been submitted previously for a degree at this or any other University.

Dedicated to my Mother, and my Fiancée, Helen, without whose love and support I would have given up long ago.

Acknowledgements

Most importantly, I would like to thank my supervisor, Prof. David Parker for his continual help and encouragement throughout this project, and for refusing to give up when others might.

I am also indebted to Julia Say and Dr. Alan Kenwright for running N.M.R. spectra and helping me with their interpretation, and to Dr. Mike Jones for being equally helpful with mass spectra. Lenny Lauchlin was of great help in teaching me to use g.c. equipment, and with practical details of the early parts of the synthetic work. The glass blowers Ray and Gordon must also be thanked for cheerfully keeping me supplied with equipment despite my bouts of clumsiness.

Dr Christine Tachon and Dr Jim Denness, who worked with me on the early and later stages of this project, provided help and advice throughout, and supplied some of the samples studied. Dr Hugh Hubbard and Simon Wellings of the Leeds University section of the I.R.C. performed the conductivity analysis, and ran many of the D.S.C. measurements.

Finally, I would like to thank all my former colleagues from Lab 27 for the lively and friendly atmosphere I enjoyed while in Durham, and especially Dr. Chris Drury for his entertaining conversation and willing help.

Abstract

A series of 12-, 13-, and 14-membered crown ether rings bearing polymerisable side-chains has been synthesised. The crown ethers were attached to a methacrylate or acrylate polymerisable group either via a short link (Ring-CH_2-O-Polymer) or via a spacer group. Both hydrocarbon and ethylene oxide spacer groups were used, giving structures of the form (Ring-CH_2-O-$(CH_2)_6$-O-Polymer) and (Ring-CH_2-O-$((CH_2CH_2)_2O)$-Polymer). The ethylene oxide chain can potentially bind to a Li^+ dopant ion.

The relative Li^+ binding affinity of 12-, 13-, and 14-membered mono- and disubstituted crown ethers has been assessed by variable temperature ^{13}C and ^{7}Li NMR.

The crown ether bearing monomers were polymerised using standard free-radical polymerisation methods to yield amorphous materials whose glass transition temperature (T_g) was controlled principally by the nature of the spacer group. On doping with lithium triflate ($LiCF_3SO_3$), the polymers exhibit high ionic conductivity. The conductivity was primarily dependent on polymer T_g, but was also found to be higher for 12-crown-4 based systems than for 13-crown-4 and 14-crown-4 based analogues. This behaviour was consistent with the results of the NMR studies, which showed that Li^+ exchange occurs more readily between 12-crown-4 rings than 13- or 14-crown-4 rings. The NMR studies also showed that 12-crown-4 systems have a higher tendency to form 2:1 (ring : Li^+) complexes. Within a polymer matrix, the presence of 2:1 complexes allows Li^+ migration via an association-disassociation mechanism, avoiding the high energy intermediate state of a free or weakly bound Li^+ ion. The greater encapsulation provided by 2:1 complexation may also aid in ion pair separation.

1. Introduction

1.1. Introduction.

Ion conduction in polymers has been extensively studied since the early 1970's.[1,2], due to the *potential* application of polymer electrolytes in electrochromic devices and high energy density rechargeable batteries. The latter application is technologically more demanding, but a successful polymer electrolyte would offer many advantages over conventional systems. These include not only reduced weight and chemical stability, but also an all solid-state construction, leading to freedom from leakage of electrolyte and evolution of gases, and resistance to damage by shock or impact. Furthermore, polymer electrolytes may afford ease of manufacture, through the use of the many techniques developed for the production of conventional plastic items.

The high chemical stability typical of polymeric materials allows the use of more reactive (and hence higher energy capacity) materials for the electrochemical reactants. Aqueous based electrolytes are limited to electrode materials which do not react at significant rates with water. This limit is not very important for the cathode, as few materials are capable of oxidising water, but prevents metals much above zinc in the electrochemical series being used as the anode. This limits the open circuit voltage of most common cells to ~1-2 volts, and requires ~20-30 g per faraday of charge stored for the anode alone.

The use of low atomic mass metals as anode materials allows significantly higher energy densities to be achieved, most strikingly so in the case of lithium anodes. Lithium is the lightest of all metallic elements, with a relative atomic mass of only 6.95, and is also a powerful reducing agent. Lithium cells can thus have open circuit voltages of 3-3.5 volts, depending on the cathode material chosen, and require only 7 g per faraday stored for the anode, although the overall energy density is much lower than this would imply, due to the much larger weight of the cathode.

To be useful in practical applications, an electrochemical cell system must not only store energy compactly, but also be able to deliver that energy at a sufficiently high rate. This requires that the electrochemical reactions at the cell electrodes have rapid kinetics, and that the cell electrolyte has a low resistance. High electrolyte resistance has been the main obstacle to the adoption of polymer electrolyte lithium cells, although it is possible to use much thinner layers of polymer electrolyte (50-200 μ) than of the aqueous electrolytes used in conventional cells (1-5 mm).[1] Figure 1.1 shows the relationship between power– and energy density for several cell systems, on a "Ragone" plot. The data are from reference 1.

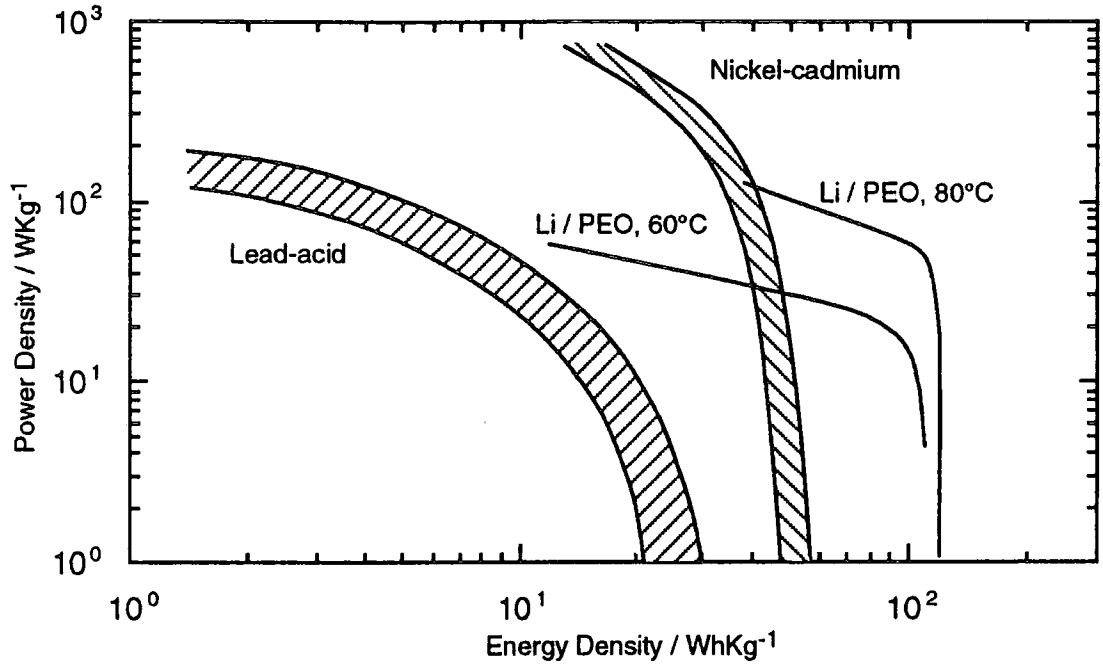

Figure 1.1 The Relationship Between Power– and Energy Density for Lead-Acid and Nickel-Cadmium Cells, and a Lithium Cell with PEO Electrolyte.

Figure 1.1 shows that although lithium cells can have very high energy densities, the use of PEO as an electrolyte limits the power density severely, unless the cells are operated at a high temperature. Consequently, efforts have been made to develop better polymer electrolytes, and to understand the ion migration process within them.

1.2. Development of lithium ion conducting polymers.

Ion containing polymers fall into two basic categories: polyelectrolytes, in which ionic groups are chemically bound to the polymer chain, and charged polymers, which consist of a non-ionic polymer to which a salt has been added. Although there is a vast literature on polyelectrolytes and their many practical applications, studies on their potential as ionic conductors are relatively rare. Charged polymers have been investigated much more thoroughly, with the initial work being published by Wright[3] in 1973, with a more detailed report in 1975 [4]. He investigated mixtures of poly(ethylene oxide) [PEO] with a variety of lithium salts, and showed them to form solid solutions, in which the cations are solvated by the oxygen atoms on the polymer backbone, and pointed out that the complexes showed definite preferred stoicheiometries and were ionic conductors.

1.2.1. Solvation of ions by polymers.

As a first approximation, for a polymer to dissolve a salt to form a homogeneous solution there must be sufficient favourable interactions between the polymer and the ions of the salt to compensate for the loss of the lattice energy of the solid salt.[2] The entropy changes on dissolution, for both the salt and the polymer, must also be considered. In practice, favourable conditions for the formation of a homogeneous solution are most easily achieved when the polymer contains suitable electron donor groups, which are able to complex the cations of the salt. Interactions between the polymer and the anion are not usually significant. A wide variety of donor groups exist, usually involving oxygen, nitrogen, or sulfur atoms as the electron donors. The most suitable donors for a given cation may be found by considering hard / soft acid-base effects. "Hard" cations such as the alkali metals are most strongly solvated by oxygen donors, while "soft" cations such as Ag^+ are most easily dissolved in polymers which have sulfur as the donor atom.

These considerations of suitable donor groups give only a very rough guide to the solvent properties of a polymer, as its detailed structure can have a great effect. Amongst simple polymers, PEO is the best solvent for alkali metal salts. Neither poly(oxymethylene), $(-CH_2-O)_n$ nor poly(trimethylene oxide), $(-CH_2-CH_2-CH_2-O-)_n$ will form a homogeneous salt solution[5], despite the high density of donor groups in poly(oxymethylene). It has been suggested by Armand[6] that PEO represents the best compromise between chain flexibility and donor atom density, and that the geometry of the repeat unit is uniquely suited to complexation of cations. PEO chains can form themselves into a helical structure, with the centre of the helix lined with oxygen atoms. No other polymer can adopt such a conformation. The closest approximation is given by poly(propylene oxide), PPO, but the extra methyl groups give rise to unfavourable eclipsing interactions and force a less tightly coiled helix.[2] However, PPO systems do offer some advantages over PEO, as will be discussed later.

Most of the polymers capable of dissolving alkali metal salts contain some elements of the PEO chain. Examples include poly(epichlorohydrin),[7] poly(ethylene succinate), $(-O-(CH_2)_2-O-CO-(CH_2)_2-CO-)_n$[8] and poly(ethylene imine), $(-CH_2-CH_2-NH)$.[9]. Poly(ethylene imine) forms a helical structure almost identical to that of PEO, and its nitrogen donor atoms are better solvators of lithium ions, in particular, than the oxygens of PEO.

1.2.1.i Experimental Evidence for Solvation.

The early evidence for interactions between polymers and salts was from observations of the physical properties of the mixtures. For low molecular weight PEO the viscosity of the polymer is increased greatly by the addition of salt,[10] indicating that the two components are interacting on a molecular level. Similar effects are seen with PPO.[11] Other early workers[2] measured volume changes in PPO diol when mixed with $LiClO_4$. The initial work of Wright et al[3,4] on the conductivity of PEO complexes was originally intended as an additional method of assessing how well PEO solvated a variety of salts, rather than as an investigation of conductivity for its own sake. Studies of solvation by measurements of bulk physical properties continue, a recent example being the work of Wixwat et al.[12] on the changes in refractive index, density, and viscosity of poly(propylene glycol) on the addition of various salts.

For Li salts, ^7Li NMR can provide a more detailed picture of the type and variety of environments encountered by a cation in a polymer electrolyte.[13, 14] X-ray diffraction patterns also provide some useful information,[15] especially for those polymers, including PEO, in which some fraction of the added salt forms a solvated crystalline complex with the polymer, rather than an amorphous solid solution. Those materials which do include a crystalline component may also be usefully studied by differential scanning calorimetry (DSC). This reveals the melting points of crystalline phases, and by measuring the size of the melting endotherms the proportion of crystalline material present may be estimated. Further information may be obtained by infra-red and Raman spectroscopy, particularly by observing changes in the spectra of the anions on dissolution.[2]

The application of these techniques to a variety of polymer-salt systems has revealed a wide range of behaviours, in particular the existence of many crystalline complexes. This information is best expressed in phase diagrams, such as those shown in figure 1.2 for the PEO - $LiCF_3SO_3$ and PEO - $LiClO_4$ systems.[16] Figure 1.3 shows the conductivity of these systems, measured at several temperatures. It is clear that the onset of crystallinity at high concentrations of lithium salt dramatically reduces the conductivity of the complex, but the complex shapes of the conductivity isotherms, particularly those for the $LiCF_3SO_3$ system, indicates that many other factors play a part. The presence of ion pairs and clusters within the liquid/amorphous phase may be responsible for the drop in conductivity between 0.05 and 0.1% $LiCF_3SO_3$.

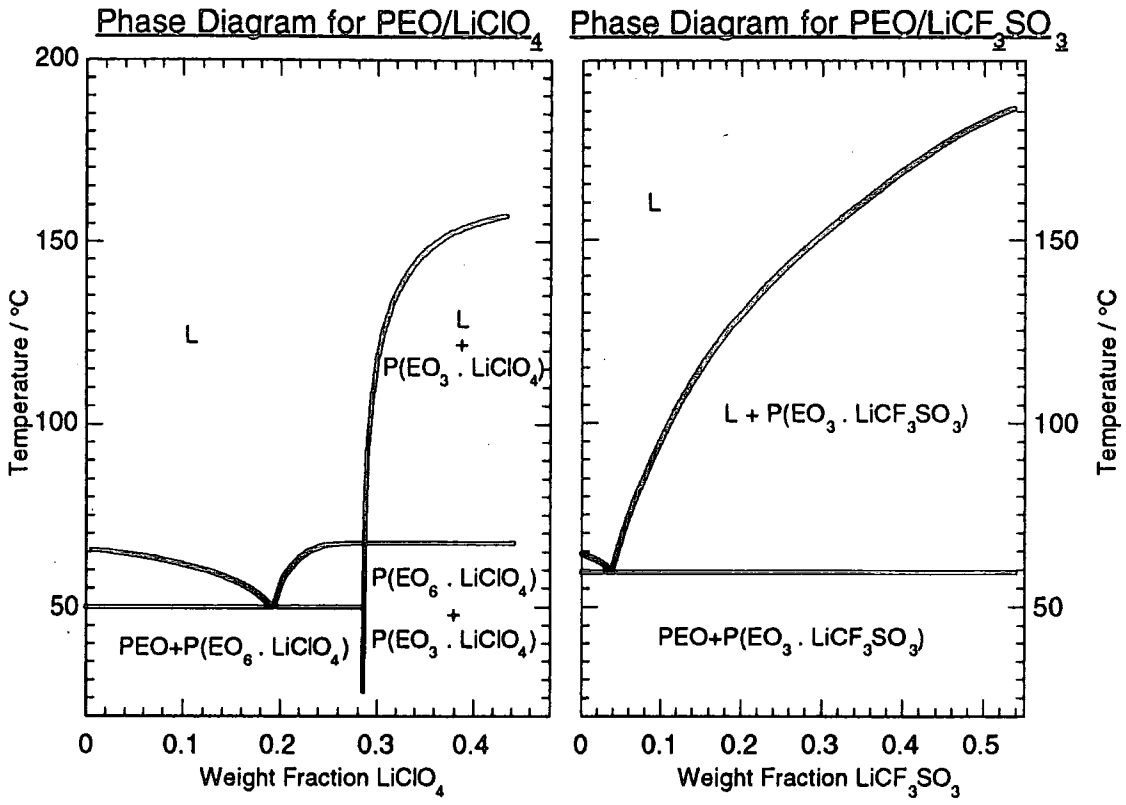

Figure 1.2 *Phase Diagrams for the PEO complexes of $LiClO_4$ and $LiCF_3SO_3$.*

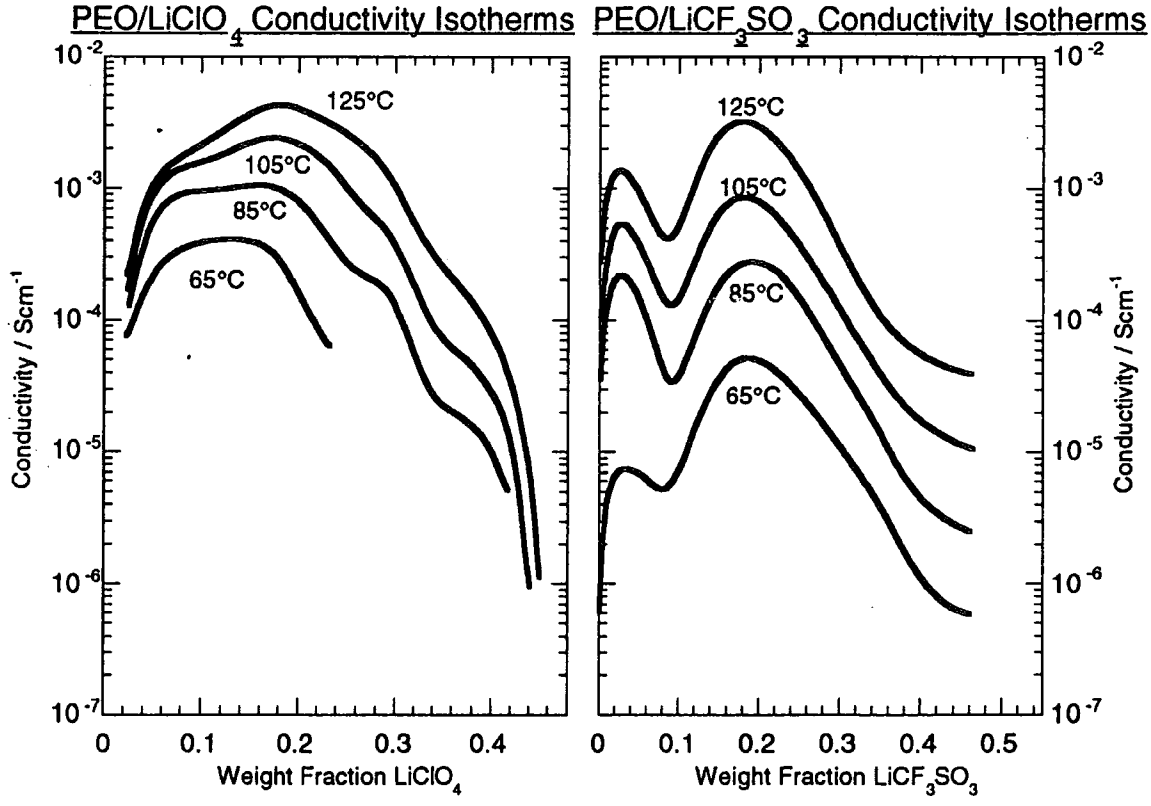

Figure 1.3 *Conductivity Isotherms for PEO-Lithium Salt Complexes*

1.2.2. Ion Transport.

The first mechanism for lithium ion transport in PEO was proposed by Armand[5], who noted that PEO - lithium complexes are partially crystalline, and adapted theories of conduction mechanisms in crystalline solids to include the helical conformation adopted by PEO chains in these complexes, discussed above. The cations were supposed essentially to hop along the channels formed by the polymer helices. Since the basic PEO - lithium complex has a stoicheiometry of four oxygens to each lithium, this model predicted that maximum conductivity would be found at a ratio of eight oxygens per lithium, as this provides (on average) alternating full and vacant sites along a helical channel, which maximises the tendency of the cations to hop between sites.

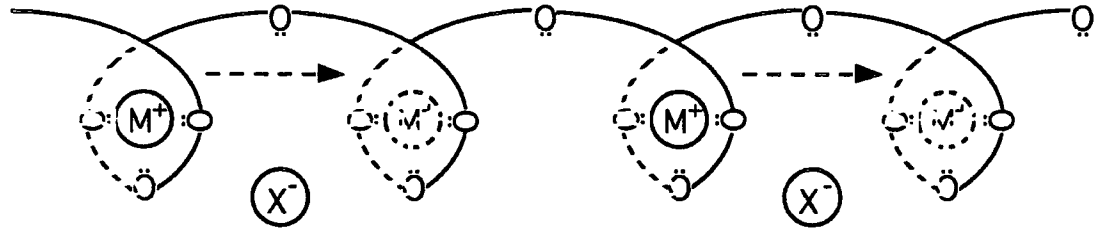

Figure 1.4 Schematic Diagram of Ion Migration Through a PEO Helix

This agreed with the observation of maximum conductivity at an O to Li ratio of ≈8-9 to 1, and led to initial acceptance of the model. However, later NMR studies by Berthier et. al.[13] (^{1}H NMR) showed that lithium ion transport occurs only in the amorphous regions of the polymer-salt complex, while the crystalline regions are essentially ionic insulators. Further studies[15] (^{7}Li, ^{19}F and ^{1}H NMR) have confirmed this picture, and the ^{19}F NMR studies (on PEO complexes of lithium triflate ($LiCF_3SO_3$)) also showed that the anions were mobile, and made a significant contribution to the total conductivity of the complex, whereas in Armand's model the anions are completely immobile.

These observations led to the adoption of explanations of ion transport based on the ability of the polymer segments and their associated cations to move and adopt new conformations. Models for ionic conduction are provided by adapting the free volume and configurational entropy theories of polymer mobility to ion containing systems.[17]

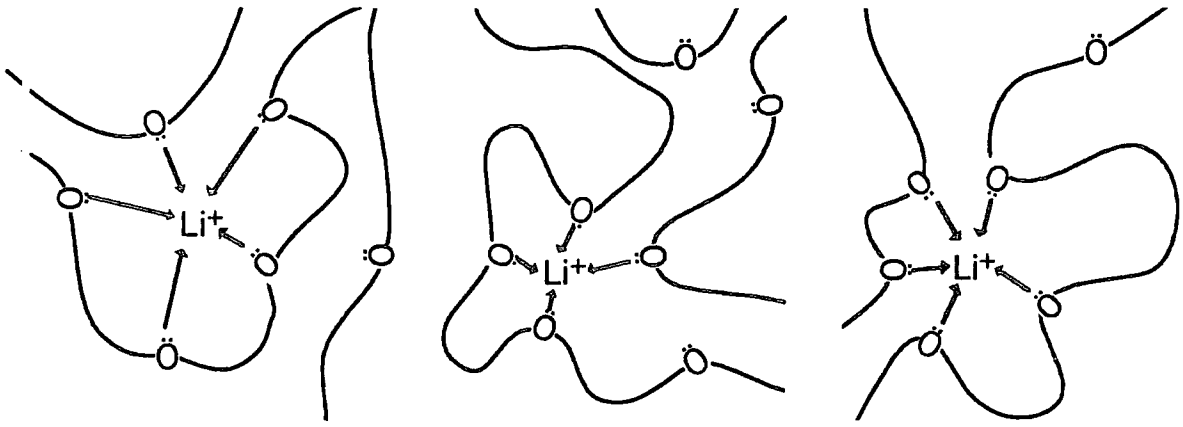

Figure 1.5 *The movement of solvated lithium ions in PEO, through rearrangements of the polymer backbone.*

1.2.2.i Free Volume Theory.

A free volume model for the diffusion of small molecules through organic liquids was published by Cohen and Turnbull[18] in 1959. They modelled the diffusion process as a series of jumps, in which the diffusing particle moves from its current position into a neighbouring hole left by the random motion of the solvent molecules. They proposed the relationship:-

$$D = gvd\exp\left\{-\frac{\gamma V^*}{V_f}\right\} \qquad \ldots.(1.1)$$

where D is the diffusion coefficient, d is the distance moved on each jump, v is the velocity of the diffusing species during the jump, and g is a numerical constant, with a value of about 1/6. The factor γ allows for the overlap of free volume, and the volumes V_f and V^* are the free volume per molecule and the free volume required for a jump, respectively. The exponential term thus represents the likelihood of the available free volume being concentrated into a void large enough to accommodate the diffusing particle. The velocity v is taken as the thermal velocity of the diffusing species, $=\{3kT/m\}^{1/2}$, where k is Boltzmann's constant, T is the absolute temperature and m is the particle's mass.

The free volume increases with temperature, as the material undergoes thermal expansion. If the expansion coefficient is α, then the free volume at temperature T is given by:-

$$V_f = V_m\alpha\{T-T_0\} \qquad \text{....(1.2)}$$

where V_m is the volume per molecule at T_0, the temperature at which free volume vanishes. Combining (1.1) and (1.2) gives:-

$$D = gvd\exp\left\{-\frac{\gamma V^*}{V_m\alpha(T-T_0)}\right\} \qquad \text{....(1.3)}$$

The diffusion coefficient must now be related to the conductivity. For any mobile charged species, the conductivity σ due to that species is given by:-

$$\sigma = nze\mu \qquad \text{....(1.4)}$$

where n is the number of charge carriers, z is their valency, e is the electronic charge and μ is the mobility of the charge carriers.

The mobility is related to the diffusion constant by the Nernst - Einstein equation:-

$$\mu = zeD/kT \qquad \text{....(1.5)}$$

Combining equations (1.3), (1.4),and (1.5) gives the relationship:-

$$\sigma = \left(\frac{nz^2e^2gvd}{kT}\right)\exp\left\{-\frac{\gamma V^*}{V_m\alpha(T-T_0)}\right\} \qquad \text{....(1.6)}$$

Remembering that v is $(3kT/m)^{1/2}$ equation (1.6) can be simplified by defining two constants:-

$$A = nz^2e^2gd(3/mk)^{1/2} \quad \text{and} \quad B = \gamma V^*/V_m\alpha \qquad \text{....(1.7a,b)}$$

Substituting these in gives the usual form of the **Vogel–Tamman–Fulcher (VTF)** equation:-

$$\sigma = AT^{-1/2} \exp\left\{\frac{-B}{T - T_0}\right\} \qquad \ldots.(8)$$

Although the above derivation gives some theoretical justification for the form of the VTF equation, it is in fact best to regard this as a basically empirical relationship. In practice the constants A and B and the temperature T_0 are found by measuring the conductivity–temperature relationship for the polymer under study and fitting a VTF curve to the experimental points. The Cohen and Turnbull relationship, equation (1), was derived for simple liquids, and its application to a solid polymer is of dubious validity. The constant A in equation (8) is found to be proportional to the ion concentration, n, as predicted by equation (7a), but *quantitative* predictions for the constants A and B on the basis of the Cohen and Turnbull relationship are impossible.

An alternative approach to understanding the temperature-conductivity relationship is the configurational entropy theory proposed by Adam and Gibbs in 1965[19] This sets out to explain the temperature dependence of a range of mechanical and electrical properties of polymeric materials on the basis of the freedom of segments of the polymer to re-arrange themselves.

Both these models indicate the importance of rearrangements of the polymer backbone for the conductivity of PEO – salt complexes. Since the glass transition temperature T_g is usually taken as the point of onset of such motions, it is necessary to produce materials which have a low T_g and do not contain a large percentage of crystalline material. This in turn requires the study of the phase diagram of the complexes in order to try and understand the factors which influence the stability of the crystalline and amorphous phases. Much of the research effort on lithium ion transport in polymers has been directed to this end[1], and to finding ways of reducing Tg and crystallinity.

1.2.3. Modification of Tg and crystallinity.

Ordinary, linear PEO is a highly regular polymer, and consequently has a high tendency to crystallise, being ~80% crystalline at room temperature. It has a Tg of -60°C, and a melting point of ~65°C. The addition of lithium salts tends to rapidly increase these transition temperatures. Consequently the conductivity of PEO-lithium salt complexes at room temperature is very low, typically $<\sim 10^{-7}$S/cm.[1] To tackle this problem, various techniques have been used to try and develop a polymer with the solvation and transport properties of amorphous PEO, with a lower Tg and without its tendency to crystallise at temperatures below 40-60°C. These can be divided into chemical and structural modifications of PEO, and attempts to find completely new polymer-salt systems, with polymer donor groups other than ether oxygens.

1.2.3.i Chemical modifications.

These are copolymers of ethylene oxide with a variety of other monomers which introduce sufficient disorder to prevent crystallisation. Block, random and alternating copolymers of PEO have been synthesised using many types of both solvating and non-solvating comonomers[20,21,22,23] The conductivities of these polymers are generally ~1-5 $x10^{-5}$S/cm, at room temperature, or a few hundred times better than that of PEO. This is, however, still too low for use in a practical battery, a further order of magnitude improvement being required.[1]

1.2.3.ii Structural modifications.

The structure of PEO may be altered by adding side-chains to the ethylene oxide monomer units,[24,25] by using a different polymer backbone to which PEO side-chains are attached,[26,27] or by cross-linking the PEO chains with polyfunctional units[28,29] or irradiation at high temperature,[30] which fixes the amorphous state. Combinations of two or more of these methods may be used, which allows more flexibility in the polymer design and improves the overall performance. An example of such an approach is a PEO-PPO-PEO block copolymer cross-linked with a trifunctional urethane,[31] the lithium perchlorate complex of which has a room temperature conductivity of $\sim 3x10^{-4}$ S/cm, which is approaching the useful range. A plot of conductivity against reciprocal temperature for a selection of lithium-polymer systems[1, 24-31] is shown in figure 1.6.

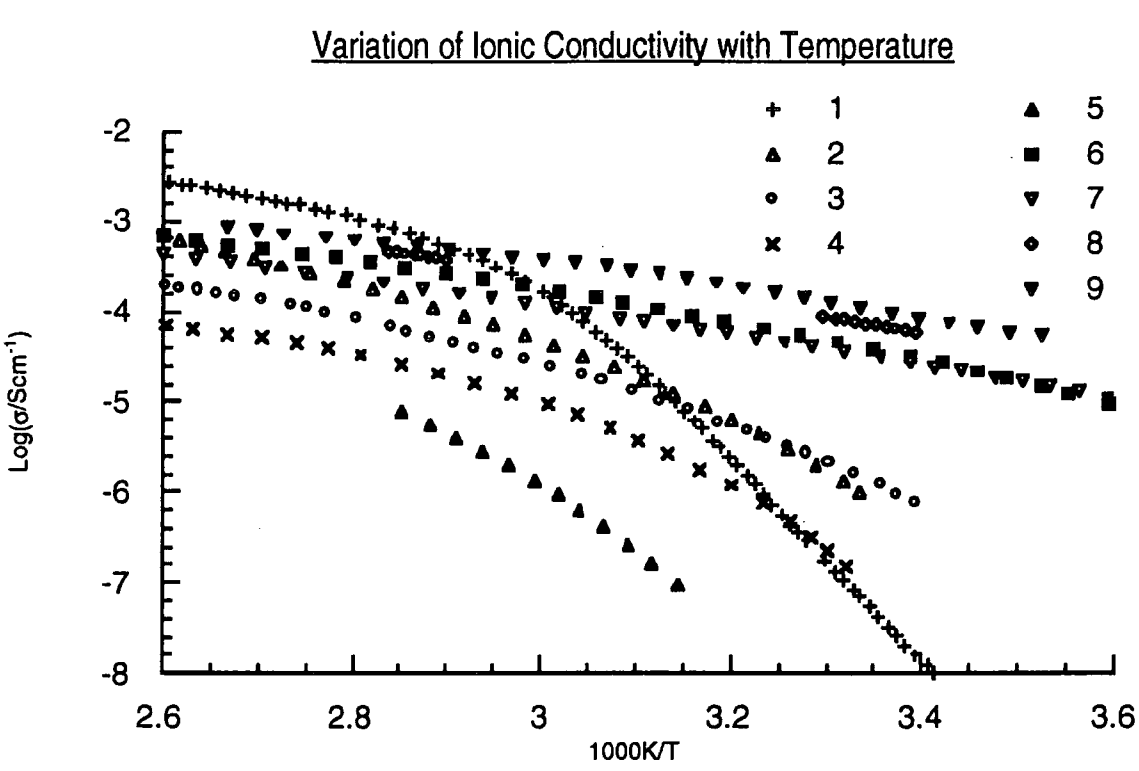

Figure 1.6 *Conductivity vs. 1000 K/T of selected polymer-salt complexes.*[1]

1) *PEO, $LiClO_4$ 12/1).*

2) *PEO, gamma-radiation cross-linked, $LiClO_4$ (8/1).*

3) *PPO, $LiCF_3SO_3$ (9/1).*

4) *Polyethylene adipate, $LiCF_3SO_3$ (4/1).*

5) *Polyethylene succinate, $LiClO_4$ (6/1).*

6) *Polyphosphazene ME7P, Li CF_3SO3 (16/1).*

7) *Polyphosphazene cross-linked 1X MP, Li CF_3SO_3 (32/1).*

8) *Polysiloxane PMM57 linear, $LiClO_4$ (25/1).*

9) *PEO-PPO-PEO block copolymer cross-linked with trifunctionalised urethane, $LiClO_4$ (20/1).*

The ratios given are donor atoms/cation.

1.3. Crown Ethers.

Crown ethers, one of the first synthetic macrocycles, were discovered by Pedersen in 1962 while working on polymerisation catalysts for du Pont Chemicals. Recognising the significance of his accidental discovery (which was a synthesis of dibenzo-18-crown-6), Pedersen made and studied over 30 crown ethers before publishing the work in 1967.[32]

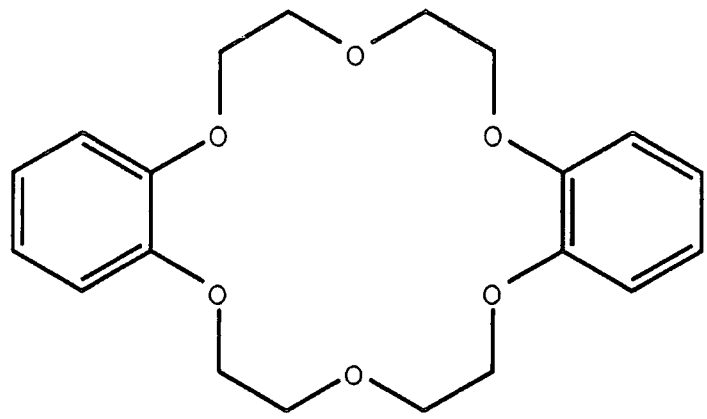

Figure 1.7 Dibenzo 18-Crown-6

These compounds were the first synthetic ligands to give strong complexes with the alkali metal cations, and were also more selective between these ions than earlier systems. Since that time, a new branch of chemistry has grown from the study of crown ethers and their more complex relatives.

The most direct change to the basic crown ether system is the replacement of the oxygen donor atoms by the more polarisable nitrogen or sulfur atoms to give a much "softer" ligand suitable for binding to transition metals. More fundamental alterations to the structure of crown ethers give the bicyclic cryptands, initially reported by Lehn and Sauvage [33,34] and the highly rigid spherands devised by Cram. Examples of these compounds are shown in figure 1.8.

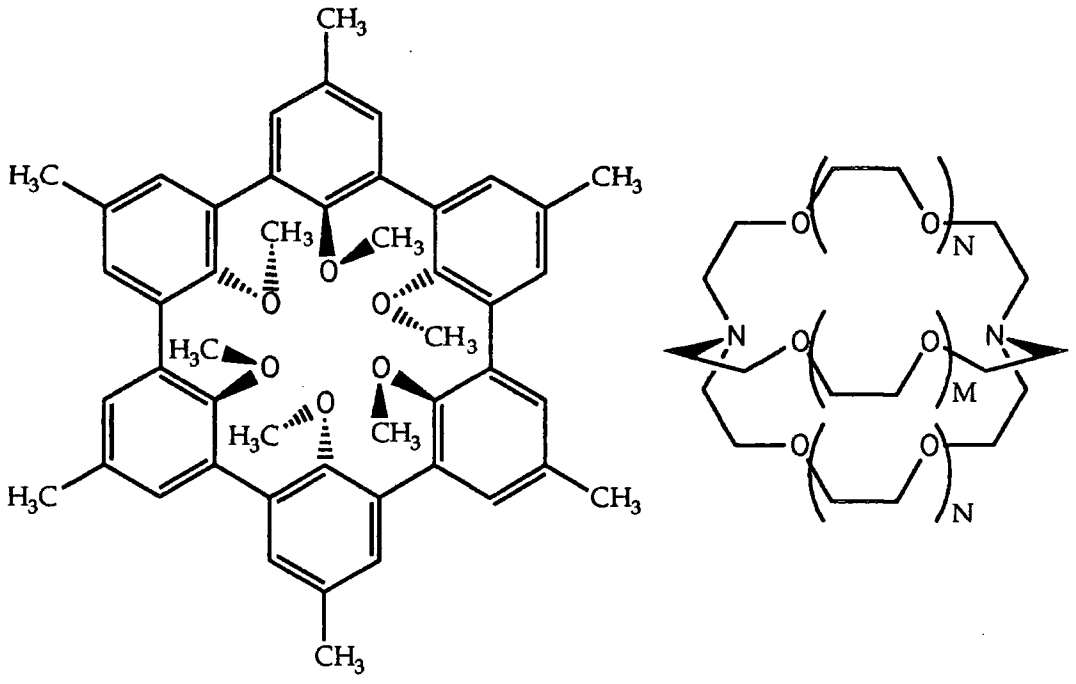

Figure 1.8 *A Spherand* *Cryptand ((M+1) (N+1) (N+1))*

1.3.1. Thermodynamics of complexation.

Measurements of the thermodynamics of complexation are almost invariably performed in solution, with the stability of the complex being determined relative to that of the separate solvated salt and ligand. The use of solvated ions and ligands as the reference state is clearly not directly relevant to the dissolution of salts in solvent free polymer systems. However, relative strengths of complexation by different ligands will still be meaningful so long as all comparisons refer to a common solvent, since all solvation processes, whether by solvent molecules or complex ligands, must first overcome the lattice enthalpy of the salt.

The overall reaction for the complexation of a metal ion M^+ with a ligand L in a solvent S may be written as:-

$$M^+S_x + LS_y \Leftrightarrow (ML)^+S_z + S(x+y-z) \qquad ....(9)$$

The equilibrium constant for this reaction is the stability constant for the complex, denoted K_s, which is defined in the usual way from the equilibrium concentrations of the three species:-

$$K_S = [ML] / [M^+][L] \quad ....(10)$$

This equilibrium constant is related to the free energy change for complexation, ΔG, which may be split into enthalpy and entropy terms, according to:-

$$\Delta G = -RT \ln K_S = \Delta H - T\Delta S \quad ....(11)$$

The main contributions to the entropy and enthalpy changes involved in complexation may be briefly summarised as:-

(1) Desolvation of the metal ion. This is entropically favoured but enthalpically disfavoured.

(2) Desolvation of the binding sites on the ligand. This is also entropically favoured but enthalpically disfavoured.

(3) Attachment of the ligand to the metal. The binding of the donor atoms to the metal is enthalpically favoured, but the ligand must first adopt a suitable conformation, which involves the loss of entropy and an increase in conformational enthalpy.

The strength of a given complex will depend on the relative importance of each of these factors, which are related to properties of the cation and solvent, as well as the ligand. Some of the important variables are discussed below.

1.3.1.i Cation Desolvation

The free energy change on desolvation will depend on:

(a) The charge density of the ion, with small and highly charged ions being more strongly bound than large and singly charged species. Thus $Li^+ > Na^+ > K^+$ and $Al^{3+} > Mg^{2+} > Na^+$, for solvation enthalpy.

This may be illustrated by the hydration enthalpies of these ions,[35] which are given in table 1.1. In other, less polar, solvents, the absolute values are smaller, but the overall trend is maintained.

Variations in the entropy change on desolvation of ions tend to parallel those in solvation enthalpy, since a stronger cation–solvent interaction gives more tightly bound solvent molecules which have lost more of their freedom of movement. This effect partially offsets the enthalpic term, but is

considerably smaller. Table 1.2 shows the size of the entropy change on hydration[35] for some common metal ions, and the "energy equivalent" at 298 K. These data are relative to ΔS°(hydration) = 0 for H^+. Compare the range of only 125 kJ mol^{-1} for the entropic effects with the 4300 kJ mol^{-1} range for hydration enthalpies of the same ions.

ION	$\Delta H^{\ominus}$(hydration) / kJ Mol^{-1}
Al^{3+}	4690
Mg^{2+}	1920
Li^+	520
Na^+	405
K^+	321

Table 1.1 *Hydration Enthalpies of Metal Cations*

ION	$\Delta S^{\ominus}$(hydration) / J Mol^{-1} K^{-1}	$\Delta S^{\ominus}$ x 298K / kJ Mol^{-1}
Al^{3+}	-321.7	-95.9
Mg^{2+}	-138.1	-41.1
Li^+	13.4	3.99
Na^+	59.0	17.6
K^+	102.5	30.5

Table 1.2 *Hydration Entropies and their Energy Equivalents at 298 K*

(b) The dipole moment, dielectric constant, and donicity of the solvent. Highly polar solvents will solvate cations more strongly, so complexes will appear weaker.

The complexation constants[36,37] for 12-crown-4 complexes in a range of solvents are given in table 1.3. These illustrate the effect of solvent polarity, as well as that of charge density in comparing the lithium and sodium complexes

in methanol. The highly unfavourable enthalpy term for desolvating lithium in this highly polar solvent dominates the free energy change, giving a weak complex.

ION	LIGAND	SOLVENT	LOG K_S
Li^+	12-crown-4	propylene carbonate	2.23
Li^+	12-crown-4	THF	1.0
Li^+	12-crown-4	MeOH	-0.57
Na^+	12-crown-4	MeOH	2.05
Na^+	12-crown-4	H_2O	----

Table 1.3 *Binding Constants for 12-Crown-4 Complexes in a Range of Solvents*

1.3.1.ii Ligand Desolvation

Prior to complexation, the ligand itself must be partially desolvated. both the enthalpic and entropic effects being larger for acyclic ligands than for macrocycles since the extended conformations adopted by free acyclic ligands are more strongly solvated than the relatively compact macrocycles. Ligand donor sites are most strongly solvated in protic solvents, which form hydrogen bonds with the O, N, S, or P donor atoms of the ligand, and in highly polar solvents. The trends in ligand solvation therefore tend to parallel those of cation solvation for common low molecular weight solvents, although the difference in solvent quality between a protic solvent and a highly polar aprotic solvent will be greater for the ligand than for the cation.

1.3.1.iii Ligand Attachment

The thermodynamics of the final step in the complexation reaction, the binding between the donor atoms of a ligand and a metal cation, depends on a great variety of factors. Some of these are similar to the factors governing solvation of cations by polymers, discussed in section 1.2. They include:–

(a) The nature of the donor atoms, particularly whether they are "hard" or "soft" bases, and whether the metal is a "hard" or "soft" acid

(b) The relative sizes of the ligand cavity and the ionic radius of the metal

(c) The degree to which the ligand is pre-organised into the correct conformation to receive the cation.

(d) Whether the basic geometry of co-ordination (octahedral, planar, etc.) preferred by the metal can be accommodated by the ligand.

1.3.1.iv The Macrocyclic effect

When comparing macrocyclic ligands with similar open chain species, most of the influences discussed above favour macrocyclic ligands. Macrocycles are generally less strongly solvated than their linear counterparts, reducing the ligand desolvation term, although the favourable desolvation entropy change is also reduced. Most importantly, macrocycles are more highly organised prior to complexation than acyclic ligands, and so undergo less conformational change on binding to a cation. The greater the distance between the free and complexed conformations, the more likely it is that unfavourable conformations, such as eclipsed hydrogens, will be present in the bound form of the ligand but absent from the free form. For ligands which have a large number of conformations of similar energy in the free state, but only one bound conformation, there will be a loss of configurational entropy on complexation, giving an unfavourable entropy change on complexation.

The term "macrocyclic effect" is used widely, but a strict definition requires the comparison of the complexation constants of a macrocycle and its nearest acyclic equivalent with a given cation in a given solvent, so as to eliminate as many extraneous influences as possible. For example, the comparison of the complexation constants for 18-crown-6 and its acyclic analogue, 2,5,8,11,14,17 hexaoxaoctadecane, with potassium give an estimate of the macrocyclic effect for 18-crown-6 under the given conditions.[38] In 99% methanol at 20° C this has a value of approximately 6,000.

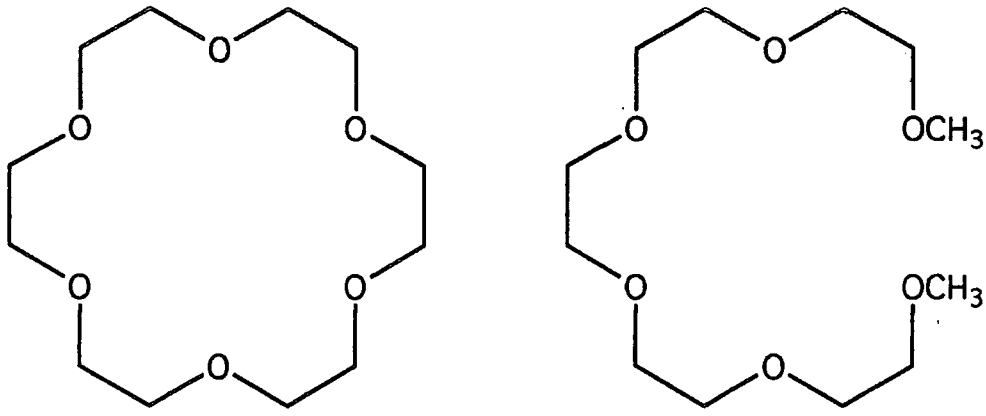

$\log K_s(K^+)$	6.05	2.27

Figure 1.9 *18-Crown-6 and its Acyclic Analogue and their Potassium Binding Constants in Methanol*

1.3.1.v Selectivity of crown ethers

The high binding constants achievable with macrocyclic ligands are only found when the correct macrocycle is used for a given metal ion. For the alkali metals, which are hard cations, hard donor atoms are needed, so suitable macrocycles are the original crown ethers and their derivatives. The interplay between the various factors influencing complex stability may be illustrated by the variation in complexation constant with ring size and cation size for the crown ether - alkali metal complexes. Selected data[38] are shown in table 1.4 and figure 1.10.

Compound	Cavity Diameter/Å	Ion	Ionic Diameter/Å
12-crown-4	1.2	Li^+	1.46
14-crown-4	1.54	Li^+	1.46
15-crown-5	1.8	Na^+	2.04
18-crown-6	2.8	K^+	2.76
21-crown-7	3.8	Rb^+	2.98

Table 1.4 *Diameters of Crown Ether Cavities and Alkali Metal Ions*

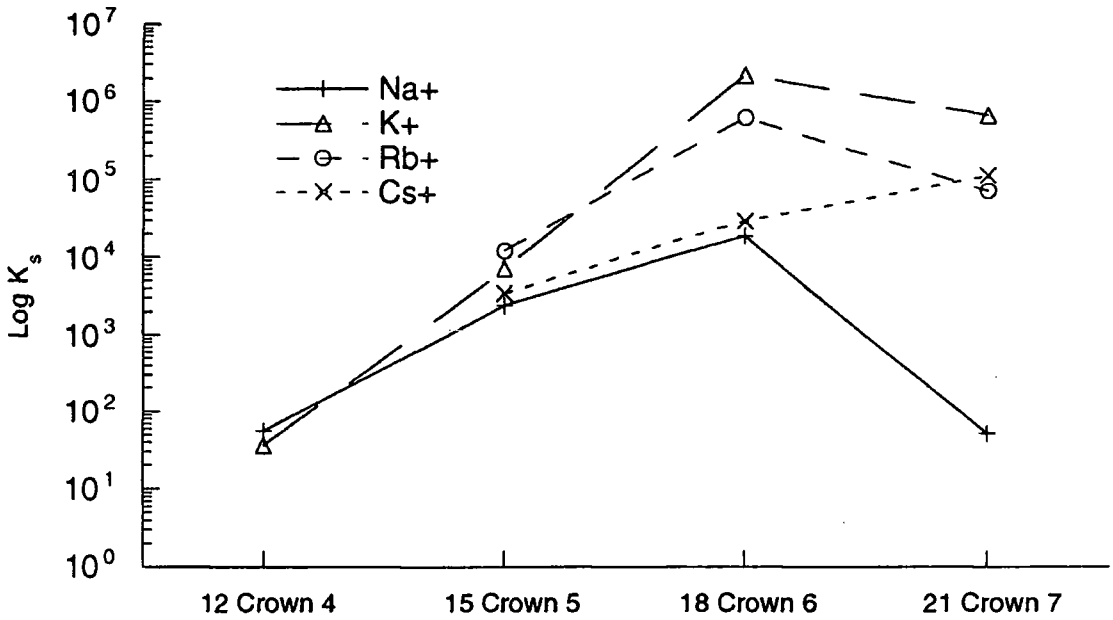

Figure 1.10 *Binding Constants for Alkali Metal Cation–Crown Ether Complexes in Methanol at 25°C*

Lithium ions are best solvated by 14-crown-4 and its derivatives, which have the best match to the ionic radius. 12-crown-4 derivatives also form reasonably strong complexes, but with the lithium ion positioned above the plain of the donor atoms. This encourages the formation of "sandwich" compounds, if insufficient lithium is present to bind to all the macrocycles in 1:1 complexes. 12-crown-4 also forms a strong 2:1 complex with sodium, with a much higher binding constant than the 1:1 lithium complex in methanol. The apparent weakness of the lithium complex is due to the high solvation enthalpy of lithium, discussed in section 1.3.1.i.

1.3.2. Kinetics of complexation.

For an effective polymeric electrolyte, the kinetics of exchange of metal ions between ligands must be rapid. This in turn requires that both the complexation and decomplexation reactions must be fast.

Two early suggestions for the mechanism of the complexation process of crown ethers and related compounds were put forward by Eigen[39] and by Chock [40]. Eigen's proposal was for a three-step process, represented as :–

$$M^+ + C \underset{k_{-1}}{\overset{k_{+1}}{\rightleftharpoons}} M^+ \cdots\cdots C \underset{k_{-2}}{\overset{k_{+2}}{\rightleftharpoons}} MC^+ \underset{k_{-3}}{\overset{k_{+3}}{\rightleftharpoons}} (MC)^+ \qquad \ldots.(12)$$

where M^+ is a metal cation, C is the macrocycle, $M^+ \cdots C$ is a loose "encounter" complex, with solvent molecules still attached to M^+, MC^+ is an "exclusive" complex, with the metal bound outside the ring, and $(MC)^+$ is the "inclusive" species, with the metal bound in the ligand cavity.

Chock suggested a simpler scheme with two basic steps :-

$$\text{(a)} \qquad C_1 \underset{k_{-0}}{\overset{k_{+0}}{\rightleftharpoons}} C_2 \qquad \text{"fast"} \qquad \ldots.(13)$$

$$\text{(b)} \qquad M^+ + C_2 \xrightarrow{k_f} MC_2^+ \qquad \text{"slow"} \qquad \ldots.(14)$$

where C_1 is the normal conformation of the free ligand, and C_2 is the conformation required for binding to the metal cation M^+, which will have a higher free energy. This mechanism thus involves a rapid pre-equilibrium of the ligand conformations, with the rate limited by the reaction of the ligand with the metal. In this mechanism, the overall rate of reaction is given by :-

$$\text{Rate} = k_f [M^+] [C_2] \qquad \text{with} \qquad [C_2] = K [C_1] \qquad \ldots.(15)$$

where K is the equilibrium constant for process (a)

Chock's mechanism appeared plausible as the reaction of C_2 with M^+ involves the removal of solvent molecules from M^+, a process likely to have a high activation energy. Chock provided supporting evidence from temperature jump relaxation studies of complexation between monovalent cations and crown ethers[40], which showed that a process with a relaxation time much shorter than that for metal-ligand interaction was involved, and his proposal was generally accepted for the following decade.

Unfortunately, this simple picture was later shown to be misleading. Chen et al[41] studied 18-crown-6 and alkali metal cations in methanol and dimethylformamide and determined the rate constants k_{+0} and k_{-0}. They found that Eigen's mechanism was appropriate and that k_{+0} is comparable to k_2. The

confusion had arisen because Chock's measurements were of relaxation times, which are always dominated by the faster of a pair of rate constants, and k_{-0} is much faster than k_{+0}.

More recent work by Cox and Schneider[42] has confirmed the necessity of the multi-step model, with the further refinement of breaking up step 3 of Eigen's model into individual reactions each involving the substitution of a single solvent molecule by a ligand donor atom. Their model indicates that the rates of complexation are very high for most alkali metals with most ligands, with the differences in thermodynamic stability of the complexes being expressed almost entirely in the rates of decomplexation. Somewhat surprisingly, the transition state for complexation is found to be early in the reaction, at a point when most of the solvent molecules are still attached to the ligand. To achieve fast cation exchange between ligands, the rate of decomplexation must be maximised, and this implies that the complexes must be relatively week.

1.4. Aims of this work

This project sought to investigate possible solutions for some of the remaining problems in constructing room-temperature solid-state lithium cells with high power outputs by applying macrocyclic chemistry to this area. The initial approach was to try and produce a variant of structurally modified PEO in which lithium-binding macrocycles are attached to a non-solvating polymer backbone with a low Tg. Poly(methyl methacrylate) was chosen as a suitable backbone as it is easy to prepare functionalised versions of this material, and it has been used previously in polymer electrolyte research.[27] It was also intended to try and correlate the properties of such polymers with those of the macrocycle-containing monomers, and related compounds. It was hoped that this would lead to some understanding of the importance of such factors as the strength and rate of formation of the lithium complexes of the ligands used, and how variations in these properties influence the conductivity of polymers containing them.

1.5. References

1. Gauthier, M., Armand, M. B. and Muller, D., in *Electroresponsive Molecular and Polymeric Systems,* ed. Skotheim, T. A., Marcel Dekker, New York, 1988, p. 41-97.

2. Cowie, J. M. G. and Cree, S. H., *Annu. Rev. Phys. Chem.*, **40** 85-113 (1989).

3. Fenton, D. E., Parker, J. M. and Wright, P. V., *Polymers,* **14** 589 (1973).

4. Wright, P. V., *British Polymer Journal,* 7 319 (1975).

5. Armand, M. B., Chabagno, J. M. and Dulcot, M. J., in *Fast Ion Transport in Solids,* ed. Vashishta, P., North Holland, New York, 1979, p. 131.

6. Armand, M. B., *Solid State Ionics,* **(9/10)**, 745-754 (1983).

7. Payne, D. R. and Wright, P. V., *Polymer,* **23** 690-693 (1982).

8. Dyson, R., Papke, B. L., Ratner, M. A. and Shriver, D. F., *J. Electrochem. Soc.*, **131** 586-89 (1984).

9. Cowie, J. M. G., in *Polymer Electrolyte Reviews,* ed. MacCallum, J. R. and Vincent, C. A., Elsevier, New York, 1987, vol. 1, p. 69-102.

10. Eisenburg, A. and King, M., *Ion -Containing Polymers: Physical Properties and Structure,* Academic, New York / London, 1977.

11. Watanabe, M., Ikeda, J. and Shinohara, I., *Polym. J.*, **15** 65 and 175 (1983).

12. Wixwat, W., Fu, Y. and Stevens, J. R., *Polymer,* **32 (7)**, 1181-1185 (1991).

13. Berthier, C., Gorecki, W., Minier, M., Armand, M. B., Chabagno, J. M. and Rigaud, P., *Solid State Ionics,* **11** 91-95 (1983).

14. Greenbaum, S. G., Pak, Y. S., Wintersgill, M. C. and Fontanella, J. J., *Solid State Ionics,* **31** 241 (1988).

15. Greenbaum, S. G., Adamic, K. J., Abraham, K. M., Alamgir, M., Fontanella, J. J. and Wintersgill, M. C., *Chem. Mater,* **3 (3)**, 534-538 (1991).

16. Robitaille, C. D. and Fauteux, D., *J. Electrochem. Soc.*, **133** 315 (1986).

17. *Polymer Electrolyte Reviews,* ed. MacCallum, J. R. and Vincent, C. A., Elsevier, New York, 1987.

18. Cohen, M. H. and Tunbull, D., *J. Chem. Phys.*, **31** 1164 (1959).

19. Adam, G. and Gibbs, J. H., *J. Chem. Phys.*, **43 (1)**, 139-146 (1965).

20. Gilles, J. R., Knight, J., Booth, C., Hobs, R. H. and Owen, J. R., PCT, No. WO 86/01643,

21. Armand, M. B., Muller, D., Duval, M., Harvey, P. E. and Chabagno, J. M., U. S. Pat., No. 4,758,483, Jul. 19, 1988

22. Ward, I. M., McIntyre, J. E., Bannister, D. J. and Hall, P. J., PCT, No. WO 85/02713,

23. Nagoaka, K., Naruse, H. and Shinohara, I., *J. Polym. Sci,* **22** 659 (1984).

24. Chabagno, J. M., Doctoral Thesis, University of Grenoble, 1980

25. Ballard, D. G. H., Cheshire, P., Mann, T. S. and Przeworski, J. E., *Macromolecules,* **23** 1256-1264 (1990).

26. Xia, D. W. and Smid, J., *J. Polym. Sci.*, **22** 617 (1984).

27. Bannister, D. J., Davies, G. R., Ward, I. M. and McIntyre, J. E., *Polymer,* **25** 1600 (1984).

28. Killis, A., LeNest, J. F., Gandini, A., Cheradame, H. and Cohen-Addad, J. P., *Solid State Ionics,* **14** 231 (1984).

29. Watanabe, M., Sanui, K. and Ogata, N., *Macromolecules,* **19** 815 (1986).

30. MacCallum, J. R., Smith, M. J. and Vincent, C. A., *Solid State Ionics,* **11** 307 (1984).

31. LeNest, J. F., Doctoral Thesis, University of Grenoble, 1985

32. Pedersen, C. J., *J. Am. Chem. Soc.*, **89** 7017 (1967).

33. Lehn, J. M. and Sauvage, J. P., *Tet. Lett.*, 2885 (1969).

34. Lehn, J. M. and Sauvage, J. P., *J. Am. Chem. Soc.*, **97** 6700 (1975).

35. Atkins, P. W. *Physical Chemistry,* Oxford University Press, Oxford, 1986.

36. Christensen, J. J., Eatough, D. J. and Izatt, R. M., *Chem. Rev.*, 351-81 (74).

37. Bradshaw, J. S., Christensen, J. J., Izatt, R. M., Lamb, J. D. and Nielson, S. A., *Chem. Rev.*, 271-339 (85).

38. Nicholson, P. E., Doctoral Thesis, University of Durham, 1989

39. Eigen, M. and Winkler, R., in *The Neurosciences: Second Study Program,* ed. Schmitt, F. O., Rockefeller University Press, New York, 1970, p. 685-96.

40. Chock, P. B., *Proc. Natl. Acad. Sci. USA,* **69** 1939-42 (1972).

41. Chen, C., Eyring, E., Petrucci, S. and Wallace, W., *J. Phys. Chem.*, **88** 2541-47 (1984).

42. Cox, B. G. and Schneider, H., *Coordination and Transport Properties of Macrocyclic Compounds in Solution,* Elsevier, Amsterdam, 1992.

2. Synthesis

2.1. Introduction

This work required the synthesis of a macrocyclic ligand capable of facilitating the transport of lithium ions within a polymer. The use of free macrocycles dissolved in a PVC polymer had been investigated previously in these laboratories,[1,2] but this approach is not suitable for use in lithium batteries or other applications where a significant charge is to be transported, as all the ligands present would be rapidly transported to the cathode along with the lithium ions, and could only return to the anode by diffusion. The resistance of such a system would therefore increase sharply during use, until the current drawn was limited to the rate of back diffusion of free ligands.

To avoid this problem, the macrocycles must be anchored to the polymer backbone, so a suitable group must incorporated into the ligands during their synthesis. A different mechanism for ion transport is also required. Instead of binding strongly to an ion and moving with it through the polymer, the ligands must bind relatively weakly, allowing ions to migrate from one binding site to another without themselves moving relative to the polymer. In designing a suitable macrocycle a compromise must be reached between fast exchange kinetics, which implies weak binding to the ion, and sufficient complexation strength to separate ion pairs and give a true solid solution. For use in a lithium battery, the ligands must also be chemically stable against reaction with lithium and likely cathode materials, and against electrochemical reaction with inert electrodes.

Candidates which fulfil the above requirements are derivatives of 12-, 13-, or 14-crown-4. These compounds contain only the ether functional group, which is known to be stable in lithium cells from studies on PEO itself. They also form weak to moderate complexes with lithium ions, and have fast exchange kinetics.

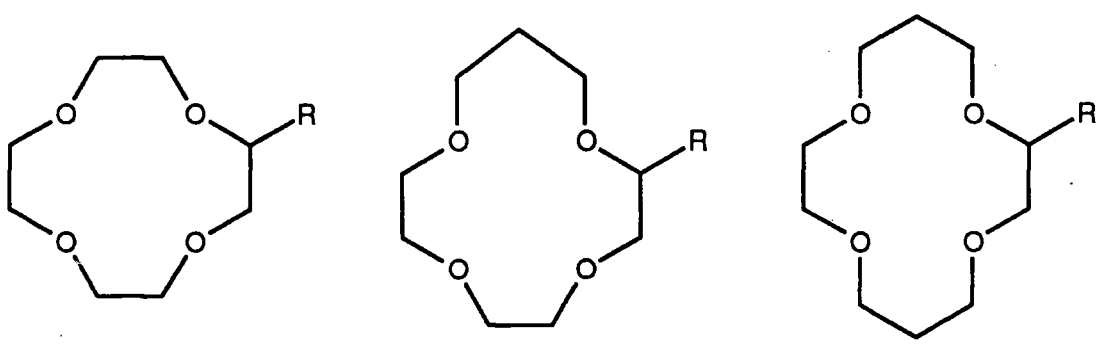

Figure 2.1. *12-, 13-, and 14-crown-4 rings with a side-group 'R'*

The side group 'R' (see fig. 2.1) must provide attachment to the polymer backbone. It may also be made to participate in binding to the lithium ion by incorporating additional donor atoms, to give a C-pivoted lariat ether. This may help ion pair separation by more effectively solvating the lithium ion. It may also aid lithium exchange by enabling the ion to leave the ring without losing all solvating oxygen atoms. This effect should lower the activation energy for decomplexation, which is the rate limiting step in lithium ion exchange.[3]

Reacting a ligand with a pre-formed polymer was expected to be difficult, as even simple reactions on polymer backbones do not go to completion, and attaching a bulky ligand would inevitably cause steric crowding as the extent of substitution increased. This problem is solved by preparing a substituted monomer, containing the cyclic ligand, and then polymerising this by standard methods once it has been purified. For a methacrylate polymer backbone, the simplest such monomer is one of the cycles shown in figure 2.1 with the side group R = $CH_2OCOC(CH_2)CH_3$. Since substituted 14-crown-4 ligands had been prepared in this laboratory for previous work[1], this was the first synthetic target.

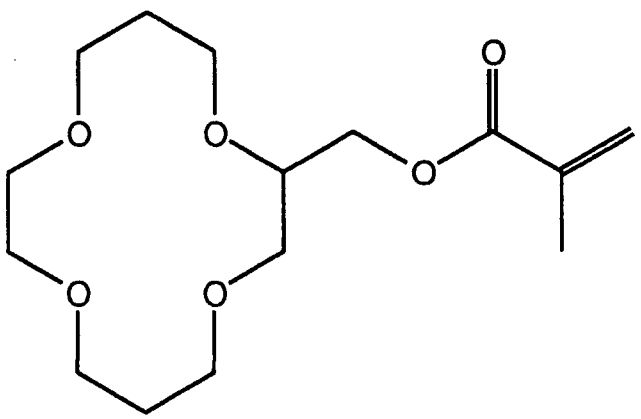

Figure 2.2 *Monomer (A), 2-(2'-Methylpropenoatomethyl)-1,4,8,11-tetraoxacylotetradecane*

2.2. Synthesis of the first Macrocycles

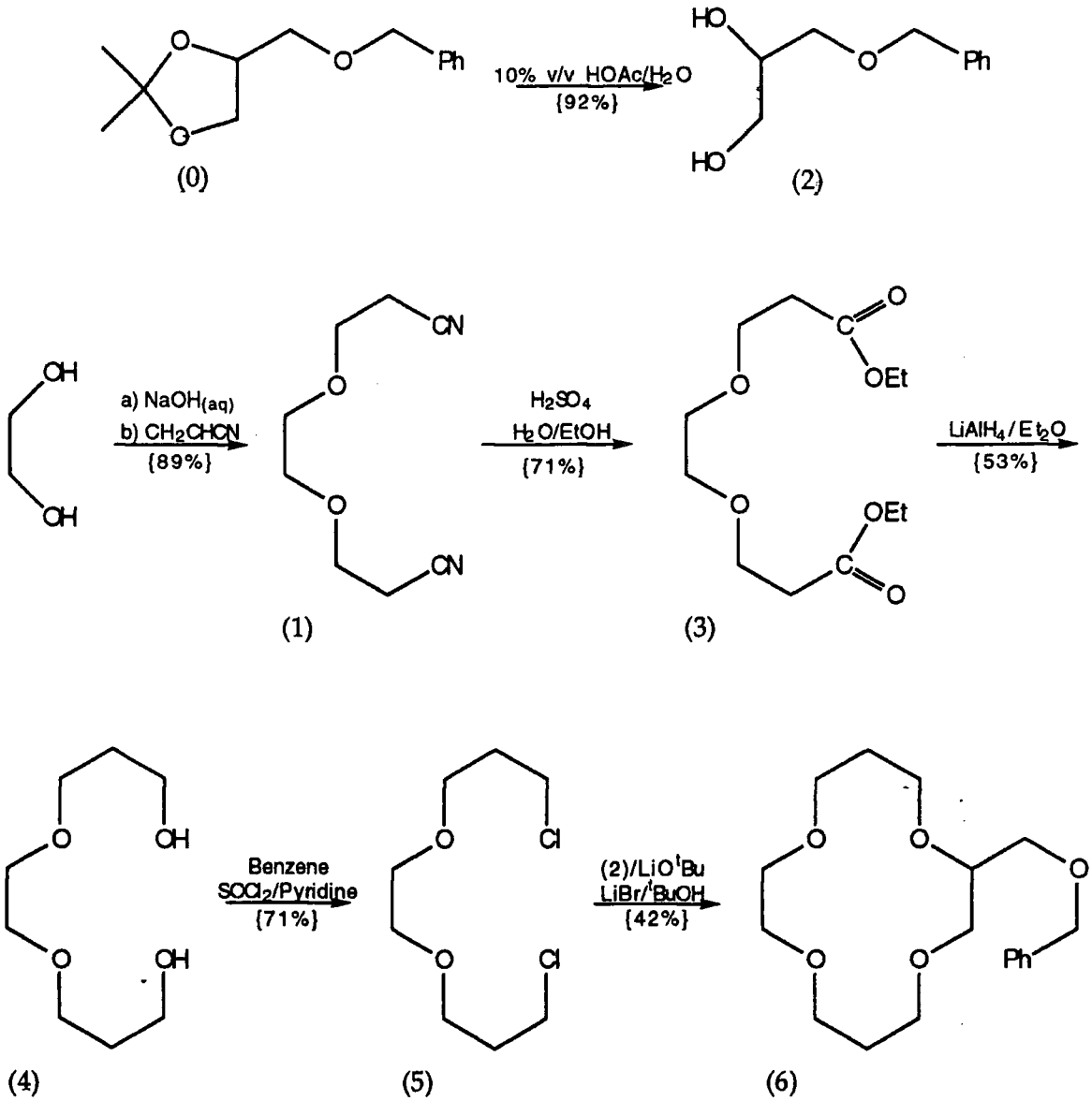

Scheme 2.1 *Synthesis of the first cyclic intermediate, 2-Benzyloxymethyl-1,4,8,11-tetraoxacyclotetradecane, (6).*

The initial steps in the synthesis of monomer (a) are illustrated in scheme 2.1. The compounds had all been prepared previously in this laboratory,[1] and the literature methods were used unmodified at first. The Michael addition to form compound **(1)** requires only very mild conditions and goes to completion in 24 hr at room temperature, although the reaction mixture must be stirred quite rapidly to mix the aqueous and organic phases. The hydrolysis of the benzyl dioxolane to the 1,2-diol, **(2)**, is also simple and high yielding. For both **(1)** and **(2)** the formation reactions themselves are almost quantitative, losses in yield occurring mostly in the purification step.

Like almost all the compounds used in this work, **(1)** and **(2)** are oils, and require purification by distillation under a pressure of 0.1 mbar or less to remove the last traces of solvents and any excess starting materials. The benzyl dioxolane **(0)** was initially obtained from Fluka, but later synthesised when larger quantities were required.

2.2.1. Alternative Routes

The hydrolysis of the dinitrile **(1)** to the diester **(3)** proved to be much more difficult than should be expected for such an apparently simple reaction. According to the literature method,[1,2] the hydrolysis can be effected by refluxing the nitrile in ethanol and sulfuric acid (20% acid, by volume) for 24 hours. In practice it was found that even extending the reaction time to a week failed to drive the reaction to completion. In an attempt to avoid this problem, the synthesis of the diester directly from ethane-1,2-diol was investigated. Michael addition of ethane-1,2-diol to methyl methacrylate in place of acrylonitrile would yield the methyl ester analogue of the ethyl ester **(3)** directly, and this reaction was attempted using metallic sodium to deprotonate the ethane-1,2-diol, in place of the aqueous sodium hydroxide used in the synthesis of the dinitrile **(1)**.

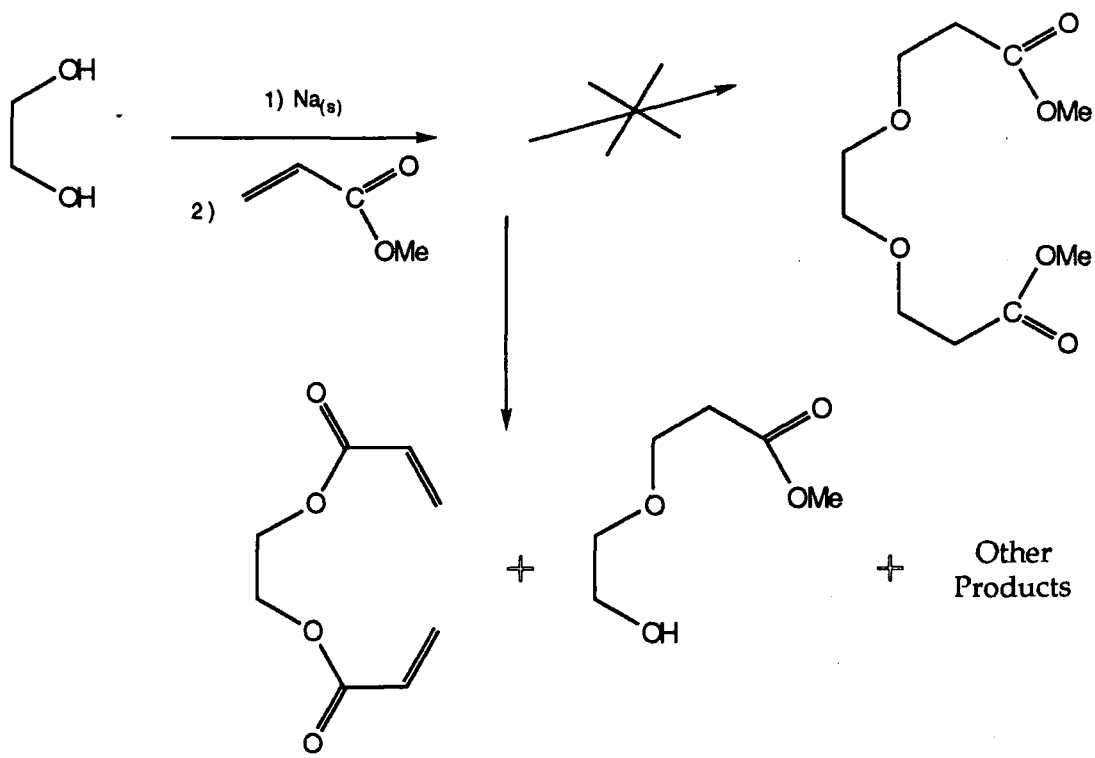

Scheme 2.1.a *Attempted direct synthesis of a suitable diester*

Unfortunately, the alkoxide ion attacks predominantly at the ester site of methyl methacrylate, giving a mixture of trans-esterified products with a small percentage of Michael addition of both ethan-1,2-diol and methanol, as shown in scheme 2.1(a). This is the predicted result for a hard base such as an ethoxide ion, and the synthesis of **(1)** is dependent on the relative inertness of the nitrile function.

The difficulty of the conversion of **(1)** into the diester **(3)** was eventually traced to the use of *too pure* a grade of ethanol. This contained insufficient water to hydrolyse the nitrile, a problem that had not been noted in the literature method. Addition of water, bringing the total present to 2 moles per mole of dinitrile, enabled the reaction to go to completion in reasonable yield.

The conversion of the diester **(3)** to the diol **(4)** proceeded with a disappointingly low yield of 53%. This is unfortunately typical of reduction by lithium aluminium hydride, at least for difunctional substrates, and is similar to the literature reported yield[2] of 51%. Rapid stirring of the reaction mixture, and careful addition of the ester solution to the centre of the stirring vortex proved essential to the success of this step, particularly at the relatively large batch size, 31 g (120 mmol) of diester, used. Further scale-up of this step would be difficult, and in view of this and the low yield, other methods of reduction were investigated. Dissolving metal reduction of an ester to an alcohol is possible, and can be used at larger scales, so this was attempted according to the method of Vogel.[4] Unfortunately, the conditions of this reaction promote a retro-conjugate addition, presumably initiated by the removal of a proton from **(3)**, rather than the desired electron transfer. There are no other readily available alternatives to hydride reduction for this step, and all subsequent batches of material were reduced as shown in scheme 2.1, using $LiAlH_4$.

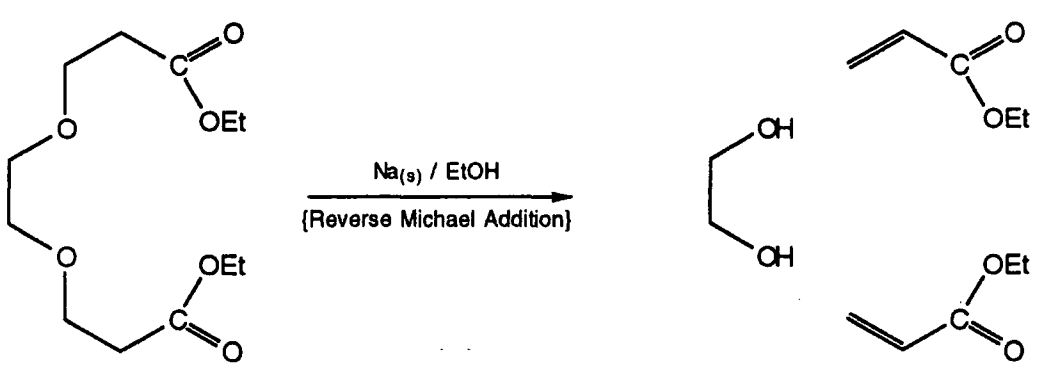

(3)

Scheme 2.1.b — *Reaction of the diester (3) with sodium gives reverse Michael addition in preference to reduction*

Conversion of the diol **(4)** to the dichloride **(5)** proceeded readily according to the literature method,[2] and in a somewhat improved yield (71% against a quoted 62%). This was probably due to the use of a Kugelrohr bulb-to-bulb distillation apparatus for the purification step, in place of a conventional distillation.

2.2.2. Cyclisation using the Literature Method

The first cyclisation reaction was carried out according to the literature method,[1] which was developed from the procedure of Okahara [5] for the synthesis of the 12-crown-4 analogue of the benzylated cycle **(6)** and of Bartsch[6], who adapted the method to produce **(6)**. This reaction is a templated cyclisation with an apparent mechanism of two successive S_N2 substitutions on the dichloride **(5)** by the lithium alkoxide of the diol **(2)**. In fact it is likely that the dichloride is first converted to the dibromide by the LiBr catalyst, and also that the reaction has at least one heterogeneous step, as neither LiBr nor the lithium alkoxide derived from the diol **(2)** are soluble in the reaction medium. The presence of solid alkoxide particles is necessary for the success of the reaction, as has been demonstrated by Okahara[5] and by Nicholson.[1] Okahara attempted the synthesis of 12-crown-4 by a method analogous to that shown in scheme 2.1, using 1,8 dichloro-3,6 dioxaoctane and ethane-1,2-diol, which has an alkoxide soluble under the reaction conditions, and obtained no product. Nicholson attempted another analogous reaction using the dichloride **(5)** and RR(+)-N,N,N`,N`-tetramethyl tartramide. This amide also gave rise to a soluble lithium alkoxide derivative, and failed to react. It therefore seems likely that the reaction involves attack on the dichloride **(5)** or its dibromide derivative by the lithium alkoxide of the diol **(2)** while both reactants are immobilised on a grain surface.

The cyclic product is too involatile to be purified by distillation, and so after neutralisation, removal of the reaction solvent and washing to extract salts, the crude product required purification by column chromatography. The cycle **(6)** has an Rf. value of 0.5 on alumina TLC. plates in 5:1 hexane : ethyl acetate. Using a gradient of solvent polarity from pure hexane to 5:1 hexane : ethyl acetate (by volume) on an alumina column the product was found to elute after a total of approximately 3 column volumes of solvent had been passed through the column. The only detectable impurity with a significant Rf. value under the conditions used was unreacted dichloride, **(5)**, which elutes before the product cycle, having an Rf. value of 0.7 in 5:1 hexane : ethyl acetate. All the other impurities present, which are likely to include oligomers of the two starting materials and some unreacted diol, **(2)**, remain on the baseline

In order to study the effects of ring size on lithium transport, a 12-membered ring analogue of the 14-membered ring (6) was synthesised by a similar method. Since the analogue of the dichloride (5) is the readily available dichloride of trigol, 1,8-dichloro-3,6 dioxadecane, the synthesis of the 12-membered ring is much simpler than that of the cycle (6), as shown in scheme 2.2. The yield of the cyclisation step is almost identical to that of the 14-membered ring (6).

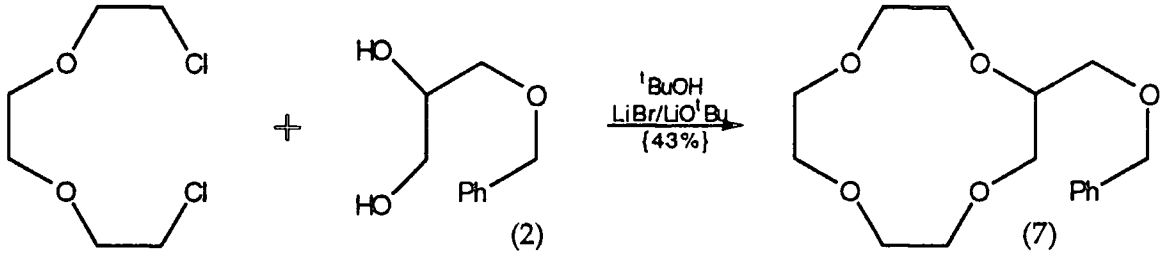

Scheme 2.2 *Synthesis of 2-Benzyloxymethyl-1,4,7,10-tetraoxacyclododecane, (7), from the readily available dichloride of trigol and the diol, (2).*

Purification of the product cycle (7) was achieved by column chromatography on alumina, as with the analogous 14-membered cycle, although (7) is somewhat more polar, having an Rf. of 0.1 in 5:1 hexane : ethyl acetate compared to 0.5 for (6).

2.2.3. Modified Cyclisation Route for Improved Yield

Although the route used in schemes 2.1 and 2.2 provided sufficient material for initial studies, the yield for the cyclisation step is rather low at 42-43 %. For the 14-membered ring (6) the overall yield from ethylene glycol is just under 10%, which makes the synthesis of large quantities of this material impractical. The yields are all the same as or slightly better than those reported by Nicholson,[2] and it was thought unlikely that modifying the reaction conditions would increase this yield significantly. The requirement of adding LiBr to the reaction mixture, presumably to form a bromide from the chloride starting material by halogen exchange, suggests that the chloride ion is not a sufficiently good leaving group to undergo the cyclisation reaction, so the use of a better leaving group in the starting material might be helpful. The obvious choice would be to use bromides as reactants directly, but trigol dibromide is known to be highly carcinogenic, and the bromide equivalent of the dichloride (5) might also be difficult to purify as it is likely to be less volatile and more unstable than the dichloride. Both problems would be considerably reduced if a solid reagent were used rather than a slightly volatile

oil. The tosylate (p-toluene sulfonate) group is known to form crystalline derivatives of many alcohols, and is a much better leaving group than chloride. Since the appropriate reagent for the synthesis of the 12-membered ring, 1,8-bis(p-toluene sulfonato)-3,6-dioxaoctane, (trigol ditosylate) can be prepared from the readily available triethylene glycol (trigol) this was used to test the modified cyclisation reaction, as shown in scheme 2.3.

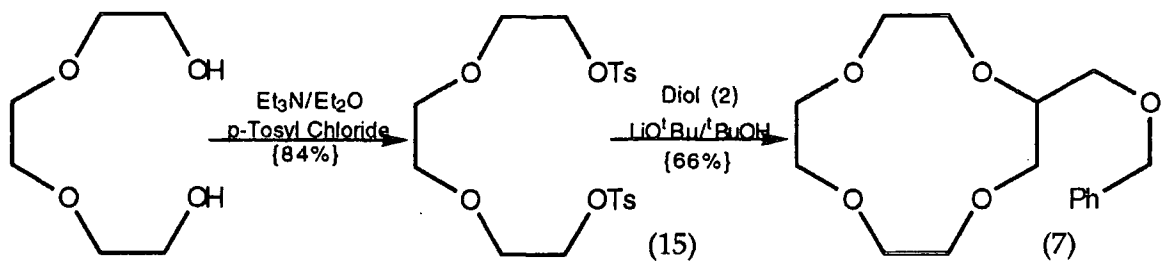

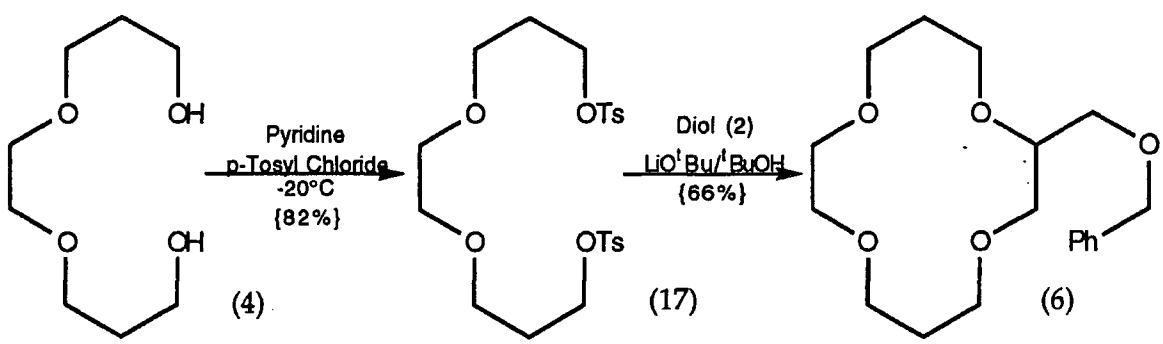

Scheme 2.3 *Synthesis of the cycles (6) and (7) in improved yield using Tosylate intermediates.*

Trigol ditosylate **(15)** precipitated as off-white lumps from a refluxing mixture of trigol, tosyl chloride and triethylamine in dry ether, along with triethylamine hydrochloride. After removal of the ether the product was readily extracted into dichloromethane by shaking with a mixture of dichloromethane and water (to dissolve the salts). Recrystallisation from ethanol gave a brilliant white powder, in a yield of 84%. This was used in place of trigol dichloride and lithium bromide in the synthesis of cycle **(7)**, without otherwise modifying the reaction conditions. The result was not an improvement on the literature method as a larger number of impurities were formed, making separation of the desired product difficult.

Although a full analysis of the impurities was never attempted, earlier work in this laboratory[1] had indicated that the main impurities are likely to be starting materials and their oligomers, and products of an elimination reaction

which competes with the desired substitution. Elimination is made more likely by increased reaction temperatures and particularly by the presence of free base (LiO^{t}Bu). The greater bulk of the tosylate group, compared to a halogen, may also encourage elimination over substitution.

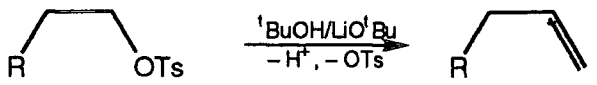

Scheme 2.3 (a)
Elimination of TsOH gives rise to unwanted alkene by-products.

A second attempt at this cyclisation was then made, with the reaction conditions modified to minimise elimination. The reaction temperature was reduced from 80 to 60 °C, and the initial concentration of lithium ^{t}-butoxide reduced by half to 0.75 equivalents. The rest of the base was added stepwise, after 30 hours and 5 days of reaction. After the last addition, the reaction was heated to 80 °C for a final 24 hours. TLC analysis confirmed that no by-products were formed in significant amounts, and after 6 days the reaction mixture appeared to contain only the product and traces of starting materials.

After removal of solvent and water-soluble impurities, the residue was found to contain approximately 72% product, 24% unreacted tosylate **(15)** and 4% other impurities (assuming that all were detected equally well by GLC.). Separation of the product and tosylate is difficult by column chromatography as they have very similar Rf. values, but the product is soluble in hot hexane, while the tosylate is not, so the residue was extracted with several portions of boiling hexane. This separated out an insoluble dark-brown viscous oil, from which some crystals of the tosylate **(15)** later precipitated, and a pale yellow oil, which was 97-98% pure product, in a yield of 64-66%. This could be used without further purification.

Following the success in increasing the yield of the cyclisation reaction of the 12-membered ring **(7)**, an attempt was made to prepare the 14-membered ring **(6)** by the same route. Unfortunately, the reaction of the diol **(4)** with tosyl chloride under the same conditions used for the preparation of trigol ditosylate **(15)** did not produce any crystallisable product. An alternative route, described in Vogel,[7] was therefore adopted, which was successful, the product **(17)** being obtained in 82% yield (see scheme 2.3). This was used in place of the tosylate **(15)** under the optimised conditions described above. Column chromatography isolated the product cycle **(6)** in 65% yield.

2.3. Deprotection of the Benzylated Cycles

Before the cycles (6) and (8) can be incorporated into other materials, the protecting benzyl group must first be removed. The literature method[2] is hydrogenation using Pearlman's catalyst (Aldrich), which is dispersed palladium hydroxide on carbon. This reaction is illustrated in scheme 2.4. Unfortunately, the hydrogenation step is not reliable. Yields varied considerably from one batch of catalyst to another, and for one period of several months no product could be obtained at all, the reactant being recovered unchanged. It was initially suspected that the batch of catalyst being used had deteriorated, but a freshly ordered batch was also ineffective. Since it was assumed that new and unopened catalyst must be active, its failure led us to believe that some impurity in the reactant must be poisoning the catalyst. Purification by repeated column chromatography did not make any noticeable difference to the results, however, nor did distillation of the reaction solvent or recrystallisation of the p-toluene sulfonic acid co-catalyst.

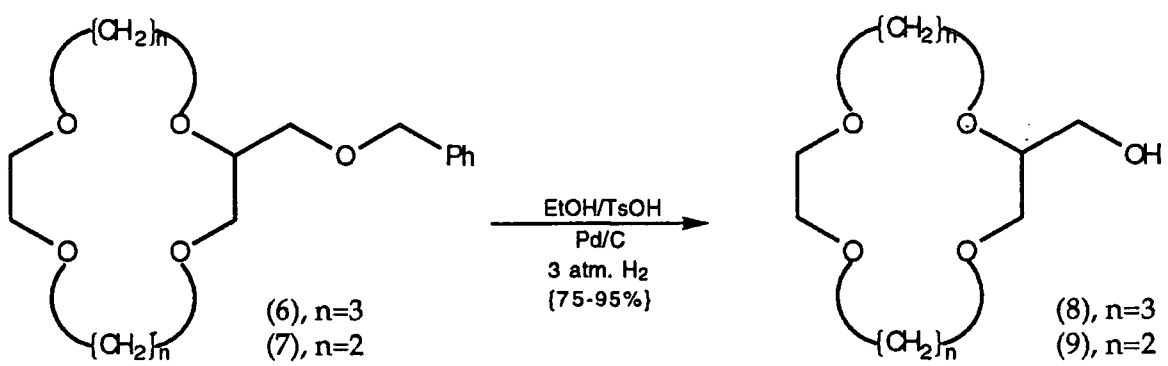

Scheme 2.4 *Conversion of the benzylated cycles (6) and (7) to the alcohols (14) and (16).*

In an attempt to overcome this difficulty, the hydrogenation reaction was attempted under forcing conditions of 100 atm. of hydrogen at a temperature of 50°C in the high-pressure laboratory. This was no more successful than the low-pressure method, so alternative means of cleaving the benzyl ether linkage were investigated.

The use of trimethylsilyl iodide[8, 9] or a mixture of sodium iodide and trimethylsilyl chloride[10] is mentioned in the literature as a method for selective ether cleavage, and the later procedure was repeated on a small scale using the 12-crown-4 derivative (7). No products were detectable by TLC after the recommended reaction period, and this route was not pursued further.

An alternative reagent for ether cleavage is boron tribromide.[11, 12] The reaction takes place overnight at room temperature in a solution of dichloromethane, to give an intermediate trialkoxy boride which is then hydrolysed. On following the literature procedure with a sample of **(7)** as the starting material a mixture of the desired product, **(9)**, benzyl alcohol, benzyl bromide and 2-bromomethyl-1,4,7,10-tetraoxacyclododecane was obtained. Some other by-products, possibly resulting from cleavage of the ring ether functions, were also detected by GLC. but were not identified.

Although the boron tribromide route could have been used, by converting the bromide products into alcohols with base and then separating them, the yield from such a multi-step process would never have been very high. A further attempt was therefore made to use the hydrogenation route, using a third batch of catalyst and operating on a reduced scale. This proved successful, and was scaled back up. Further investigations found that the batches of catalyst available in the laboratory varied greatly in activity, and that age was not a reliable guide to catalyst usefulness as the newest samples sometimes gave no reaction at all. Once a "good" batch of catalyst had been found it was used for the rest of the project, and was successful even on rather impure samples.

2.4. Extended Side-Chain Macrocycles

In order to investigate the links between polymer structure, glass transition temperature T_g and ionic conductivity, it was necessary to prepare monomers with other structural elements in addition to the macrocycle. It was hoped that in all the polymers, lithium solvation would be dominated by the macrocycle, so that this would not vary greatly. The glass transition temperature of any polymer will be reduced by the incorporation of flexible groups, whether attached to the polymer backbone or simply dissolved in the polymer as a separate plasticiser. The glass transition temperature T_g, and ionic conductivity, σ, are closely linked. According to the VTF equation, reproduced below, the relationship is similar in form to the Arrhenius equation for reaction rates. :-

The VTF Equation :- $$\sigma = AT^{-1/2} \exp\left\{\frac{-B}{T - T_0}\right\} \qquad T_0 = T_g - \text{(a constant)}$$

(See section 1.2.2.i for its justification.)

The incorporation of an internal "plasticiser" into the monomer structure is therefore likely to have a large effect on the measured conductivity. If the "plasticised" and "unplasticised" polymers fit onto the same VTF plot, once differences in T_g have been taken into account, it may be concluded that the mechanisms of ion transport are identical in the two polymers. Deviations from this behaviour may indicate that barriers to ion movement have been modified by the inclusion of the plasticising group.

Two plasticising groups were studied, and were incorporated into the polymer as extensions to the ring side-chain. The extensions were a C_6 hydrocarbon chain, and an oxydiethylene group. The hydrocarbon group plasticises the polymer, but can take no part in ion transport. The oxyethylene group is somewhat more flexible than a simple hydrocarbon, so it was expected to be a better plasticiser, but it can also solvate lithium ions, either independently of the crown ether or in conjunction with some of the ring oxygens. It was thought that this might provide an intermediate state between crown ether bound and free lithium ions, reducing the energy barrier to lithium migration.

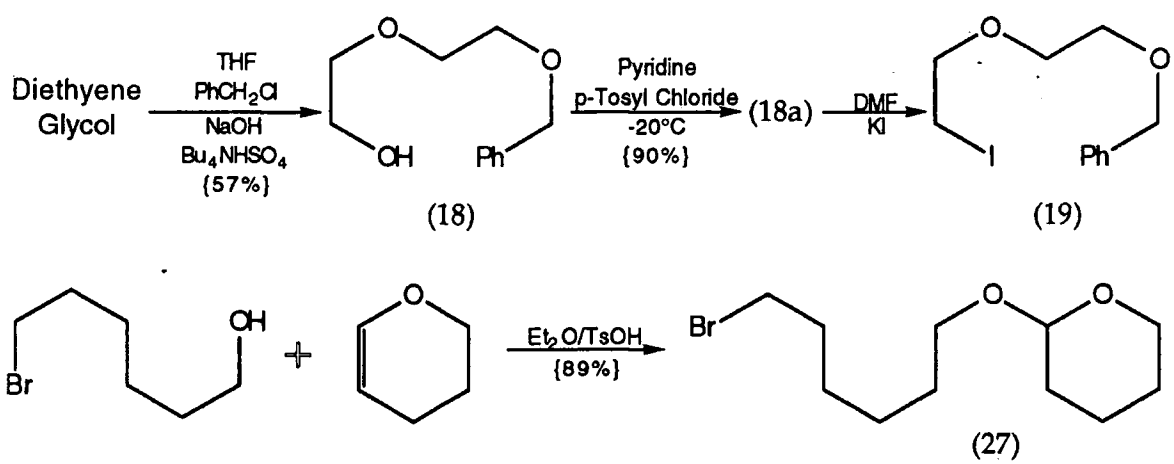

Scheme 2.5 *Synthesis of the extension groups (19) and (27).*

The extension groups were prepared for coupling to the ring alcohols **(8)** and **(9)** as shown in scheme 2.5. The conditions for the monobenzylation of diethylene glycol were derived from a procedure used previously in this laboratory[13]. The Bu_4NHSO_4 acts as a phase transfer catalyst for base, so that an aprotic reaction solvent can be used. The Bu_4N-diethylene glycoxide ion pair is much more soluble in THF than Bu_4N-OH, so the formation of benzyl alcohol is minimised. The product alcohol **(18)** is purified by fractional distillation under reduced pressure, and tosylated by the same method used for the preparation of the ditosylate **(17)**, described in section 2.2.3. Conversion of the tosylate to the iodide **(19)** requires only stirring at room temperature

overnight. However, the iodide is easily oxidised, so the reaction mixture was sealed under nitrogen and portions purified as required.

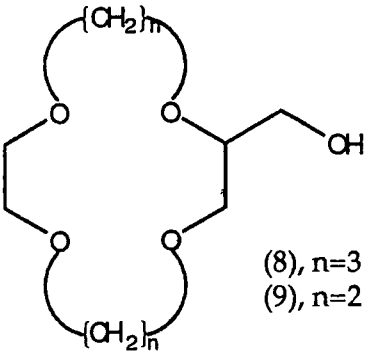

(8), n=3
(9), n=2

a) TlOEt/Toluene
b) (19)/MeCN
{65-70%}

a) TlOEt/Toluene
b) (27)/MeCN
{60-65%}

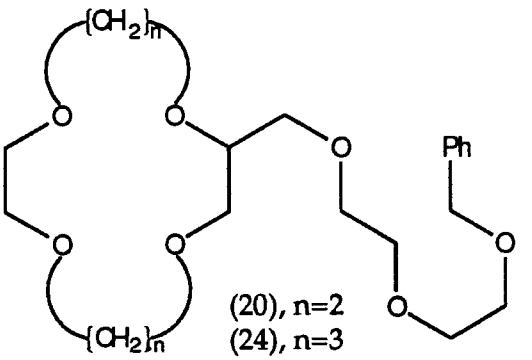

(20), n=2
(24), n=3

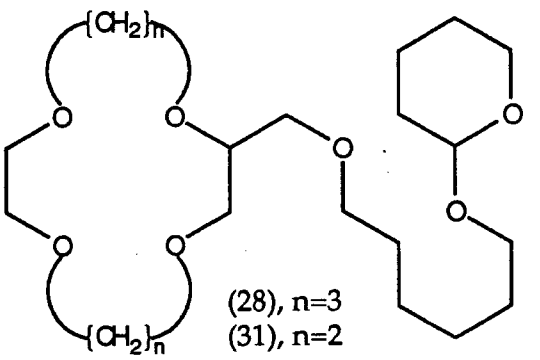

(28), n=3
(31), n=2

MeOH/TsOH
Pd/C
3 atm H_2
{86-88%}

0.1M HCl in MeOH
{100%}

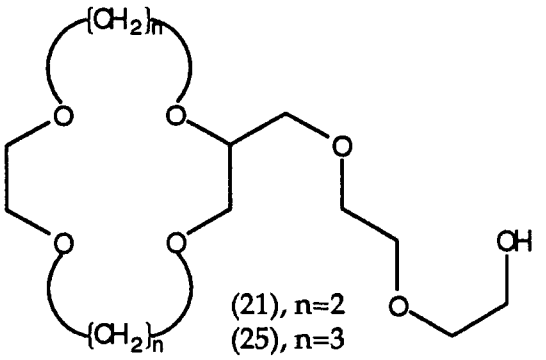

(21), n=2
(25), n=3

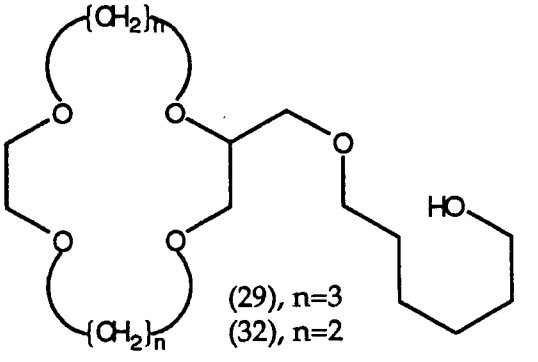

(29), n=3
(32), n=2

Scheme 2.6 *Preparation of Extended-chain Macrocycles*

The hydrocarbon chain extension was prepared by protecting the readily available 6-bromo hexanol with a tetrahydropyranyl (THP) group, according to the literature method[14]. The addition and removal of the THP group is simpler than that of the benzyl group used for the ethylene oxide-based extension. No suitable monosubstituted derivative of diethylene glycol (analogous to 6-bromo hexanol) was available. To protect just one hydroxy group of diethylene glycol with THP would have required the use of a large excess of the diol, and the difficulty of purifying the resulting mixture made the use of a benzyl protecting group the more attractive option.

The conversion of the "short chain" crown ether alcohols to the "extended chain" variants is shown in scheme 2.6. The initial coupling of the extensions to the ring side-chain is carried out via an intermediate thallium alkoxide[15]. This route was chosen as the reaction of thallium alkoxides with alkyl iodides is cleaner and higher yielding than most S_N2 reactions. It is driven by the extreme insolubility and high lattice energy of thallium iodide, which can be formed at or near the transition state of the substitution reaction, but does not assist the competing elimination pathway. The reaction with the alkyl bromide **(27)** was similar to the standard iodide method, although the yield is slightly reduced.

The extended chain cycles were purified by column chromatography, and then deprotected by hydrogenation or acidification[16], as appropriate. The by-products of the removal of the THP group are all volatile, so the pure product could be recovered by simply evaporating the by-products under reduced pressure. The ethylene oxide extended alcohol required purification by column chromatography.

2.5. Preparation of Macrocycle-containing Monomers

The final step in synthesising the methacrylate monomers, shown in scheme 2.7, is relatively easy, provided that dry reagents are used to avoid the formation of methacrylic acid before the cyclic alcohol reacts with the acid chloride. However, the first attempts at isolating the product resulted in its spontaneous polymerisation to form an insoluble gel during the removal of solvents. Possible initiating agents for this polymerisation include radicals produced by atmospheric oxidation and by light, so the synthesis reaction was repeated using a foil-wrapped apparatus to exclude light, and with more care to exclude oxygen, although even the first attempts had been made under an atmosphere of dry nitrogen.

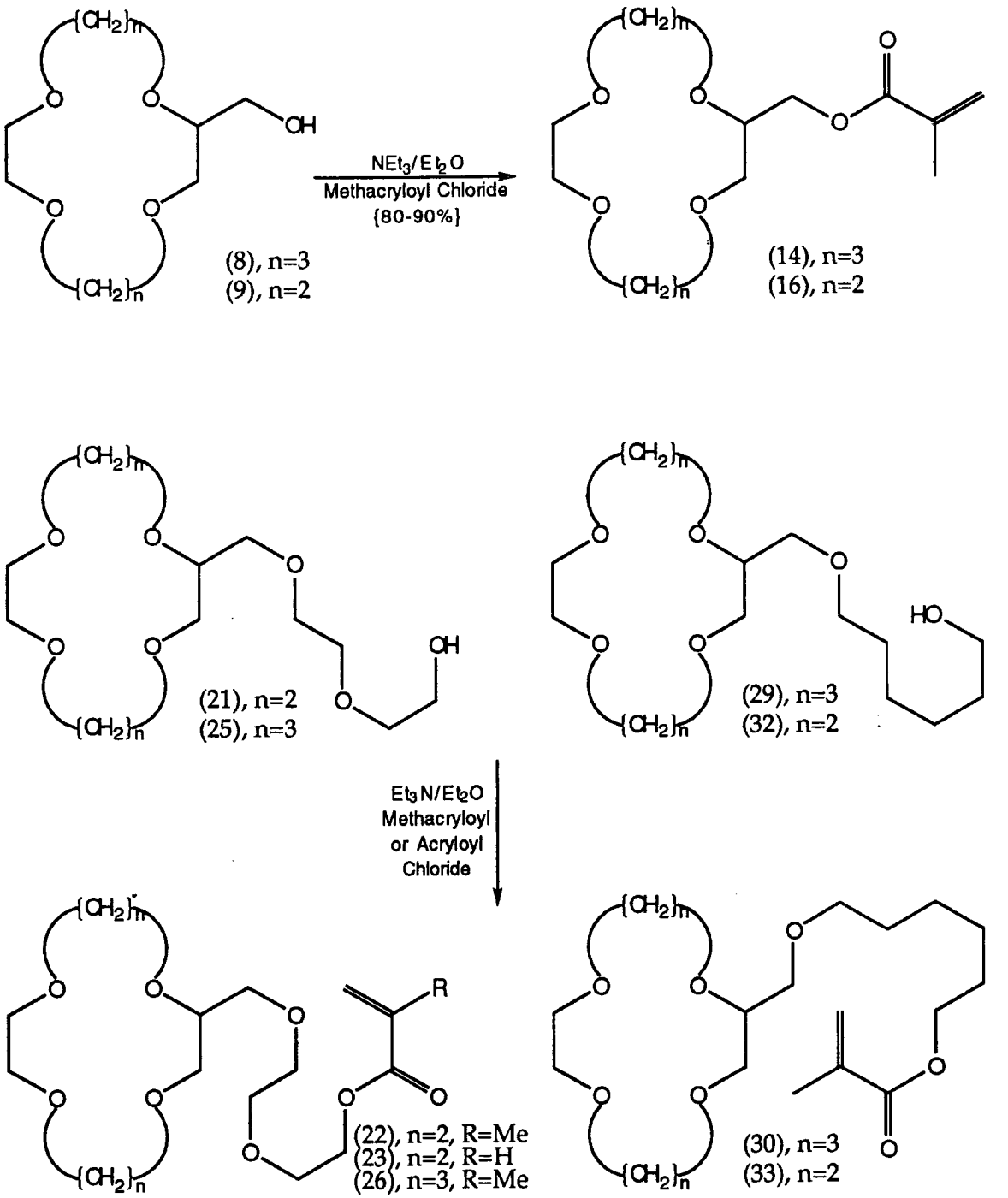

Scheme 2.7 *Synthesis of Macrocycle-containing Monomers*

Unfortunately, it is necessary to purify the product monomer before attempting a controlled polymerisation, to remove excess methacryloyl chloride and other impurities, and this requires column chromatography. Although it is possible to prepare an oxygen-free column, and run it under nitrogen, this involves considerable extra effort, and should not be necessary as methacrylate monomers can normally be handled in the open laboratory, provided they are stored in a freezer and used quickly. For longer term storage, an inhibitor (a radical trap) is required. Although the methacryloyl chloride used in the synthesis of **(14)** and **(16)** contained an inhibitor, this appeared to be insufficient to stabilise the macrocyclic monomers. A few crystals of the strong radical inhibitor hydroquinone were therefore added to the reaction flask before the start of the reaction This amounted to an inhibitor concentration of several parts per thousand, compared with a typical concentration of a hundred parts per million in commercially supplied monomers. With this addition, it was possible to remove the solvent from the crude product, provided that the material was not heated. The product could be stored in a freezer (about -20°C) for up to several days, but the chances of spontaneous polymerisation are greatly reduced by storing it while still diluted by the reaction solvent.

In practice, the crude product was usually placed immediately onto a pre-prepared chromatography column and purified. This removes the inhibitor, but the monomer is stable in air, at least for a few hours, so long as it remains diluted in the eluted solvent. The final removal of this solvent must be done under a good vacuum, in the flask intended for the controlled polymerisation reaction, and the product then used immediately.

The instability of the monomers **(14)** and **(16)** is surprising as the density of polymerisable groups is low compared to that in simple monomers due to the presence of the bulky rings. This may be due to the possible additional site for radical formation at the 2- position on the rings. Hydrogen abstraction here gives rise to a carbon radical stabilised by interaction of the singly occupied carbon p–orbital with the lone pair orbital (approximately an sp^3 hybrid) on the neighbouring oxygen,[17] illustrated in figure 2.2. Further stabilisation is provided by interaction with the C—H bonds of the adjacent carbons, (hyperconjugation) and by the electron-withdrawing effect of the methacrylate group. This will lower the energy of the lone electron, and so increase its interaction with the oxygen lone pair.

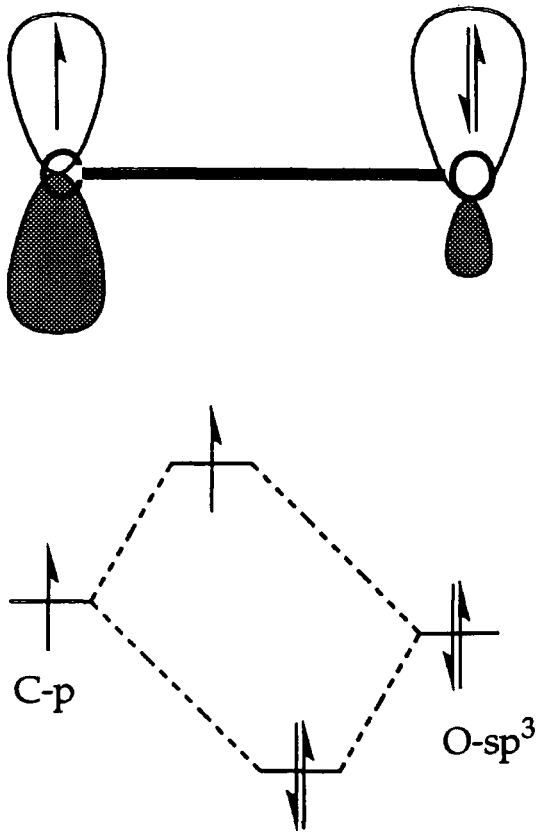

Figure 2.2 *Stabilisation of a carbon radical (carbon—p-orbital) by interaction with a lone pair on a neighbouring oxygen atom.*

2.6. Model Polymers

When the first difficulties with the spontaneous polymerisation of the target monomers were encountered, it was decided that some simple model compounds should be prepared to establish the required conditions for their preparation and controlled polymerisation. In place of the alcohols **(6)** and **(7)** the readily available 2 methoxyethoxy ethanol was reacted with methacryloyl and acryloyl chloride. The resulting compounds are in fact much more stable than the target monomers, and could be stored safely in the freezer without additional stabiliser.

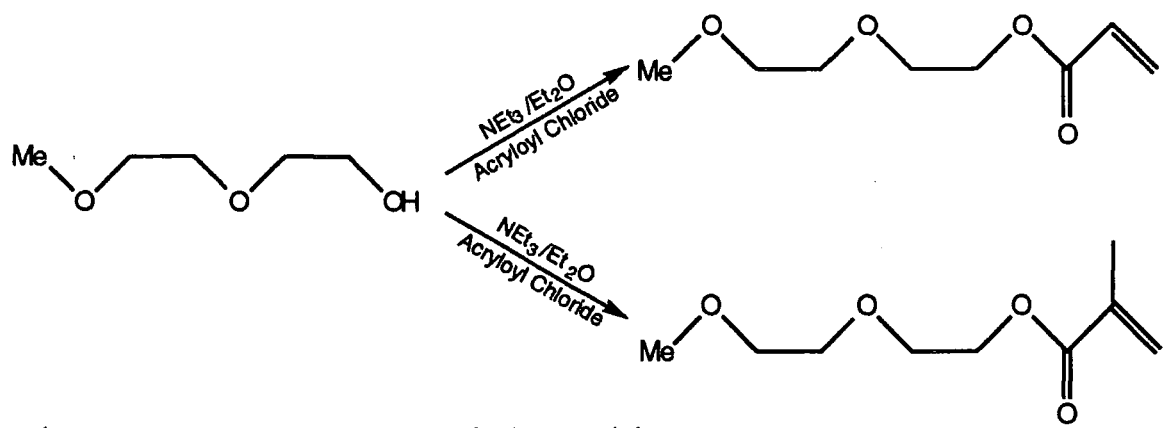

Scheme 2.8 *Synthesis of the model monomers*

The model monomers were polymerised according to the method used by Bannister et al[18] on a series of similar compounds. This method uses the reaction between $K_2S_2O_8$ and $FeSO_4$ to generate $SO_4^{\cdot-}$ radicals, which initiate the polymerisation. For the literature compounds, both the monomer and the polymer are soluble in the aqueous reaction medium, but due to the use of a shorter ethylene oxide chain, our model polymers were found to be insoluble and precipitated as a milky suspension. This was coagulated by the addition of Na_2SO_4. The reaction was performed using degassed water under an atmosphere of nitrogen, as oxygen from the air traps the radicals which propagate the polymerisation. The acrylate and methacrylate monomers **(12)** and **(13)** behave very similarly, except that the methacrylate is somewhat more reactive, the polymerisation reaction occurring readily at room temperature rather than at 60°C.

The literature polymerisation method[18] recommended purification of the polymer by dissolution in acetone followed by filtration to remove salts and precipitation in acetone/heptane, in which the monomers, and the hydroquinone used to terminate the polymerisation reaction, are soluble. The polymers of **(12)** and **(13)** were found to contain substantial quantities of acetone-insoluble material, although the soluble polymer could be extracted and purified as suggested. The insoluble material, comprising 50-70% of the total weight, appeared to be a cross-linked and/or very high molecular weight polymer, as prolonged stirring with a variety of solvents resulted only in swelling the material, rather than dissolution of it.

The formation of the high molecular weight or cross-linked material was probably due to the insolubility of the polymer in the reaction solvent. This resulted in the precipitation of microscopic polymer granules early in the reaction. Since the monomer was miscible with the polymer, polymerisation could continue within the polymer granules, effectively giving rise to a bulk polymerisation environment. Towards the end of the reaction, viscosity within the granules will increase greatly, immobilising the radical at the end of the polymer chain. In the absence of other molecules to react with, the radical will attack a neighbouring polymer chain, leading to branched and eventually to cross-linked material. In an attempt to avoid this problem, the polymerisation was repeated using ethanol as the solvent, but this resulted in very little reaction, with most of the monomer being recovered unchanged. The salt based initiation mechanism is not suitable for other common solvents, as the salts will not be soluble.

2.7. Formation of Crown Ether Polymers

2.7.1. Redox Initiation

The first controlled polymerisation of the crown ether functionalised monomers **(14)** and **(16)** was carried out using the aqueous method described above for the model compounds. As with the model polymers, the crown ether polymers were found to be insoluble in water, resulting in a heterogeneous reaction, and consequently in the formation of a proportion of insoluble gel-like material. Due to the relative ease of hydrogen atom abstraction at the 2 position on the rings, discussed in section 2.5, the tendency to gel formation was even greater than for the model compounds. Although this presented some difficulties in characterising the polymers, as only the soluble fraction could be thoroughly analysed, it was not necessarily a hindrance to the use of polymers prepared by this method for lithium electrolytes. A small degree of cross-linking is desirable in a polymer electrolyte, as it increases the mechanical strength of the material without greatly reducing the mobility of the polymer segments, except at the relatively small number of cross-linking sites. Cross-linking also greatly reduces polymer crystallinity, as it is impossible for a randomly cross-linked gel to rearrange into an ordered crystalline state. Since crystalline regions are ionic insulators, this effect will increase the overall conductivity of the sample. Analysis of the molecular weight distribution of the soluble fraction by gel permeation chromatography (GPC) revealed that some very high molecular weight material (molecular weight $>10^6$) had been formed, although the polydispersity was very large (Mw/Mn = 4.04). High molecular weight polymers may also offer superior properties, as chain entanglement will improve mechanical stability.

2.7.2. AIBN Initiation

To increase the yield of soluble polymer, so that a full characterisation as well as electrical measurements could be performed on the same material, required a method of polymerisation that gave a homogeneous reaction. Both the monomers **(14)** and **(16)** and their polymers **(A)** and **(B)** were known to be soluble in acetone, dichloromethane, and ethyl acetate. The usual initiator for the polymerisation of methacrylate monomers in organic solvents is azo-isobutyronitrile, $[(CH_3)_2(CN)CN]_2$, usually abbreviated as AIBN[19]. On heating this liberates nitrogen gas, leaving two $[(CH_3)_2(CN)C]^{\cdot}$ radicals which initiate the polymerisation. The decomposition reaction has a half-life of $1\frac{1}{2}$ – 2 hours at 80°C, or 15 – 20 hours at 60°C. Chlorinated hydrocarbons are unsuitable as

solvents for radical reactions as chlorine radicals are readily removed from the solvent molecules, which destroys the polymerisation chain reaction. Both acetone and ethyl acetate are chemically suitable, but the low boiling point of acetone (56°C) would result in a slow rate of reaction at reflux. Ethyl acetate, boiling at 77°C, was therefore the initial choice.

The polymerisation was carried out using freshly purified monomers, which were transferred into the reaction flask in solution. The transfer solvent was removed using a vacuum pump, with the monomer being kept cold and dark to minimise the chance of spontaneous polymerisation. The pure monomer was frozen in liquid nitrogen, and the ethyl acetate reaction solvent transferred into the flask as vapour. This procedure ensured that the neat monomer was never allowed to stand at room temperature, and also removed dissolved oxygen from the reaction solvent. The AIBN initiator was added to the reaction vessel whilst the reactants were still frozen, and oxygen was purged from the system by repeated freeze-thaw cycles under alternating nitrogen and vacuum. The polymerisation was started by heating the reaction vessel in an oil bath set to 80°C, and carried out under a slight positive pressure of nitrogen. The reaction was terminated by the addition of hydroquinone after 12 – 18 hours.

The polymer was recovered by dropping the reaction solution into a large excess of hexane, which precipitated it, and further purified by dissolution in a small quantity of acetone, and reprecipitation into clean hexane. The unreacted monomers and oligomers were hexane soluble. It was found to be necessary to avoid using too much acetone in the purification steps, as a dilute polymer solution precipitated into a fine suspension of particles, which could not be recovered except by evaporating off all the solvents and redissolving the residue in fresh acetone. When sufficiently concentrated solutions were used, the polymer formed a continuous thread which adhered to the sides of the flask.

Although the ethyl acetate route gave much less insoluble material than the previous aqueous route, some gel sometimes formed, and significant quantities of unreacted monomer were sometimes present at the end of the reaction period, after sufficient time for all but a few percent of the initiator to decompose had been allowed. The use of butanone (boiling point 79°C) in place of ethyl acetate was suggested[19], and this eliminated gel formation entirely, and reduced the proportion of unreacted monomer.

Polymer	Monomer	Ring Size	Extension	Backbone
A	14	14	None	Methacrylate
B	16	12	None	Methacrylate
C	22	12	Oxyethylene	Methacrylate
D	23	12	Oxyethylene	Acrylate
E	26	14	Oxyethylene	Methacrylate
F	30	14	Hydrocarbon	Methacrylate
G	33	12	Hydrocarbon	Methacrylate

Table 2.1 *Summary of the Structures of the Polymers Studied in this Work*

2.8. Polymer Characterisation.

The soluble portions of the macrocycle-containing polymers were characterised by proton and carbon NMR, and by GPC (gel permeation chromatography). Differential scanning calorimetry was used to obtain measurements of the T_g of the polymers, both in the pure state and when doped with varying quantities of lithium trifluoromethane sulfonate (lithium triflate, $LiSO_3CF_3$). More detailed T_g studies, and measurements of the conductivities of the doped polymers, were performed by our collaborators at the University of Leeds, and will be discussed fully in chapter 4.

The first analysis performed on the purified polymers was the measurement of their proton and carbon NMR spectra, using the 400 MHz Varian spectrometer. The proton spectra consisted of broad resonances, due to a combination of the slow tumbling of the large polymer molecules, and the range of environments encountered by each type of proton along the polymer chain. The most sharply resolved protons are those attached to carbons 6 and 13 of the 14-membered rings. These are not closely coupled to the backbone, and resonate at a frequency far from most of the other protons present, at a shift of 2 ppm, compared to 3.5-4.0 ppm for the other ring protons. These features are illustrated in figure 2.3(a) by the proton spectrum of polymer **(A)** in acetone.

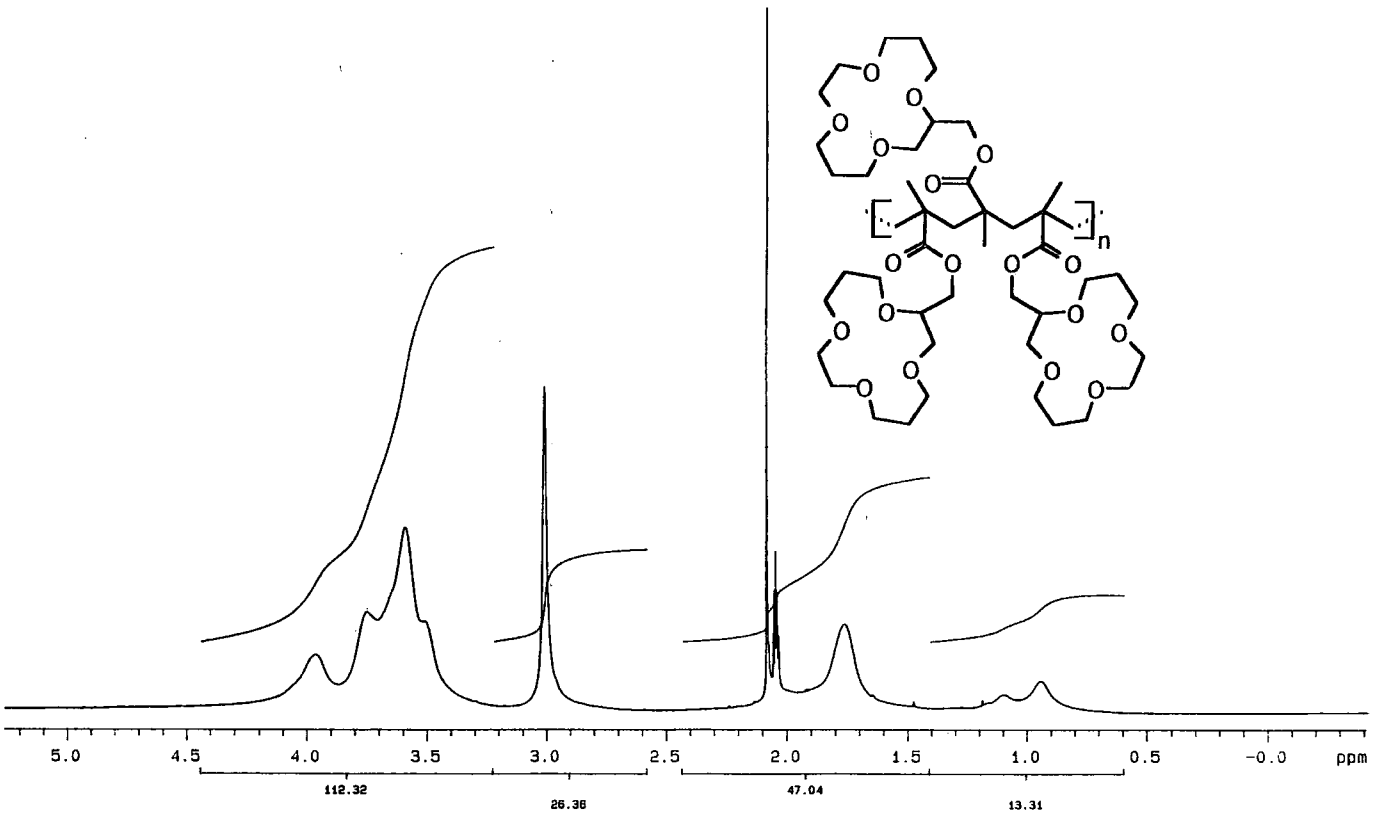

Figure 2.3(a) *Proton NMR Spectrum of Polymer (A) in $(CD_3)_2CO$*

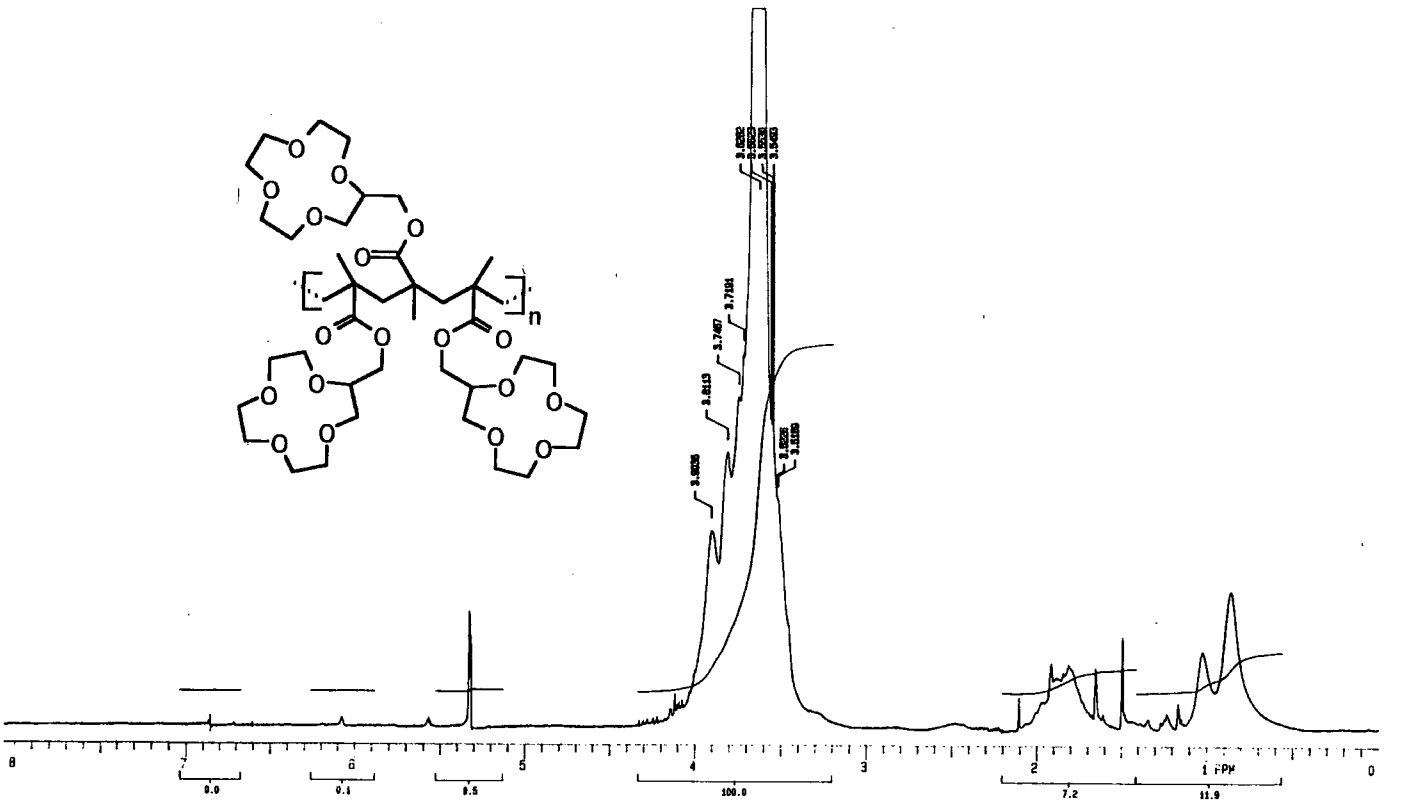

Figure 2.3(b) *Proton NMR Spectrum of Polymer (B) in CD_2Cl_2*

The most useful and unambiguous piece of information obtainable from the proton spectrum is the absence of resonances for the alkene region, which confirms that no residual monomer is present. Small amounts of monomer were sometimes detected at this stage, indicating that further purification was required. These are visible in the spectrum of a partially purified sample of polymer **(B)** in CD_2Cl_2, figure 2.3(b)

The carbon NMR spectra of the polymers are more informative than the proton spectra, due to the larger chemical shift range of carbon. Although the lines are slightly broadened compared to those observed in the spectra of the corresponding monomers, particularly for carbons in or close to the backbone, they remain easily distinguishable. Close examination of the resonances of the backbone carbons themselves shows them to be split due to the stereoirregularity of the polymer. Each polymerisation step forms a new chiral centre at the quaternary carbon. Adjacent pairs of chiral centres may have either opposite or identical chirality, which are symbolised as m (meso) or r (racemic) diads, respectively. The stereochemistry (tacticity) of the polymer can therefore be represented as a sequence of m and r diads along the chain.

A perfectly isotactic polymer would contain only the m configuration, i.e. alternating chiral configurations along the chain, while a perfectly syndiotactic polymer would have only r. The local environment of each chiral centre may be described as an rr, rm, or mm triad, depending on the relative chirality of the adjacent centres. In a completely random polymer, these configurations would be present in the ratio rr : mr : mm = 1 : 2 : 1. These different local environments are distinguishable by the NMR shifts of the chiral carbon and groups bonded to it, which appear as split lines. More distant influences are sometimes detectable, giving rise to more complicated splitting patterns corresponding to pentads of rrr, mrr, rmr, mrm, mmr, or mmm chiral centres.

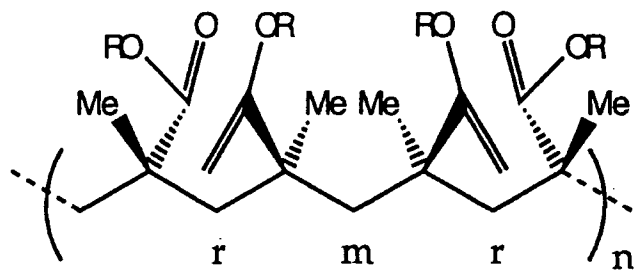

Figure 2.4 *Tacticity of a Section of a Methacrylate Polymer*

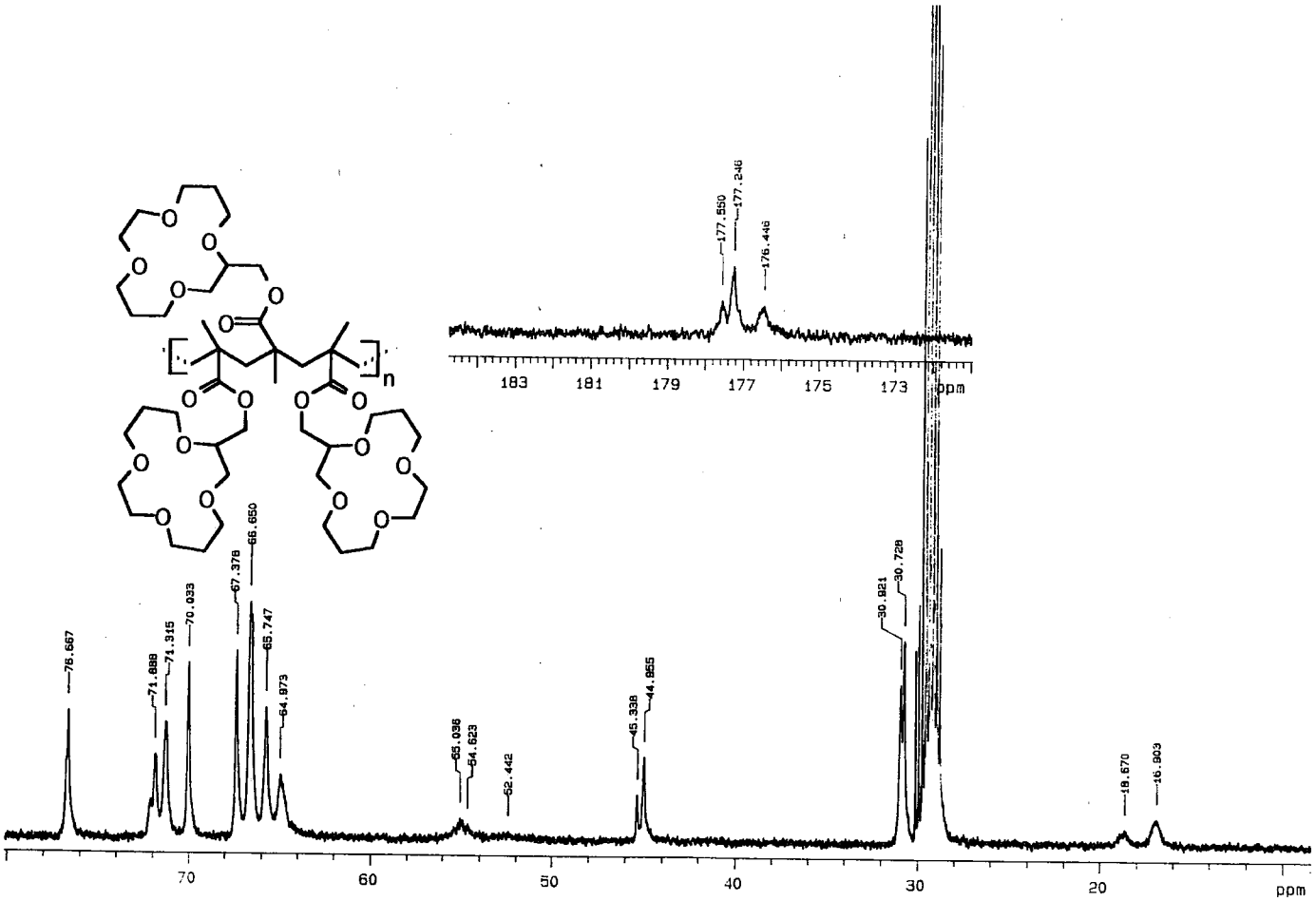

Figure 2.5(a) *Carbon NMR Spectrum of Polymer (A) in $(CD_3)_2CO$*

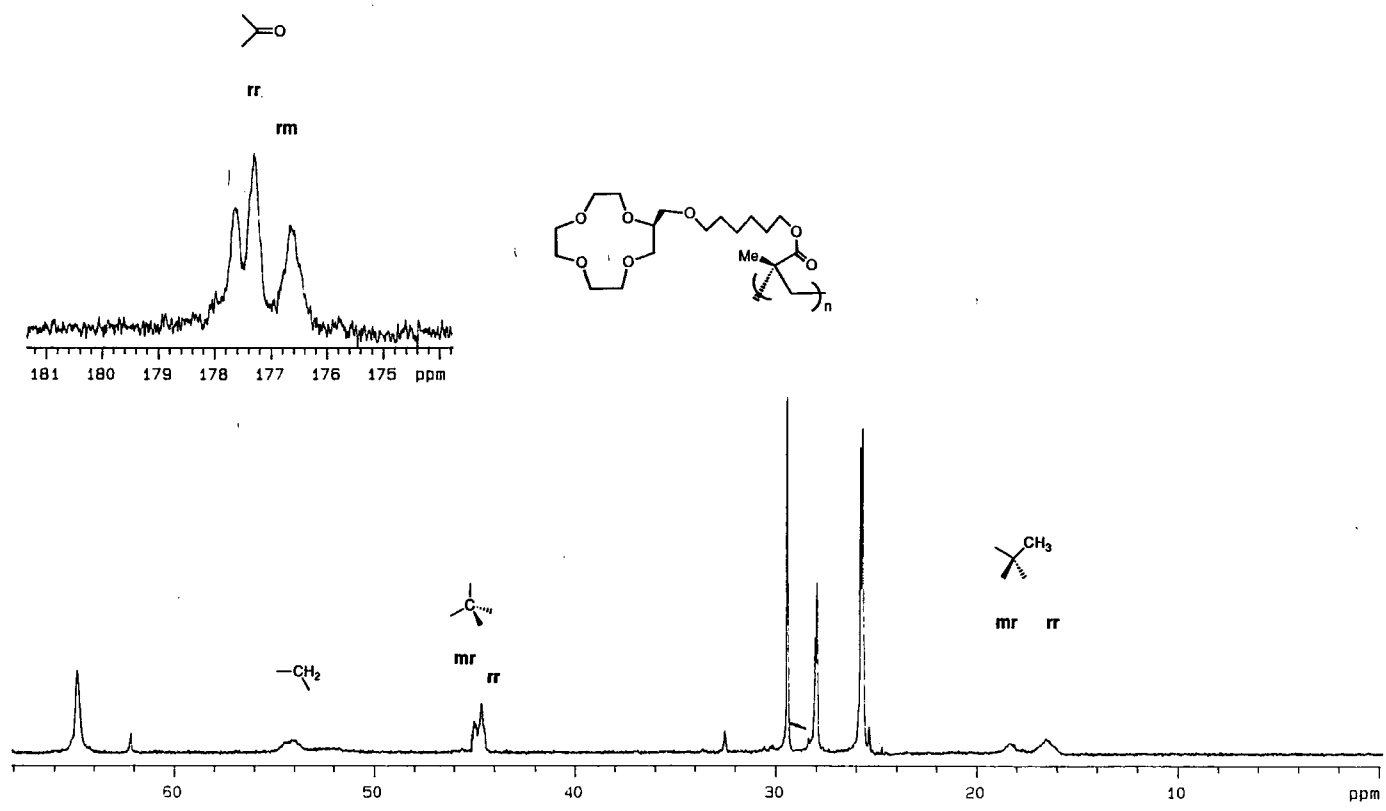

Figure 2.5(b) *Carbon NMR Spectrum of Polymer (G) in $CDCl_3$*

Methacrylate polymers formed by free radical polymerisation typically have a predominance of rr triads, but include a significant proportion of rm triads, so that only very short runs of syndiotactic polymer exist.[20] All the polymers prepared in this work follow this pattern, the nature of the substituent at the methacrylate ester position having very little effect on the polymerisation stereochemistry. This is illustrated in figure 2.5(a) and (b) by the carbon NMR spectra of polymers **(A)** and **(G)**. In both cases, the mr and rr triads can be distinguished for the quaternary carbon, methacrylate methyl and carbonyl groups. For the carbonyl group, some pentad structure is visible, with mrr and rrr pentads resolvable, although the other four are combined into a broad band, or are too rare to be detected. The aqueous polymerisation route appears to give a slightly higher proportion of rr (and rrr) conformations than polymerisation in butanone, as illustrated by the insets in figure 2.5.

A comparison of the spectra of polymer **(E)**, its monomer **(26)**, and a related extended macrocycle[21] is shown in figure 2.6. The carbons of the crown ether ring are scarcely effected by the polymerisation, and the flexible ethylene oxide spacer sufficiently decouples the motion of the rings from the backbone that the lines remain quite sharp. The single CHO resonance — the attachment point of the side-chain to the ring — is sharp and distinct at 78 ppm in the spectrum of all three compounds. This may be relevant to lithium ion transport in the solid polymer, as it indicates that the rings may move independently of the polymer backbone.

The molecular weight distributions of polymers produced by the aqueous and ethyl acetate/butanone routes are very different. Polymer **(A1)**, produced by the aqueous route, has a molecular weight M_n of nearly $2x10^5$, and a polydispersity index (M_w/M_n) of just over 4.0. This is probably due to the presence of some branched material, as discussed previously in sections 2.3.1 and 2.7.1. Polymer **(E)**, produced with the homogeneous polymerisation system using butanone produces a much smaller and less polydisperse material, having an M_n of just 7700 and a (M_w/M_n) of 1.37, a much more typical figure for a "clean" free radical polymerisation.

The DSC measurements show the expected reduction in T_g from the unextended side-chain materials **(A)** and **(B)** to the extended polymers. The ethylene-oxide extended acrylate polymer **(D)** shows the lowest T_g of all as the acrylate backbone is inherently more flexible than methacrylate.

Addition of lithium salts alters both the NMR spectra and DSC traces of all the polymers studied. These effects are discussed in Chapter 4.

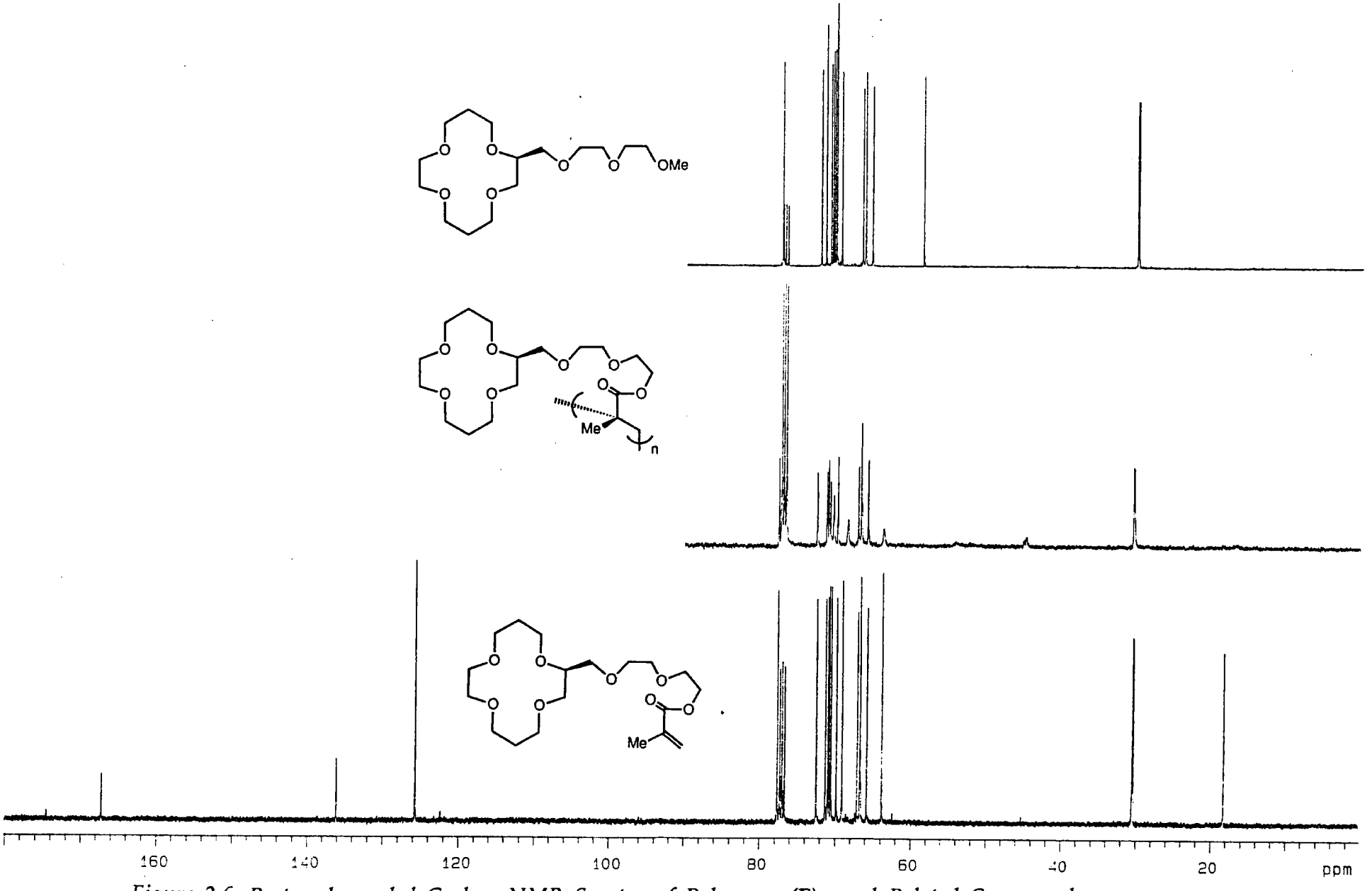

Figure 2.6 Proton-decoupled Carbon NMR Spectra of Polymer (E) and Related Compounds

2.9. References

1. Nicholson, P. E., Doctoral Thesis, University of Durham, 1989

2. Kataky, R., Nicholson, P. E. and Parker, D., *J. Chem. Soc., Perkin Trans. II*, 321 (1990).

3. Cox, B. G. and Schneider, H., *Coordination and Transport Properties of Macrocyclic Compounds in Solution*, Elsevier, Amsterdam, 1992.

4. Vogel, A. I., *Practical Organic Chemistry, 3rd Edition*, Longman, London, 1957, p 249.

5. Itoh, A., Myazaki, T. M., Okahara, M. and Yumagida, S., *Bull. Chem. Soc. Japan*, **55** 2005 (1982).

6. Babb, D. A., Bartsch, R. A., Czech, B. P. and Son, B., *J. Org. Chem.*, **40** 4805 (1984).

7. Vogel, A. I., *Practical Organic Chemistry, 3rd Edition*, Longman, London, 1957, p 825.

8. Jung, M. E. and Lyster, M. A., *J. Org. Chem.*, **42 (23)**, (1977).

9. Olah, G. A., Narang, S. C., Gupta, B. G. B. and Malhotra, R., *J. Org. Chem.*, **44** 1247 (1979)

10. Belaran, G., George, A., Narang, B. G., Olah, S. C. and Ripudaman, M., *J. Org. Chem.*, **44 (8)**, (1979).

11. Fieser and Fieser, *Reagents for Organic Synthesis*, Wiley, New York. 1967, p 66

12. McOmie, J. F., Watts, M. L. and West, D. E., *Tetrahedron*, **24** 2289 (1968).

13. Tachon, C., personal communication.

14. Bernady, K. F., Floyd, M. B., Poletto, J. F. and Weis, M. J., *J. Org. Chem.*, **44** 1438 (1979).

15. Bates, P. S., Doctoral. Thesis, University of Durham, 1993

16. Johnston, R. D., Marston, C. R., Krieger, P. E. and Goe, E. L., *Synthesis*, 393 (1988).

17. Fleming, I., *Frontier Orbitals and Organic Chemical Reactions,* John Wiley & Sons, Chichester, 1978.

18. Bannister, D. J., Davies, G. R., Ward, I. M. and McIntyre, J. E., *Polymer,* 25 1600 (1984).

19. Richards, R., personal communication.

20. Randall, J. C., *Polymer Sequence Determination,* Academic Press, London, 1977.

21. Denness, J. E., Parker, D. and Hubbard, H. S. V. A., *J. Chem. Soc., Perkin Trans. II,* 1445-53 (1994).

3. Experimental method

3.1. Introduction.

Throughout this work, temperatures are quoted in °C, and pressures in mbar. The alumina used in chromatography was Merck alumina, activity II-III, 70-230 mesh.

Proton and carbon-13 NMR spectra were recorded on a Varian VXR400, Varian Gemini 200, or a Bruker AC250 spectrometer. Proton and carbon chemical shifts are quoted in ppm to higher frequency of TMS. Coupling constants are given in Hz.

Infrared spectra were recorded on a Perkin-Elmer 577 spectrometer, as a thin film for liquid samples or a Nujol mull for solids, between NaCl plates. Mass spectra were recorded on a VG 7070E mass spectrometer, using CI or EI ionisation modes as stated. Gas chromatography was performed using a Hewlett Packard HP 5890 gas chromatograph fitted with an SE 30 capillary column, with a temperature programme of 1/2 min. at 40°C, ramp to 270°C at 10°C/min., and hold for 10 min

Glass transition temperatures were measured by differential scanning calorimetry with a calibrated Perkin-Elmer DSC-7, at a scan rate of 20 °C min^{-1}. Polymer molecular weights were determined by gel permeation chromatography of a tetrahydrofuran solution of the polymer. The column was calibrated against polystyrene standards, and used a Viscotec 200 differential viscometer detector.

The conductivity of lithium doped polymer samples was measured by our collaborators at Leeds university department of physics, using A. C. impedance spectroscopy on a Solartron 1260 frequency response analyser over the frequency range 0.1 Hz to 63 kHz. Polymer samples were dried in a vacuum oven and pressed between brass or stainless steel plates (blocking electrodes), with the sample thickness being fixed by a PTFE separator. The temperature and atmosphere of the polymer sample was controlled by passing a stream of heated dry nitrogen over it.

3.2. Synthesis of materials.

(±)-4-Benzyloxymethyl-2,2-dimethyl-1,3-dioxalane (0)[1]

Dry THF (200 ml), 4-hydroxymethyl-2,2-dimethyl-1,3-dioxalane (15 g), benzyl chloride (17 g), tetrabutyl ammonium hydrogensulphate (1.5 g), and sodium hydroxide (5.5 g), were added sequentially to a 500 ml flask and the mixture was heated to reflux under dry nitrogen for 24 hr. The mixture was filtered, and solvent removed under reduced pressure, leaving a yellow oil which was distilled to yield a colourless oil (22 g, 87%), bp 61-62°C, 0.01 mbar.

$\delta_H(CDCl_3)$: 1.26 (3 H, s, CH_3C); 3.38 (2 H, d, CH_2O);
3.57-4.17 (3 H, mult, CH_2O); 4.41 (2 H, s, CH_2Ph); 7.10 (5 H, br. s, arom).

1,8-Dicyano-3,6-dioxaoctane (1)[2]

To a solution of sodium hydroxide (0.8 g), in distilled water (40 ml), was added ethane-1,2 diol (25 g, 0.4 mol), followed by dropwise addition of acrylonitrile (57 ml, 0.87 mol), over 1 hr. The mixture was stirred for 24 hr. at room temperature and then transferred to a separating funnel. The lower, organic layer was separated and the upper layer extracted with dichloromethane (2 x 10 ml).The combined organic layers were dried (K_2CO_3), and solvent and excess acrylonitrile removed under reduced pressure, to yield a colourless oil (63.6 g, 95%). This was distilled under vacuum, and a colourless oil obtained (60.3 g, 89%), bp. 120-125°C, 0.02 mbar.

$\delta_H(CDCl_3)$: 2.55 (4 H, t, J=6 Hz, CH_2CN); 3.51 (4 H, s, CH_2O);
3.55 (4 H, t, J=6 Hz, CH_2O).

$\delta_C(CDCl_3)$: 17.9 (CH_2CN); 64.9, 69.5 (CH_2O);117.7 (CN)

υ_{max} (thin film): 2230 cm^{-1} (CN); 1110 cm^{-1} (C-O-C); 845 cm^{-1}

GC t_R: 20.7 min.

(±)-3-Benzyloxy-propan-1,2-diol (2)[3]

(±)-4-Benzyloxymethyl-2,2-dimethyl-1,3-dioxalane.(17 g, 76 mmol)) was heated in 10% acetic acid (45 ml) at 100°C for 2 hr, after which time the initial emulsion had cleared. Solvents were removed under reduced pressure, and

the residue purified by vacuum distillation, to yield a colourless oil (12.8 g, 92%), bp 115-120°C, 0.1 mbar

$\delta_H(CDCl_3)$: 3.55-3.75, (5 H, broad mult. CH_2O+CHO);
4.57 (2 H, s, CH_2Ph); 7.3 (5 H, br. s, arom.).

Diethyl-4,7-dioxadecan-1,10-dioate (3)[2]

Sulphuric acid (98%, 20 ml), distilled water (9 ml), and the dinitrile (1) (66 g, 0.39 mol), were added sequentially to ethanol (130 ml) and the mixture boiled under reflux for 24 hr.. Further sulphuric acid (10 ml) was then added, and the reaction allowed to continue for a further 40 hr.. The solvent was then removed under reduced pressure, and distilled water (100 ml) and dichloromethane (30 ml) added. After shaking and settling, the organic layer was removed and the aqueous layer extracted with dichloromethane (3 x 20 ml). The combined organic layers were then washed with dilute brine (2 x 20 ml), dried (K_2CO_3), filtered, and solvent removed under reduced pressure to yield an orange oil, which was distilled to give a colourless oil (73.4 g, 71%), bp 95-100°C, 0.015 mbar

$\delta_H(CDCl_3)$: 1.27 (6 H, t, J=7 Hz, CH_3); 2.60 (4 H, t, J=6.3 Hz, CH_2CO);
3.63 (4 H, s, CH_2O); 3.76 (4 H, t, J=6.3 Hz, CH_2O);
4.16 (4 H, q, J=7 Hz CH_2CH_3).

$\delta_C(CDCl_3)$: 13.9 (CH_3); 34.8 (CH_2C); 60.2 (CH_2CO_2);
66.3, 68.7 (CH_2O); 171.3 (CO_2).

υ_{max}(thin film): 1735 cm^{-1} (C=O); 1115 cm^{-1}, 1185 cm^{-1} (C-O-C).

GC t_R: 21.7 min.

1,10-Dihydroxy-4,7-dioxadecane (4)[2]

To a suspension of lithium aluminium hydride (11.3 g) in dry ether (100 ml) under an atmosphere of dry nitrogen at 0°C was added, dropwise, a solution of the diester (3) (40 g, 0.15 mol) in dry ether (100 ml), maintaining a gentle reflux. The mixture was stirred rapidly, and left at room temperature overnight. It was then cooled to 0°C, and distilled water (11 ml) added dropwise, followed by sodium hydroxide solution (15%, 22.5 ml), and then distilled water (11 ml), rapid stirring being maintained. The resulting suspension was filtered, and the solid washed with ether (6 x 50 ml). The ether

solutions were combined and solvent removed under reduced pressure to leave a viscous oil, which was distilled to give a colourless viscous oil (11.6 g, 53%),bp 110-115°C, 0.03 mbar

$\delta_H(CDCl_3)$: 1.82 (4 H, quint., J=6 Hz, CH_2C); 3.58 (4 H, s, CH_2O); 3.63 (4 H, t, J=6 Hz, CH_2O); 3.74 (4 H, t, J=6 Hz, CH_2OH)

$\delta_C(CDCl_3)$: 31.8 (CH_2C); 59.1 (CH_2OH); 68.3, 68.7 (CH_2O).

υ_{max}(thin film): 3500-3100 cm^{-1} (br, OH) 1105 cm^{-1}, 845 cm^{-1} (C-O-C).

1,10-Dichloro-4,7-dioxadecane (5)[2,4]

To a stirred solution of the diol (4) (10.6 g, 60 mmol), pyridine (11 g, 140 mmol) and dry benzene (50 ml) was added thionyl chloride (16.7 g, 140 mmol), dropwise. The mixture was heated to reflux under dry nitrogen for 24 hr., cooled to 0°C, and hydrochloric acid (3 M, 6 ml) slowly added. The organic layer was separated, and the reaction flask and aqueous layer washed with dichloromethane (3 x 10 ml). The combined organic fractions were then washed with distilled water (2 x 20 ml) dried (K_2CO_3), filtered, and solvent removed under reduced pressure. The residue was distilled in a Kugelrohr apparatus to obtain a very pale yellow oil (9.1 g, 71%), bp 75-85°C, 0.01-0.02 mbar

$\delta_H(CDCl_3)$: 1.95 (4 H, tt, J=6 and 6.1 Hz, CH_2C); 3.45-3.75 (12 H, mult CH_2O + CH_2Cl)

$\delta_C(CDCl_3)$: 32.4 (CH_2C); 41.6 (CH_2Cl); 67.3, 69.9 (CH_2O).

υ_{max}(thin film): 1120 cm^{-1} (C-O-C); 655 cm^{-1} (C-Cl).

GC t_R: 26.5 min.

2-Benzyloxymethyl-1,4,8,11-tetraoxacyclotetradecane (6)[2,4]

Method 1: Dichloride route.

To dry t-butanol (200 ml) under dry nitrogen was added lithium metal (0.4 g), and the mixture stirred overnight at 60°C to dissolve the lithium. To the resulting suspension of lithium t-butoxide was added, sequentially, the diol (2) (3.39 g, 18.6 mmol), anhydrous lithium bromide (1.62 g, 18.6 mmol), and the dichloride (5) (4 g, 18.6 mmol). The mixture was heated to reflux and

stirred for 12 days, the reaction being monitored by TLC. Solvent was then removed under reduced pressure, and distilled water (50 ml) added to the residue. this solution was brought to pH 7 with hydrochloric acid (6 M) and extracted with dichloromethane (5 x 40 ml). The combined extracts were washed with distilled water (2 x 20 ml), dried (K_2CO_3), filtered, and solvent removed to yield a dark orange oil, which was chromatographed on neutral alumina, eluting with hexane: ethyl acetate 5:1 to give a colourless oil (2.5 g, 42%).

Method 2: Ditosylate route.

Lithium metal (0.2 g) was added to t-butanol (200 ml) and the mixture stirred overnight at 60°C under dry nitrogen to dissolve the lithium. The diol (2) (3.56 g, 19.5 mmol) was then added, followed by the ditosylate (17) (9.5 g, 19.5 mmol) The suspension was stirred for 24 hr. at 60°C under dry nitrogen, and a further addition of lithium metal (0.14 g) was then made. The reaction was allowed to continue under the same conditions for 4 days and then checked by TLC Some ditosylate remained, so more lithium was added (0.1 g, bringing the total to 0.44 g, 63 mmol) and the reaction mixture heated to 80°C for 24 hr.. Solvent was then removed under reduced pressure, and distilled water (50 ml) added to the residue. The solution was brought to pH 7 with hydrochloric acid (6 M), and extracted with dichloromethane (2 x 50 ml, 2 x 25 ml). The combined extracts were washed with distilled water (10 ml) dried (K_2CO_3), filtered, and solvent removed to yield a yellow oil. This was purified by column chromatography as described above to obtain a colourless oil (4.1 g, 65%)

$\delta_H(CDCl_3)$: 1.74 (4 H, mult, CH_2C); 3.44-3.86 (17 H, mult. CH_2O + CHO); 4.55 (2 H, s, CH_2Ph); 7.21-7.35 (5 H, mult. arom.)

$\delta_C(CD_3OD)$: 31.3, 31.5 (CH_2C);
66.8, 67.6, 67.7, 68.2, 70.8, 71.1, 71.8, 73.3 (CH_2O); 74.3 (CH_2Ph);
79.1 (CHO); 128.7, 128.8, 129.4 (CH arom.); 139.6 (C arom.)

υ_{max}(thin film): 1650-1600 cm^{-1} (ring); 1117 cm^{-1} (C-O-C).

GC t_R: 31.0 min.

M/e found: 325=(M+1).

2-Benzyloxymethyl-1,4,7,10-tetraoxacyclododecane (7)[5]

Method 1: Dichloride route.

This is the same as the procedure for preparing (6), described above, using lithium metal (0.42 g, 60 mmol), t-butanol (200 ml), lithium bromide (1.74 g, 20 mmol), (2 (3.64 g, 20 mmol) and 1,8 dichloro-3,6 dioxadecane (3.74 g, 20 mmol). Purification by column chromatography on alumina, eluting with hexane/ethyl acetate 3:1, gave a colourless oil (2.6 g, 43%)

Method 2: Ditosylate route.

Lithium metal (0.2 g) was added to t-butanol (250 ml) and the mixture stirred overnight at 60°C under dry nitrogen to dissolve the lithium. The diol (2) (4 g, 22 mmol) was then added, followed by a solution of the ditosylate (15) (10.1 g, 22 mmol) in hot t-butanol (50 ml). The suspension was stirred for 24 hr. at 60°C under dry nitrogen, and a further addition of lithium metal (0.14 g) was then made. The reaction was allowed to continue under the same conditions for 4 days and then checked by TLC Some ditosylate remained, so more lithium was added (0.1 g, bringing the total to 0.44 g, 63 mmol) and the reaction mixture heated to 80°C for 24 hr.. Solvent was then removed under reduced pressure, and distilled water (50 ml) added to the residue. The solution was brought to pH 7 with hydrochloric acid (6 M), and extracted with ether (2 x 50 ml, 2 x 25 ml). The combined extracts were washed with distilled water (10 ml) dried (K_2CO_3), filtered, and solvent removed to yield a yellow oil. This was repeatedly extracted with boiling hexane (10 - 20 ml portions), and the hexane evaporated to leave a pale yellow oil (4.3 g, 66%)

$\delta_H(CDCl_3)$: 3.46-3.85 (17 H, mult. CH2O + CHO); 4.54 (2 H, s, CH_2Ph); 7.24-7.35 (5 H, mult. arom.)

$\delta_C(CD_3OD)$: 71.1, 71.2, 71.3, 71.5, 71.55, 71.6, 71.8, 72.6 (CH_2O); 74.3 ($PhCH_2O$); 79.8 (CHO); 128.7,128.8,129.4 (CH arom); 139.6 (C arom)

υ_{max}(thin film): ~1630 cm^{-1} (br, ring); 1132 cm-1, 1097 cm^{-1} (C-O-C).

GC t_R: 29.0 min.

M/e found: 297=(M+1).

2-Hydroxymethyl-1,4,8,11-tetraoxacyclotetradecane (8)[2,4]

The macrocycle (6) (2.2 g, 6.8 mmol), Pearlman's catalyst (220 mg), p-toluene sulfonic acid (10 mg) and ethanol (25 ml) were added sequentially to a Parr hydrogenation flask and shaken in an atmosphere of hydrogen (3 atm) at room temperature for 24 hr.. The catalyst was then filtered off, solvent removed under reduced pressure and the residue purified by column chromatography on neutral alumina, eluting with ethyl acetate (R_f 0.3), to give a colourless viscous oil (1.27 g, 80%).

$\delta_H(CDCl_3)$: 1.6-1.9 (4 H, mult. CH_2C); ~2.4 (1 H, br. s, OH);
3.6-3.9 (17 H, mult. CH_2O + CHO).

$\delta_C(CDCl_3)$: 30.3, 30.4 (CH_2C); 62.8 (CH_2OH);
66.1, 66.8, 66.9, 67.5, 69.5, 71.3, 72.5 (CH_2O); 78.7 (CHO);

υ_{max}(thin film): 3650-3100 cm^{-1} (br., OH); 1120 cm^{-1}, 1090 cm^{-1} (C-O-C).

GC t_R: 22.2 min.

2-Hydroxymethyl-1,4,7,10-tetraoxacyclododecane (9)[6]

The macrocycle (7) (1.2 g, 4.0 mmol), Pearlman's catalyst (120 mg), p-toluene sulfonic acid (5 mg) and water/methanol (10% water, 15 ml) were shaken under hydrogen (3 atm) for 48 hr. at room temperature. After filtration, and removal of solvent, the residue was chromatographed on neutral alumina, eluting with ethyl acetate/methanol (10:1) to yield a colourless, viscous oil (0.64 g, 77%).

$\delta_H(CDCl_3)$: ~2.55 (1 H, br. s, OH); 3.45-3.9 (17 H, mult. CH_2O + CHO).

$\delta_C(CDCl_3)$: 62.35 (CH_2OH);
69.89, 70.08, 70.42, 70.44, 70.5, 70.75, 71.35 (CH_2O); 79.75 (CHO);

υ_{max}(thin film): 3600-3150 cm^{-1} (br, OH); 1135 cm^{-1},1100 cm^{-1} (C-O-C).

M/e found: 207=(M+1).

2-Isobutyrylmethyl-1,4,8,11-tetraoxacyclotetradecane (10)

The 14-membered ring alcohol (8) (150 mg, 0.64 mmol), dry triethylamine (~200 mg, ~2 mmol), dry ether (5 ml) and isobutyryl chloride (~200 mg, ~1.9 mmol) were added sequentially to a 50 ml flask, under dry nitrogen. The mixture was stirred rapidly overnight at room temperature, and solvents and excess isobutyryl chloride were then removed under reduced pressure. The residue was dissolved in dichloromethane (10 ml) and water (10 ml), and the organic layer separated. The aqueous layer was extracted with dichloromethane (3 x 5 ml), and the combined organic layers washed with distilled water (2 x 5 ml), dried (K_2CO_3), filtered, and solvent removed to yield a yellowish oil (0.17 g, 87%). This was purified by column chromatography on alumina, eluting with hexane/ethyl acetate (10:1-5:1) [R_f 0.17 in 10:1]. A colourless oil (150 mg, 79%) was obtained.

$\delta_H(CDCl_3)$: 1.17 (6 H, d, CH_3C); 1.78 (4 H, mult. CH_2C);
2.57 (1 H, septet, $(CH_3)_2CH$); 3.45-4.09 (15 H, mult. CH2O + CHO);
4.11 (2 H, d, CH_2OCO).

GC t_R: 24.7 min.

M/e found: 305=(M+1).

Bis(2-methyl-1,4,8,11-tetraoxacyclotetradecane)-trans-3,6-endomethylene-1,2,3,6-tetrahydrophthalate (11)

This was prepared as described for the ester (10) using the macrocyclic alcohol (8) (60 mg, 0.26 mmol), trans-3,6 endomethylene-1,2,3,6 tetrahydrophthaloyl chloride (28 mg, 0.13 mmol) and triethylamine (~0.1 g, large excess) in dry ether (5 ml). The product was a colourless oil (49 mg, 62%). This was polymerised by J. P. Mitchell by ring opening metathesis using the catalyst di(t-butoxy)-2,2 dimethylpropenyl-2,6 di(isopropyl)aryl imido molybdenum.[7] Polymerisation was monitored by proton NMR, the distinctive resonances of the endomethylene proton at 11.2 and 11.7 ppm being absent from the polymer. However, the complexity of the material obtained precluded further analysis. The monomer itself possesses 4 different stereogenic centres and gives rise to 8 stereoisomers.

m/e found: 615=(M+1).

$\delta_H(C_6D_6)$: (polymer) 0.9-1.5 (4 H, mult., CH + CH_2 backbone);
1.7-1.85 (8 H, mult., CH_2 ring); 2.9 (4 H, mult., $CHCO_2$);
3.2-3.85 and 3.95-4.35 (34 H, CH_2O + CHO); 5.5-5.8 (2 H, mult., alkene).

2-(Methoxyethoxy)ethyl propenoate (12)[8]

2 methoxyethoxy ethanol (6.9 g), dry triethylamine (6.7 g) and dry ether (60 ml) were added sequentially to a 500 ml flask fitted with reflux condenser and dropping funnel. The mixture was stirred rapidly and cooled to 0°C, and a solution of acryloyl chloride (5.4 g) in dry ether (40 ml) added dropwise. The mixture was stirred overnight at room temperature under dry nitrogen, transferred to a separating funnel, and distilled water (100 ml) added. After shaking and settling the organic layer was removed, and the aqueous layer extracted with ether (3 x 50 ml). The combined ether layers were washed with hydrochloric acid (2 M, 2 x 10 ml), potassium carbonate solution (1 M, 2 x 10 ml), dried (K_2CO_3), filtered, and solvent removed under reduced pressure, leaving a pale yellow oil (5.6 g, 56%),

$\delta_H(CDCl_3)$: 3.39 (3 H, s, CH_3O);
3.57, 3.67, 3.75, (each 2 H, t, CH_2O); 4.33 (2 H, t, CH_2OCO);
5.84 (1 H, dd {J=1.5, 10.3 Hz}, $^{H}_{H}C=C^{H}$);
6.16 (1 H, dd {J=10.3, 17.5 Hz}, =CH);
6.43 (1 H, dd {J=1.5, 17.5 Hz}, $^{H}_{H}C=C^{H}$).

2-(Methoxyethoxy)ethyl methylpropenoate (13)[9]

This was prepared as described for the acrylate (12), using 2 methoxyethoxy ethanol (6.4 g), methacryloyl chloride (6.1 g) and triethylamine (6.5 g). The product was again a pale yellow oil (8.3 g, 83%).

2 -(2'-Methylpropenoatomethyl)-1,4,8,11-tetraoxacyclotetradecane (14)

The macrocyclic alcohol (8) (0.9 g, 3.85 mmol), triethylamine (~0.8 g, ~8 mmol), dry ether (~10 ml) and methacryloyl chloride (0.6 g, 5.8 mmol) were added sequentially to a 50 ml round bottomed flask under dry nitrogen. A few crystals of hydroquinone were added as stabiliser and the mixture stirred for 1 hr. The solvent was removed under reduced pressure and the residue purified by column chromatography on alumina, eluting with hexane followed by

hexane/ethyl acetate (5:1). A colourless oil (1.04 g, 89%) was obtained, and used directly for polymerisation.

δ_H(C6D6): 1.7-1.8 (4 H, mult. CH_2CH_2 ring); 1.85 (3 H, mult. CH_3);
3.3-3.8 and 3.85-4.15 (17 H, mult. CH2O + CHO);
5.30 (1 H, mult. alkene H cis to Me);
6.11 (1 H, mult. alkene H trans to Me)

δ_C(C6D6): 18.8 (CH_3); 31.35, 31.45 (CH_2CH_2 ring);
64.9, 66.55, 67.15, 67.2, 67.8, 70.6, 72.05, 72.82 (CH_2O);
77.55 (CHO) 125.7 (=CH_2); 137.2 (=C-); 167.1 (CO_2)

M/e (d.c.i.). Found: 303.1801; (M^++1) $C_{15}H_{27}O_6$ requires 303.18087

1,8-Bis(p-toluene sulfonato)-3,6-dioxaoctane (15)[10,11]

Triethylene glycol (20 g) and triethylamine (41 ml) were added to dry ether (100 ml) in a 500 ml flask under dry nitrogen. A solution of p-toluene sulfonyl chloride (53.4 g) in dry ether (200 ml) was added dropwise to this mixture, which was stirred rapidly. The apparatus was then heated until a gentle refluxing began, and left stirring under nitrogen overnight. The resulting suspension was filtered, the solid being washed with ether (3 x 20 ml), and solvent removed from the filtrate under reduced pressure. However, there was little residue after evaporation, so it was concluded that the product was only slightly soluble in ether. The solid previously filtered off was therefore shaken in dichloromethane (100 ml) and distilled water (100 ml), the layers separated, and the aqueous (upper) layer extracted with dichloromethane (3 x 20 ml). The combined organic fractions (ether and dichloromethane) were dried (K_2CO_3), filtered, and solvent removed, leaving a pale yellow oil. This was recrystallised from ethanol to obtain a white solid (51.2 g, 84%).

δ_H($CDCl_3$): 2.3 (6 H, s, CH_3 Ph); 3.4 (4 H, s, CH_2O); 3.6, (4 H, t, CH_2O);
4.0 (4 H, t, CH_2OTs); 7.5 (8 H, ABsys{J=8.25 Hz, Δu=0.48 ppm}, OTs).

m. p. 77-78°C

2 -(2'-Methylpropenoatomethyl)-1,4,7,10-tetraoxacyclododecane (16)

This was prepared as described for (14), using the 12-membered ring alcohol (9) (1.5 g, 7.3 mmol), methacryloyl chloride (1.1 g, 10.9 mmol) and

triethylamine (~1.5 g, ~14.6 mmol) in dry ether (~10 ml). After purification by column chromatography, a colourless oil was obtained (2.26 g, 80%), and used directly for polymerisation.

$\delta_H(CDCl_3)$: 1.87 (3 H, dd, J=1 Hz and 1.5 Hz, CH3);
3.45-3.9 and 4.0-4.1 (17 H, mult. CH_2O and CHO);.
5.51 (1 H, mult. alkene H cis to Me);
6.03 (1 H, mult. alkene H trans to Me)

$\delta_C(CDCl_3)$: 17.92 (CH_3);
63.8, 69.88, 69.93, 70.25, 70.31, 70.42, 70.60, 70.95 (CH2O);
77.07 (CHO); 125.4 (=CH_2); 135.7 (=C-); 166.6 (CO_2)

M/e (d.c.i.). Found: 275.1526; (M^++1) $C_{13}H_{23}O_6$ requires 275.1528

1,10-Bis(p-toluene sulfonato)-4,7-dioxadecane (17)

The triethylamine route described above for the ditosylate (15) was found to give poor yields for this compound. An alternative route using pyridine as the solvent was therefore adopted. The 1,10 diol (4) (20.8 g, 0.12 mol) and pyridine (100 ml), were placed in a conical flask fitted with a dropping funnel and cooled in a dry ice/acetone bath. p-Toluene sulfonyl chloride (69.0 g, 0.36 mol) was dissolved in pyridine (150 ml) and the solution poured into the dropping funnel and added slowly to the conical flask over a period of 20 min. The reaction flask was then stoppered and placed in a freezer (~-20°C) for 72 hr. After this time the reaction mixture had become yellow-orange and some yellow crystals had precipitated out. This mixture was poured onto 300-400 g of crushed ice, stirred for 30 min and filtered. The solid was washed with ice cold water and recrystallised from ethanol to obtain the product, a white solid (46.7 g, 82%).

$\delta_H(CDCl_3)$: 1.90 (4 H, quint, CH_2C); 2.45 (6 H, s, CH_3C);
3.46 (8 H, mult., CH_2O); 4.10 (4 H, t, CH_2O); 7.33 - 7.77 (4 H, dd, Ar).

$\delta_C(CDCl_3)$: 21.47 (CH_2C); 29.10 (CH_3Ph); 66.42, 66.59, 70.0 (CH_2O);
127.73, 129.73, 132.90, 144.64 (arom C).

υ_{max}(nujol):.1600 cm^{-1} (C=C, arom); 1380 cm^{-1}, 1170 cm^{-1} (S=O).

M/e (c.i.) 504 (M^+ + 18, 100%), 213 (12%).

Elemental Analysis. Found: C=54.0%; H=6.20%.
$C_{22}H_{30}S_2O_8$ requires C=54.3%; H=6.21%.

6-Hydroxy-1-benzyl-1,4-dioxahexane (18)

Dry THF (300 ml), diethylene glycol (57 ml, 0.6 mol) benzyl chloride (23 ml, 0.2 mol), tetrabutyl ammonium hydrogensulphate (0.6 g), and sodium hydroxide (10 g, 0.25 mol), were added sequentially to a 500 ml flask and the mixture was heated to reflux under dry nitrogen for 24 hr. The mixture was filtered, and solvent removed under reduced pressure, leaving a yellow oil which was distilled to yield a colourless oil (22.3 g, 0.11 mol, 57%), bp 91-93°C, 0.005 mbar.

$\delta_H(CDCl_3)$: 2.91 (1 H, br. s, OH); 3.56 - 3.72 (8 H, mult, CH_2O); 4.56 (2 H, s, OCH_2Ph); 7.33 (5 H, mult, Ph).

$\delta_C(CDCl_3)$: 62.2 (CH_2OH); 69.9, 70.9, 73.0, 73.8 (CH_2O); 128.2, 128.3, 128.9 (CH arom.); 138.5 (C arom.)

M/e (e.i.): 196 (M^+, 3%), 107 (19%),.42 (19%), 91 (100%)

6-(p-Toluenesulfonato)-1-benzyl-1,4-dioxahexane (18a)

Pyridine (50 ml) and the alcohol (18) (15 g, 76.5 mmol) were placed in a 500 ml flask cooled in a dry ice/acetone bath. p-Toluene sulfonyl chloride (16 g, 84 mmol) was then dissolved in pyridine (150 ml) and added to the reaction flask over a period of about 20 min. from a dropping funnel, the reaction temperature being kept below -70°C. The reaction flask was then stoppered and shaken, and placed in a freezer at ~-20°C for 72 hr. After this time the solution had become a pale yellow/pink in colour. This was poured over ~300 g of crushed ice, and an oily lower layer formed and was separated off. The upper, aqueous layer was extracted with dichloromethane (3 x 100 ml) and the combined organic layers acidified with dilute hydrochloric acid and the resulting aqueous layer separated off. The organic layer was dried (K_2CO_3), filtered, and solvent removed under reduced pressure to leave the product, a pale yellow oil (24 g, 90%). This was found to be almost pure by TLC and was used without further purification.

$\delta_H(CDCl_3)$: 2,47 (3 H, s, CH_3-C_6H_4); 3.59-3.83 (6 H, mult. CH_2O);
4.22 (2 H, t, 6.7 Hz, CH_2OTs); 4.58 (2 H, s, CH_2OPh);
7.3-7.42 (5 H, mult. CH phenyl); 7.82 and 7.86 (4 H, AB sys. CH tosyl).

$\delta_C(CDCl_3)$: 21.47 (CH_3-C_6H_4); 68.52, 69.17, 69.21, 70.63, 73.10 (CH_2O);
127.49 (para CH phenyl.); 127.56 (meta CH phenyl.);
128.24 (ortho CH phenyl.); 137.99 (C arom.).

υ_{max}(nujol):.1120 cm^{-1}, 1083 cm^{-1}, (C-O-C);
1360 cm^{-1}, 1185 cm^{-1}, 1178 cm^{-1}, (S=O).

M/e (e.i.) Found: 350.2135.(M^+), $C_{18}H_{22}O_5S$ requires 350.2139

6-Iodo-1-benzyl-1,4-dioxahexane (19)

Potassium iodide (17.1 g 103 mmol) was dissolved in DMF (100 ml) and added to the p-toluene sulfonate (18) (24 g, 68 mmol), and the solution left overnight at room temperature. A white solid, presumed to be potassium p-toluene sulfonate was found to have precipitated out, and on addition of dichloromethane to the reaction mixture further precipitate formed. This was filtered off and washed with more dichloromethane, and the combined filtrate and washings concentrated under reduced pressure to give a brown oil. This was stored in a freezer, and portions purified as needed by column chromatography on alumina, eluting first with hexane, then with hexane/ethyl acetate mixtures up to 5% ethyl acetate. The product, a colourless oil, became yellow and then brown on exposure to air and light at room temperature for a period of a few hours, and was always stored in a freezer and used within a day of purification

$\delta_H(CDCl_3)$: 3.27 (2 H, t, J=7.14 Hz, CH_2I); 3.6-3.82 (6 H, mult. CH_2O);
4.59 (2 H, s, CH_2OPh); 7.25-7.39 (5 H, mult. CH arom.).

$\delta_C(CDCl_3)$: 2.92 (CH_2I); 69.23, 70.09, 71.31, 73.09 (CH_2O);
127.45 (para CH arom.); 127.54 (meta CH arom.);
128.20 (ortho CH arom.); 137.96 (C arom.).

M/e (e.i.) Found: 306.0115 (M^+), $C_{11}H_{15}O_2I$ requires 306.0117

2-(8'-Benzyl-2',5',8'-trioxaoctyl)-1,4,7,10-tetraoxacyclododecane (20)

The 12-membered ring alcohol (9) (0.41 g, 2 mmol) and thallous ethoxide (0.5 g, 2 mmol) were added to 5 ml of dry toluene in a 50 ml round

bottomed flask, under an atmosphere of dry nitrogen. The toluene was then removed under vacuum and 15 ml of dry acetonitrile added, followed by the iodide (19) (0.67 g, 2.2 mmol). The mixture was heated to reflux, and after 1 hr. a yellow precipitate had formed. The reaction was left under reflux overnight, after which time the precipitate had become much heavier, and TLC analysis showed the reaction to be complete. The precipitate, presumed to be thallium iodide, and other thallium compounds were removed by filtering the reaction mixture through 5 cm depth of alumina, the organic components being washed through with ethyl acetate until no further product was detectable by TLC analysis of the washings. The crude product was purified by column chromatography on alumina, eluting with 10%-50% ethyl acetate in hexane. The product was a colourless oil (0.56 g, 73%).

$\delta_H(CDCl_3)$: 3.45-3.55 and 3.64-3.85 (25 H, mult. CH_2O + CHO);
4.59 (2 H, s, CH_2OPh); 7.3-7.4 (5 H, mult. CH arom.).

$\delta_C(CDCl_3)$: 69.34, 6.936, 70.01, 70.25, 70.51, 70.56, 70.57, 70.59, 70.79, 70.84, 71.27, 71.59, 73.13 (CH_2O); 78.45 (CHO); 127.47 (para CH arom.); 127.60 (meta CH arom.); 128.24 (ortho CH arom.); 138.13 (C arom.).

M/e (d.c.i.). Found: 385.2224 (M^++1), $C_{20}H_{33}O_7$ requires 385.2228

2-(7'-Hydroxy-2',5'-dioxaheptyl)-1,4,7,10-tetraoxacyclododecane (21)

The extended macrocycle (20) (500 mg, 2.6 mmol) was debenzylated as described for the original unextended macrocycles (8) and (9) using p-toluene sulfonic acid (10 mg), Pearlman's catalyst (100 mg), and 10% water in methanol (20 ml). The product was purified by column chromatography on alumina, eluting with 0% – 10% methanol in ethyl acetate, to give a colourless oil (330 mg, 86%).

$\delta_H(CDCl_3)$: 3.16 (1 H, br. s., OH) 3.3-3.7 (25 H, mult. CH_2O + CHO).

$\delta_C(CDCl_3)$: 61.9 (CH_2OH);
70.41, 70.59, 70.61, 70.88, 70.90, 71.0, 71.21, 71.28, 71.70, 71.89, 72.9 (CH_2O); 78.8 (CHO).

M/e (c.i.). Found: 295.1742 (M^++1), $C_{13}H_{27}O_7$ requires 295.1758

2-(7'-(2''-Methyl)-propenoato-2',5'-dioxaheptyl)-1,4,7,10 tetraoxacyclododecane (22)

This was prepared as described for the corresponding unextended compound (16), using the alcohol (21) (750 mg, 2.55 mmol), methacryloyl chloride (400 mg, 3.83 mmol) and triethylamine (0.6 ml, ~4.3 mmol) in dry ether (~10 ml).Column chromatography of the crude product (alumina, eluting with 20%-100% ethyl acetate in hexane) gave a colourless oil (720 mg, 78%).

$\delta_H(CDCl_3)$: 1.89 (3 H, d., J = 1, CH_3); 3.40-3.82 (23 H, mult. CH_2O + CHO); 4.24 (2 H, t., CH_2CO_2); 5.52 (1 H, dq, $^{H}_{H}C=C^{Me}$); 6.08 (1 H, d, J = 1, $_{H}{}^{H}C=C^{Me}$).

$\delta_C(CDCl_3)$: 18.21 (CH_3); 63.01 (CH_2CO_2); 69.04, 69.81, 70.02, 70.25, 70.30, 70.4, 70.45, 70.50, 70.81, 71.23, 71.31 (CH_2O); 78.2 (CHO); 125.6 (CH_2); 136.0 (C alkene); 167.2 (CO_2).

M/e (c.i.): 380 (M^++18, 79%), 363 (M^++1, 6.5%), 78 (100%), 61 (58%); Found: 363.2026 (M^++1), $C_{17}H_{31}O_8$ requires 363.2020

2 (7-Propenoato-2,5-dioxaheptyl)-1,4,7,10 tetraoxacyclododecane (23)

This was prepared as described for the methacrylate (22), above using the alcohol (21) (1.5 g, 5.1 mmol), acryloyl chloride (700 mg, 7.73 mmol) and triethylamine (1.2 ml, ~8.6 mmol) in dry ether (~15 ml).Column chromatography of the crude product (alumina, eluting with 20%-100% ethyl acetate in hexane) gave a colourless oil (1.46 g, 82%).

$\delta_H(CDCl_3)$: 3.37-3.79 (23 H, mult. CH_2O + CHO); 4.25 (2 H, t, CH_2OCO); 5.78 (1 H, dd {J=1.5, 10.3 Hz}, $^{H}_{H}C=C^{H}$); 6.10 (1 H, dd {J=10.3, 17.5 Hz}, =CH); 6.37 (1 H, dd {J=1.5, 17.5 Hz}, $^{H}_{H}C=C^{H}$).

$\delta_C(CDCl_3)$: 63.49 (CH_2CO_2); 67.91, 68.94, 70.01, 70.18, 70.4, 70.5, 70.5, 70.72, 70.76, 71.24, 71.49 (CH_2O); 78.39 (CHO); 128.1 (=CH_2); 130.71 (=CH); 167.52 (CO_2).

M/e (c.i.): 366 (M^++18, 46%), 349 (M^++1, 12.5%), 312 (100%); Found: 349.1860 (M^++1), $C_{16}H_{29}O_8$ requires 349.1864

2-(8'-Benzyl-2',5',8'-trioxaoctyl)-1,4,8,11-tetraoxacyclotetradecane (24)

This was prepared according to the same procedure used for the equivalent 12-membered ring compound (20). The 14-membered ring alcohol (8) (1 g 4.27 mmol) was reacted with thallous ethoxide (1.07 g, 4.27 mmol), followed by the iodide (19) (1.44 g, 4.7 mmol). After reaction, and removal of thallium compounds, an orange/yellow oil (1.85 g) was recovered. This was purified by chromatography on alumina, eluting with 15%-30% ethyl acetate in hexane, to give a colourless oil (1.1 g, 62%), R_f 0.35 in 3:1 ethyl acetate: hexane on alumina.

$\delta_H(CDCl_3)$: 1.7-1.85 (4 H, mult. CH_2C);
3.44-3.95 (25 H, mult. CH_2O + CHO);
4.58 (2 H, s, CH_2OPh); 7.25-7.4 (5 H, mult. CH arom.).

$\delta_C(CDCl_3)$: 30.22, 30.33 (CH_2C); 65.63, 66.53 x 2, 66.90, 69.25, 69.69, 70.48, 70.48, 70.66, 70.82, 71.11, 72.35, 73.01 (CH_2O); 77.54 (CHO);
127.35 (para CH arom.); 127.49 (meta CH arom.);
128.13 (ortho CH arom.); 138.06 (C arom.).

M/e (d.c.i.): 430.2 (M^++18), 413 (M^++1);
Found: 413.2542 (M^++1), $C_{22}H_{37}O_7$ requires 413.25407

2-(7'-Hydroxy-2',5'-dioxaheptyl)-1,4,8,11-tetraoxacyclotetradecane (25)

Compound (24) (1.1 g, 2.7 mmol)was debenzylated under the usual conditions, using Pearlman's catalyst (200 mg) and p-toluene sulfonic acid (20 mg) in 10% water in methanol (30 ml). After filtration and evaporation of solvent the residue was purified by chromatography on alumina, eluting with ethyl acetate followed by 1% methanol in ethyl acetate. The product was a colourless oil (760 mg, 88%).

$\delta_H(CDCl_3)$: 1.75-1.81 (4 H, mult. CH_2C);
3.47-3.79 (26 H, mult. CH_2O + CHO + OH).

$\delta_C(CDCl_3)$: 30.14, 30.22 (CH_2C); 61.40, 65.67, 66.56, 66.56, 67.05, 69.62, 70.10, 70.61, 70.73, 71.07, 72.13, 72.35 (CH_2O); 77.50 (CHO).

M/e (d.c.i.): 340.2 (M^++18), 327 (M^++4), 323 (M^++1);
Found: 323.2074 (M^++1), $C_{15}H_{31}O_7$ requires 323.2070

2-(7'-(2"-Methyl)-propenoato-2',5'-dioxaheptyl)-1,4,8,11-tetraoxacyclotetradecane (26)

This was prepared as described for the equivalent unextended compound (14) using the alcohol (25) (760 mg, 2.36 mmol) methacryloyl chloride (370 mg 3.54 mmol) and triethylamine (0.6 ml, ~4.3 mmol), in dry ether (10 ml). After purification of the crude product by chromatography (alumina, 0%-40% ethyl acetate in hexane) a colourless oil was obtained.(780 mg, 85%)

$\delta_H(CDCl_3)$: 1.75 (4 H, mult. CH_2C);
1.90 (3 H, dd., J = 1 Hz and 1.5 Hz, CH_3);
3.3-4 and 4.1-4.2 (25 H, mult. CH_2O + CHO);
5.58 (1 H, mult., HHC=CMe); 6.13 (1 H, mult., HHC=CMe).

$\delta_C(CDCl_3)$: 18.2 (CH_3); 30 3, 30.4 (CH_2C);
64.0, 65.8, 66.6, 66.7, 67.0, 69.1, 69.8, 70.5, 70.8, 71.0, 71.3, 72.4 (CH_2O);
77.6 (CHO); 125.7 ($=CH_2$); 136.0 (=C); 167.2 (CO_2)

M/e (c. i.) 409 (M^++19, 22%), 408 (M^++18, 100%),
391 (M^++1, 30%), 113 (9%)

2-(7'-Bromo-1'-oxaheptyl)-tetrahydropyran (27)

Tetrahydropyran (THP) (5 g, 60 mmol)), dry ether (20 ml), 6 bromo hexanol (5 g, 27.6 mmol) and p-toluene sulfonic acid (20 mg) were added sequentially to a 50 ml round bottomed flask. The mixture became warm immediately on addition of the last reagent, and after 1/2 hr. TLC analysis showed no alcohol remaining. The reaction mixture was neutralised with sodium bicarbonate solution, and the aqueous layer separated. After drying ($MgSO_4$) and filtration, the solvent and excess THP were removed under reduced pressure. The recovered product was used without further purification. (Yield: 6.5 g, 89%).

$\delta_H(CDCl_3)$: 1.1-1.8 (14 H, mult. CH_2C); 3.15-3.35 (2 H, mult. CH_2O);
3.25 (2 H, t, 13.6 Hz, CH_2Br);
3.5-3.9 (2 H, mult. CH_2O); 4.42 (1 H, t, OCHO).

$\delta_C(CDCl_3)$: 19.5, 25.28, 25.33, 27.8, 29.4, 30.55, 32.55 (CH_2CH_2);
33.63 (CH_2Br); 62.1, 67.2 (CH_2O); 98.64 (OCHO)

M/e (c.i.): 284.1, 282.1 (M^++18), 267, 265 (M^++1);
Found (e. i.): 264.0753, $C_{11}H_{21}BrO_2$ (^{79}Br) requires 264.07549

2-(9'-(2''-Tetrahydropyranyl)-2',9'-dioxanonyl)-1,4,8,11-tetraoxacyclotetradecane (28)

The 14-membered ring alcohol (8) (0.85 g, 3.63 mmol), dry toluene (10 ml) and thallous ethoxide (0.91 g, 3.63 mmol) were added to a 50 ml round bottomed flask under dry nitrogen, and solvent removed under vacuum. Dry acetonitrile (20 ml) and the bromide (27) (1.4 g, 5.4 mmol) were then added, and the mixture heated to reflux overnight. A white precipitate formed, presumed to be thallium bromide, and this was removed as described for the thallium iodide produced in the synthesis of compound (20). The crude product was recovered by removal of solvents under reduced pressure, and the residue purified by column chromatography on alumina, eluting with 0%-50% ethyl acetate in hexane, to give a colourless oil (0.92 g, 60%).

$\delta_H(CDCl_3)$: 1.2-1.75 (18 H, mult. CH_2C);
3.2-4.05 (23 H, mult. CH_2O + CHO); 4.44 (1 H, t, OCHO).

$\delta_C(CDCl_3)$: 19.36, 25.21, 25.66, 25.79, 29.25, 29.40, 30.14 (CH_2C);
30.25, 30.45 (CH_2C 14-ring); 61.89, 65.53, 66.42, 66.42, 66.78, 67.15, 69.62, 70.45, 70.75, 71.15, 72.42 (CH_2O); 77.48 (CHO); 98.43 (OCHO).

M/e (c. i.): 436.3 (M^++18), 419.3 (M^++1);
Found: 419.3010 (M^++1), $C_{22}H_{43}O_7$ requires 419.30102

2-(8'-Hydroxy-2'-oxaoctyl)-1,4,8,11-tetraoxacyclotetradecane (29)

The tetrahydropyranyl compound (28) (0.92 g), methanol (9 ml) and 1 M hydrochloric acid (1 ml) were stirred in a round bottomed flask at room temperature overnight. The solvents, acid and tetrahydropyran were removed under reduced pressure to leave the alcohol (29) (0.74 g, 100%), which was used without further purification.

M/e (d. c. i.): 352.2 (M^++18), 335.2 (M^++1);
Found: 335.2433 (M^++1), $C_{17}H_{35}O_6$ requires 335.2435

2-(8'-(2''-Methyl)-propenoato-2'-oxaoctyl)-1,4,8,11-tetraoxacyclotetradecane (30)

This was prepared as described for compound (14), using the alcohol (29) (0.74 g, 2.2 mmol), methacryloyl chloride (0.35 g, 3.3 mmol) and triethylamine (0.36 g, 3.6 mmol) in dry ether (4 ml).The product was purified by

chromatography on alumina, eluting with 0%-10% ethyl acetate in hexane, to give a colourless oil (0.63 g, 71%), Rf. 0.75 in 3:1 hexane: ethyl acetate.

$\delta_H(C_6D_6)$: 1.1-1.25 and 1.35-1.6 (8 H, mult. CH_2C of chain);
1.7-1.85 (4 H mult. CH_2C of ring); 1.93 (3 H, dd 1 Hz and 1.5 Hz, CH_3);
3.2-4.2 (21 H, mult. CH_2O + CHO); 5.30 (1 H, mult., HHC=CMe);
6.21 (1 H, mult., HHC=CMe).

$\delta_C(C_6D_6)$: 18.92 (CH_3);.26.52, 26.60, 29.38, 30.43 (CH_2C of chain);
31.51, 31.69 (CH_2C of ring); 65.13 (CH_2CO_2); 66.58, 67.34, 67.36, 67.80, 70.57, 71.90, 71.91, 72.35, 73.86 (CH_2O); 78.78 (CHO);
125.23 (CH_2=); 137.56 (C=); 167.39 (CO_2).

M/e (d. c. i.): 420.3 (M^++18), 403.3 (M^++1);
Found: 403.26910 (M^++1), $C_{21}H_{39}O_7$ requires 403.26972.

2-(9'-(2'-Tetrahydropyranyl)-2',9'-dioxanonyl)-1,4,7,10-tetraoxacyclododecane (31)

This was prepared in the same way as the equivalent 14-membered ring compound (28), using the 12-membered ring alcohol (9) (1.5 g, 7,3 mmol), thallous ethoxide (2.0 g, 8 mmol), and the bromide (27) (2.3 g 8.75 mmol).After removal of thallium salts and purification by column chromatography a colourless oil was obtained (1.86 g 65%) R_f 0.6 in ethyl acetate.

$\delta_H(CDCl_3)$: 1.1-1.2 and 1.25-1.5 (14 H, mult. CH_2C);
3.1-3.3 and 3.4-3.65 (23 H, mult. CH_2O + CHO); 4.34 (1 H, t, OCHO).

$\delta_C(CDCl_3)$: 19.13, 25.00, 25.44, 25.57, 29.05, 29.18, 30.24 (CH_2C); 61.66, 66.93, 69.67, 69.83, 70.13, 70.14, 70.15, 70.32, 70.40, 71.00, 71.26 (CH_2O);
78.07 (CHO); 98.21 (OCHO).

M/e (d. c. i.): 408.3 (M^++18), 391.3 (M^++1);
Found: 391.2624 (M^++1), $C_{20}H_{39}O_7$ requires 391.26254.

2-(8'-Hydroxy-2'-oxaoctyl)-1,4,7,10-tetraoxacyclododecane (32)

This was prepared as described for the equivalent 14-membered ring compound (29) using (31) (1.86 g, 4.77 mmol).After removal of solvents and by-products under reduced pressure, the product alcohol, a colourless oil, (1.46 g, 100%), was recovered and used without further purification.

M/e (d. c. i.): 324 (M^++18), 308 (M^++2), 307 (M^++1);
Found: 307.2124 (M^++1), $C_{15}H_{31}O_6$ requires 307.212

2-(8'-(2''-Methyl)-propenoato-2'-oxaoctyl)-1,4,7,10-tetraoxacyclododecane (33)

This was prepared as described for compound (14), using the alcohol (32) (0.78 g, 2.5 mmol), methacryloyl chloride (0.40 g, 3.8 mmol) and triethylamine (0.41 g, 4.1 mmol) in dry ether (5 ml).The product was purified by chromatography on alumina, eluting with 0%-20% ethyl acetate in hexane, to give a colourless oil (0.73 g, 75%).

$\delta_H(CDCl_3)$: 1.37, 1.52-1.72 (8 H, mult. CH_2C);
1.93 (3 H, dd J = 1 Hz and 1.5 Hz, CH_3);
3.39-3.43, 3.66-3.82 and 4.10-4.16 (21 H, mult. CH_2O + CHO);
5.54 (1 H, mult., HHC=CMe); 6.09 (1 H, mult., HHC=CMe).

$\delta_C(CDCl_3)$: 18.32 (CH_3);.25.74, 25.81, 28.55, 29.48 (CH_2C); 64.66 (CH_2CO_2);
70.23, 70.36, 70.66, 70.67, 70.68, 70.85, 70.93, 71.46, 71.78 (CH_2O);
78.62 (CHO); 125.17 (CH_2=); 136.47 (C=); 167.50 (CO_2).

M/e (d. c. i.): 392.2 (M^++18), 375 (M^++1).

Poly (2-(Methoxyethoxy)ethyl propenoate)

To the model acrylate (12) (1.0 g) in a 100 ml flask was added degased distilled water (40 ml), ferrous sulphate solution (5 mmolar, 5 ml) and potassium bisulphate solution (5 mmolar, 5 ml), sequentially, while a stream of nitrogen was bubbled through the mixture. The flask was then attached to a nitrogen line and immersed in an oil bath pre-heated to 80°C. After 24 hr of rapid stirring at this temperature no monomer was detectable by TLC, and the mixture was cooled to room temperature and hydroquinone (~10-20 ml) added. Precipitation of the polymer was induced by adding sodium sulphate (0.5 g) and warming, and the salt solution decanted off. An attempt was made to purify the polymer by dissolving it in acetone but although the polymer swelled rapidly on addition of the solvent, very little dissolved even after 12 hr of rapid stirring in 30 ml of acetone. (~20 mg was recovered after filtering the suspension and evaporating solvent from the filtrate). This was repeated using dichloromethane, DMF, and methanol.

Poly (2-(Methoxyethoxy)ethyl methylpropenoate)

This was prepared as described for (12)-polymer using the model methacrylate (13) (1.1 g) except that the reaction was carried out at room temperature, and was found to be complete after 6 hr. A much larger fraction of the polymer was found to dissolve in acetone, and after filtration the solution was reduced in volume (to ~10 ml) under reduced pressure and hexane added to induce precipitation of the polymer. Further solvent was then removed, and more hexane added. The liquid was then decanted off, and the polymer washed with hexane (2 x 10 ml). Last traces of solvent were removed under vacuum (0.05 mbar, 4 hr), leaving a clear film of polymer (0.35 g, 31%).

$\delta_H((CD_3)_2CO)$: 0.9-1.0 (1.9 H, br. mult., CH_3 rr); 1.05-1.15 (1.1 H, CH_3 mr); 1.85-1.92 (1.3 H, br. s, CH_2 rr); 1.96-2.01 (0.7 H, br. mult., CH_2 mr); 3.35 (3 H, s, OCH_3); 3.55, 3.63, 3.71 (2 H each, CH_2O); 4.12 (2 H, CH_2CO_2)

$\delta_C((CD_3)_2CO)$: 17.4 (CH_3, rr);.19.1 (CH_3, mr); 45.5 (C backbone, rr); 45.8 (C backbone, mr); 55.1 (CH_2 backbone); 59.0 (CH_3O); 64.8 (CH_2CO_2); 69.2, 71.0, 72.6 (CH_2O); 177.1 (CO_2 mr); 177.9, (CO_2 rrrr); 178.2 (CO_2 mrrr).

Poly (2 -(2'-Methylpropenoatomethyl)-1,4,8,11-tetraoxacyclotetradecane) (A)

Method 1: Redox initiation (A1)

This was prepared as described above for the polymer of the model methacrylate (13), using the 14-membered ring methacrylate (14) (2.34 g 7.7 mmol) with 0.032 mmol of the redox initiators $K_2S_2O_8$ and $FeSO_4$ in 70 ml of degased distilled water. The reaction was started at 0°C and allowed to proceed at room temperature overnight, after which time the polymer was found to have precipitated out and adhered to the flask. Acetone was added to the flask and stirred overnight, and the resulting mixture filtered to give a clear solution of the polymer. This was purified by precipitation by addition of distilled water, redisolved in acetone and precipitated again by addition of hexane. After removal of solvents, a clear film of polymer (0.57 g, 24%) was left coating the flask.

$\delta_H((CD_3)_2CO)$: 0.9-1.0 and 1.05-1.15 (3 H, br. mult., CH_3); 1.65-1.85 (6 H, br. mult. CH_2CH_2 backbone + CH_2CH_2 ring); 3.4-3.8 and 3.85-4.05 (17 H, br. mult. CH2O + CHO).

$\delta_C((CD_3)_2CO)$: 16.9 (CH_3, rr);.18.67 (CH_3, mr); 30.73, 30.92 (CH_2C ring); 44.96 (C backbone, rr); 45.34 (C backbone, mr); 55.0 (CH_2 backbone);

64.97 (CH_2CO_2); 65.75, 66.6, 66.65, 67.38, 70.03, 71.32, 71.89 (CH_2O);
76.67 (CHO); 176.45 (CO_2 mr); 177.25, (CO_2 rrrr); 177.55 (CO_2 mrrr).

M_n: 200,000. M_w: 800,000. M_w/M_n: 4.0

T_g: 31°C

Method 2: AIBN initiation (A2)

The macrocyclic methacrylate (14) (1.04 g, 3.44 mmol), distilled butanone (5 ml) and AIBN (4.4 mg, 0.42 wt% on the monomer) were added to a Schlenk tube fitted with a reflux condenser and the mixture deoxygenated by three repetitions of the cycle: cool and freeze in liquid nitrogen while evacuating the apparatus; allow to warm to room temperature under an atmosphere of argon. The tube was then placed in an oil bath heated to 85°C and the reaction left overnight under an atmosphere of argon. Hydroquinone (~2 mg) was then added to ensure no further radical reactions could occur, and the reaction mixture added dropwise to hexane (50 ml). After allowing the precipitated polymer to settle out, the solvent was decanted off and the polymer redisolved in acetone (2-3 ml). This solution was dropped into hexane, and the recovered polymer reprecipitated once more in the same way. Solvents were removed from the purified polymer under vacuum, leaving a white, hard foam (0.66 g, 63%).

M_n: 13,000. M_w: 19,100. M_w/M_n: 1.47

T_g: 31°C

Poly(2 -(2'-Methylpropenoatomethyl)-1,4,7,10-tetraoxacyclododecane) (B)

This was prepared by the method described for polymer (A2), using the 12-membered ring methacrylate (16), 1.02 g, 3.71 mmol, and AIBN 3.4 mg. After purification by precipitation in hexane, the polymer was dried in vacuum, to yield a hard, white foam (0.73 g, 72%).

$\delta_H(CD_2Cl_2)$: 0.75-0.95 and 1.0-1.1 (3 H, br. mult., CH_3);
1.75-1.95 (2 H, br. mult. CH_2CH_2 backbone);
3.4-4.0 (17 H, br. mult. CH2O + CHO).

$\delta_C(CD_2Cl_2)$: 16.9 (CH_3, rr);.18.7 (CH_3, mr);
45.0 (C backbone, rr); 45.4 (C backbone, mr); 55.0 (CH_2 backbone)

65.3 (CH_2CO_2); 70.4, 70.5, 70.6, 70.8, 70.8, 71.2, 71.2 (CH_2O);
77.3 (CHO); 177.5 (CO_2 mr); 177.8 (CO_2 rrrr); 177.8 (CO_2 mrrr).

T_g: 0°C

Poly(2-(7'-(2"-Methyl)-propenoato-2',5'-dioxaheptyl)-1,4,7,10 tetraoxacyclododecane) (C)

This was prepared by the method described for polymer (A2), using the ethylene oxide extended 12-membered ring methacrylate (22), 0.72 g, 2.0 mmol, and AIBN 3.0 mg. After purification by precipitation in hexane, the polymer was dried in vacuum, to yield a very viscous liquid (0.5 g, 69%).

$\delta_H(CDCl_3)$: 0.82-0.91 (1.8 H, CH_3 rr); 0.98-1.08 (1.2 H, CH_3 mr);
1.75-1.98 (1.2 H, br. s, CH_2 rr); 2.04-2.14 (0.8 H, br. mult., CH_2 mr);
3.46-3.55 and 3.6-3.88 (23 H, mult, CH_2O + CHO); 4.05-4.13 (2 H, CH_2CO_2)

$\delta_C(CDCl_3)$: 16.6 (CH_3, rr);.18.5 (CH_3, mr); 44.7 (C backbone, rr);
45.1(C backbone, mr); 54.1 (CH_2 backbone); 63.75 (CH_2CO_2);
68.42 ($OCH_2CH_2CO_2$ rr); 68.55 ($OCH_2CH_2CO_2$ mr);
70.12, 70.27, 70.38, 70.6, 70.6, 70.6, 70.82, 70.86, 71.37. 71.59 (CH_2O);
78.47 (CHO); 177.1 (CO_2 mr); 177.9, (CO_2 rrrr); 178.2 (CO_2 mrrr).

T_g: -39°C

Poly(2-(7'-propenoato-2',5'-dioxaheptyl)-1,4,7,10 tetraoxacyclododecane) (D)

This was prepared by the method described for polymer (A2), using the ethylene oxide extended 12-membered ring methacrylate (23), 1.4 g, 4.0 mmol, and AIBN 8.0 mg. After purification by precipitation in hexane, the polymer was dried in vacuum, to yield a very viscous liquid (0.95 g, 68%).

$\delta_H(CDCl_3)$: 0.8-0.95 (2 H, br. mult. CH_2 backbone);
1.24 and 1.39 (1 H, br. mult, CH backbone)
3.4-3.8 (23 H, mult, CH_2O + CHO); 4.1-4.2 (2 H, br. t., CH_2CO_2)

$\delta_C(CDCl_3)$: 40.9 (CH backbone); 68.8 (CH_2 backbone); 63.2 (CH_2CO_2);
68.6, 69.9, 70.1, 70.1, 70.4, 70.4, 70.4, 70.65, 70.65, 71.15. 71.4 (CH_2O);
78.3 (CHO); 172.4 (CO_2 mr); 173.8-174.4 (CO_2 rr).

M_n: 2000. M_w: 3000. M_w/M_n: 1.5 [Telomer]

T_g: -35°C

Poly(2-(7'-(2"-Methyl)-propenoato-2',5'-dioxaheptyl)-1,4,7,10 tetraoxacyclotetradecane) (E)

This was prepared by the method described for polymer (A2), using the ethylene oxide extended 14-membered ring methacrylate (26), 0.76 g, 2.0 mmol, and AIBN 3.0 mg. After purification by precipitation in hexane, the polymer was dried in vacuum, to yield a very viscous liquid (0.4 g, 53%).

$\delta_H(CDCl_3)$: 0.82-0.91 (1.8 H, CH_3 rr); 0.98-1.08 (1.2 H, CH_3 mr);
1.65-2.14 (6 H, br. mult., CH_2CH_2 backbone + CH_2CH_2 ring);
3.36-3.75 (23 H, mult, CH_2O + CHO); 4.0-4.1 (2 H, CH_2CO_2)

$\delta_C(CDCl_3)$: 16.8 (CH_3, rr);.18.6 (CH_3, mr); 30.68. 30.87 (CH_2 ring);
44.8 (C backbone, rr); 45.19 (C backbone, mr); 54.3 (CH_2 backbone);
63.85 (CH_2CO_2); 65.65, 66.5, 66.5, 67.29, 68.53, 69.89, 70.12, 70.27, 70.38, 71.22, 71.79 (CH_2O); 76.61 (CHO); 176.9 (CO_2 mr); 178.9, (CO_2 rr).

M_n: 7,700. M_w: 10,800. M_w/M_n: 1.38

T_g: -55°C

Poly(2-(8'-(2"-Methyl)-propenoato-2'-oxaoctyl)-1,4,8,11-tetraoxacyclotetradecane) (F)

This was prepared by the method described for polymer (A2), using the 14-membered ring hydrocarbon extended methacrylate (30), 0.63 g, 1.56 mmol, and AIBN 2.5 mg. After purification by precipitation in hexane, the polymer was dried in vacuum, to yield a very viscous liquid (0.73 g, 72%).

$\delta_H(CDCl_3)$: 0.8-0.9 (rr) and 1.0-1.1 (mr) (3 H, br. mult., CH_3);
1.25-1.4 and 1.45-1.65 (8 H, mult. CH_2-CH_2 extension);
1.65-1.95 (6 H, br. mult. CH_2CH_2 backbone + CH_2CH_2 ring);
3.35-3.75 and 3.75-4.05 (21 H, br. mult. CH2O + CHO).

$\delta_C(CDCl_3)$: 16. 6(CH_3, rr);.18.35 (CH_3, mr); 30.76, 30.95 (CH_2C ring);
25.68, 25.79, 28.02, 29.45 (CH_2CH_2 extension);
44.65 (C backbone, rr); 45.15 (C backbone, mr); 55.1 (CH_2 backbone);
64.87 (CH_2CO_2);
65.70, 66.80, 66.63, 67.40, 70.06, 70.06, 71.29, 71.88, 71.70 (CH_2O);
76.67 (CHO); 176.45 (CO_2 mr); 177.25, (CO_2 rrrr); 177.55 (CO_2 mrrr).

T_g: -20 °C

Poly(2-(8'-(2"-Methyl)-propenoato-2'-oxaoctyl)-1,4,7,10-tetraoxacyclododecane) (G)

This was prepared by the method described for polymer (A2), using the 12-membered ring hydrocarbon extended methacrylate (33), 0.73 g, 1.95 mmol, and AIBN 3 mg. After purification by precipitation in hexane, the polymer was dried in vacuum, to yield a very viscous liquid (0.47 g, 65%).

$\delta_H(CDCl_3)$: 0.75-0.85 (rr) and 0.9-1.1 (mr) (3 H, br. mult., CH_3);
1.2-1.35 and 1.45-1.6 (8 H, mult. CH_2-CH_2 extension);
1.75-1.95 (2 H, br. mult. CH_2CH_2 backbone);
3.3-3.4 and 3.55-3.85 (21 H, br. mult. CH2O + CHO).

$\delta_C(CDCl_3)$: 16.55 (CH_3, rr);.18.25 (CH_3, mr);
25.66, 25.76, 27.96 (rr) and 28.05 (mr), 29.42 (CH_2CH_2 extension);
44.5 (C backbone, rr); 45.0 (C backbone, mr); 55.0 (CH_2 backbone)
64.83 (CH_2CO_2);
70.08, 70.22, 70.54, 70.54, 70.54, 70.78, 70.78, 71.35, 71.65 (CH_2O);
78.48 (CHO); 176.63 (CO_2 mr); 177.28 (CO_2 rrrr); 177.62 (CO_2 mrrr).

T_g: -26°C

3.3. Complexation studies.

~50 mg of the ligand to be studied was weighed into an NMR tube, and dissolved in the appropriate quantity of CD_3OD. The ^{13}C NMR spectrum of the free ligand was recorded, and a small quantity (~2-3 mg) of lithium perchlorate weighed in. The NMR spectrum of the partially complexed ligand was then recorded, and more lithium perchlorate added. This cycle was repeated until successive spectra became similar, the quantity of lithium salt added each time being increased after sufficient had been added to form a 1:1 complex with all the ligands present. A plot of change in chemical shift of one of the spectral lines vs. quantity of salt added was then constructed.

3.4. References

1. Golding, B. T. and Ioannou, P. V., *Synthesis*, 423 (1977).

2. Kataky, R., Nicholson, P. E. and Parker, D., *J. Chem. Soc., Perkin Trans. II*, 321 (1990).

3. Howe, R. J. and Malkin, J., *J. Chem. Soc.*, 2663 (1951).

4. Babb, D. A., Bartsch, R. A., Czech, B. P. and Son, B., *J. Org. Chem.*, **40** 4805 (1984).

5. Itoh, A., Myazaki, T. M., Okahara, M. and Yumagida, S., *Bull. Chem. Soc. Japan*, **55** 2005 (1982).

6. Collie, L., Denness, J. E., Parker, D., O'Carroll, F. and Tachon, C., *J. Chem. Soc., Perkin Trans. II*, 1747-1758 (1993).

7. Mitchell, J. P., Doctoral Thesis, University of Durham, 1990.

8. Fisher, K. and Eisenbach, C. D., *Makromol. Chem., Rapid Commun.*, **9 (7)**, 503-11 (1988).

9. Andrade, J. D., Chen, C. M. and Gregonis, D. E., *Polym. Prepr. Am. Chem. Soc. Div Pol. Chem.* **16(2)** 349 (1975).

10. Dalè, J. and Kristiansen, P. O., *Acta Chemica Scand.*, **26** 1471 (1972).

11. Marvel, C. S. and Sekera, V. C., *Org. Syn. Coll. Vol.*, **3** 366 (1955).

4. Discussion

4.1. Complexation Studies.

4.1.1. Lithium Titration of the Benzylated Cycles

Carbon-13 NMR was used to monitor the extent of lithium binding by a series of ligands as a function of the total concentration of added lithium salt. In effect the ligand was titrated against lithium ions. Lithium perchlorate was used as the lithium source, as the perchlorate anion binds very poorly to metal ions, and was unlikely to interfere with lithium complexation significantly. Deuterated methanol, CD_3OD, was used as the solvent.

The variation in carbon-13 NMR chemical shift observed on the addition of lithium ions is almost entirely due to the changes in ligand conformation induced when lithium is bound to the crown ether ring[1]. The direct effect of de-shielding the carbons due to the presence of a nearby positive charge is negligible by comparison. Under the conditions used for most of the experiments (room temperature, CD_3OD solvent) the complexation and decomplexation process is fast on the time scale of NMR observation, so the chemical shift observed for a particular carbon is the weighted mean of its chemical shift in complexed and free ligands.

4.1.1.i. Derivation of a Model for 1:1 Binding[2]

For a simple 1:1 complex, the observed chemical shift of a line, δ, is given by :-

$$\delta = \frac{\delta_0[L] + \delta_1[LiL]}{[L] + [LiL]} \qquad \ldots.(4.1)$$

where δ_0 is the position of the line in the free ligand, and δ_1 is its position in the complexed ligand. The concentrations of free and complexed ligand are [L] and [LiL] respectively. The denominator is the total ligand concentration, which is fixed initially as $[L]_{int}$.

In practice, the measured quantities are the change in observed chemical shift $\Delta\delta_0 = (\delta - \delta_0)$ and the quantity of lithium added, which can be expressed as a mole fraction M of the amount of ligand present. The desired parameter is the complexation constant K_1, defined as :-

$$K_1 = \frac{[LiL]}{[L][Li]} \qquad \ldots.(4.2)$$

Since [LiL] + [L] = $[L]_{int}$ and [LiL] + [Li] = $M[L]_{int}$ equation 4.2 may be rewritten using only two unknown quantities, [LiL] and K_1.

$$K_1 = \frac{[LiL]}{\{[L]_{int} - [LiL]\}\{M[L]_{int} - [LiL]\}} \qquad ....(4.3)$$

Similarly, equation 4.1 may be expressed in terms of the measured parameters $\Delta\delta_0$ and δ_0 and only two unknowns, [LiL] and the chemical shift δ_1 of the complexed ligand. :-

$$\Delta\delta_0 = \frac{[LiL]\{\delta_1 - \delta_0\}}{[L]_{int}} \qquad ....(4.4)$$

Equation 4.3 may be rearranged into a quadratic in [LiL]. :-

$$K_1[LiL]^2 - [LiL]\{1 + K_1[L]_{int} + K_1[L]_{int}M\} + K_1[L]^2_{int}M \qquad ....(4.5)$$

Solving for [LiL], one obtains :-

$$[LiL] = \frac{\{1+K_1[L]_{int}+K_1[L]_{int}M\}}{2K_1} \pm \frac{\sqrt{\{1+K_1[L]_{int}+K_1[L]_{int}M\}^2 - 4K_1^2[L]_{int}^2 M}}{2K_1} \qquad ....(4.6)$$

The positive root is not physically allowed, as it requires [LiL] to be greater than $[L]_{int}$. Combining equations 4.4 and 4.6 by eliminating [LiL] gives :-

$$\Delta\delta_0 = \frac{(\delta_1 - \delta_0)}{2K_1[L]_{int}}\left\{(1+K_1[L]_{int}+K_1[L]_{int}M) - \sqrt{(1+K_1[L]_{int}+K_1[L]_{int}M)^2 - 4K_1^2[L]_{int}^2 M}\right\} \qquad ....(4.7)$$

Equation 4.7 was used as a model for the observed data, which is plotted as a graph of $\Delta\delta_0$ against M. By numerically fitting equation 4.7 to such a plot, the values of K_1 and the "limiting shift" (δ_1 - δ_0) may be determined.

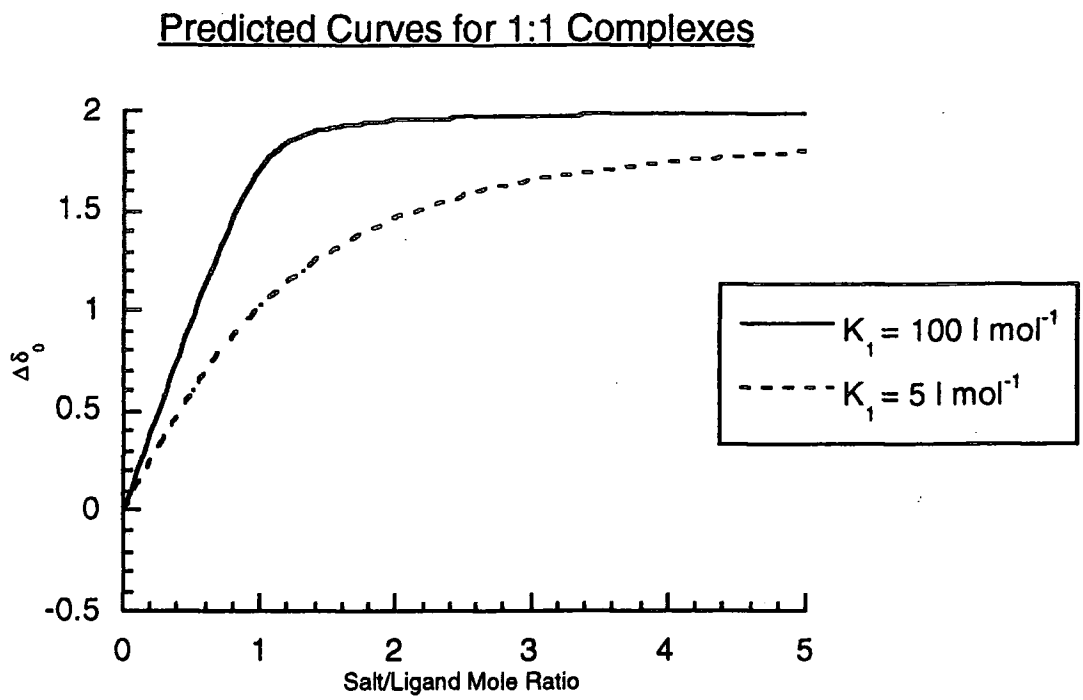

Figure 4.1 *The Variation of $\Delta\delta_0$ with Added Lithium for Complexes with Binding Constants K_1 of 5 l mol^{-1} and 100 l mol^{-1} as Predicted by Equation 4.7*

4.1.1.ii. Lithium Titration Results

The first experiments were carried out on compound (7), the monobenzylated 12-membered ring. The most easily identified resonance is that of C-1, the methylene carbon to which the side-arm is attached. Figure 4.1 shows the plot of chemical shift change against the mole ratio of added lithium to ligand. The "raw data" plot, which is simply ($\delta - \delta_0$) as discussed above, is somewhat scattered, and a smoother plot was produced by taking the difference in chemical shift between C-1 and another carbon. In the absence of noise, the "raw data" and "corrected" plots should be related by a simple scale factor common to all points, but in practice the "corrected" plot removes scatter due to miss-referencing of the spectrum as a whole. A similar method of noise reduction was used for all subsequent plots.

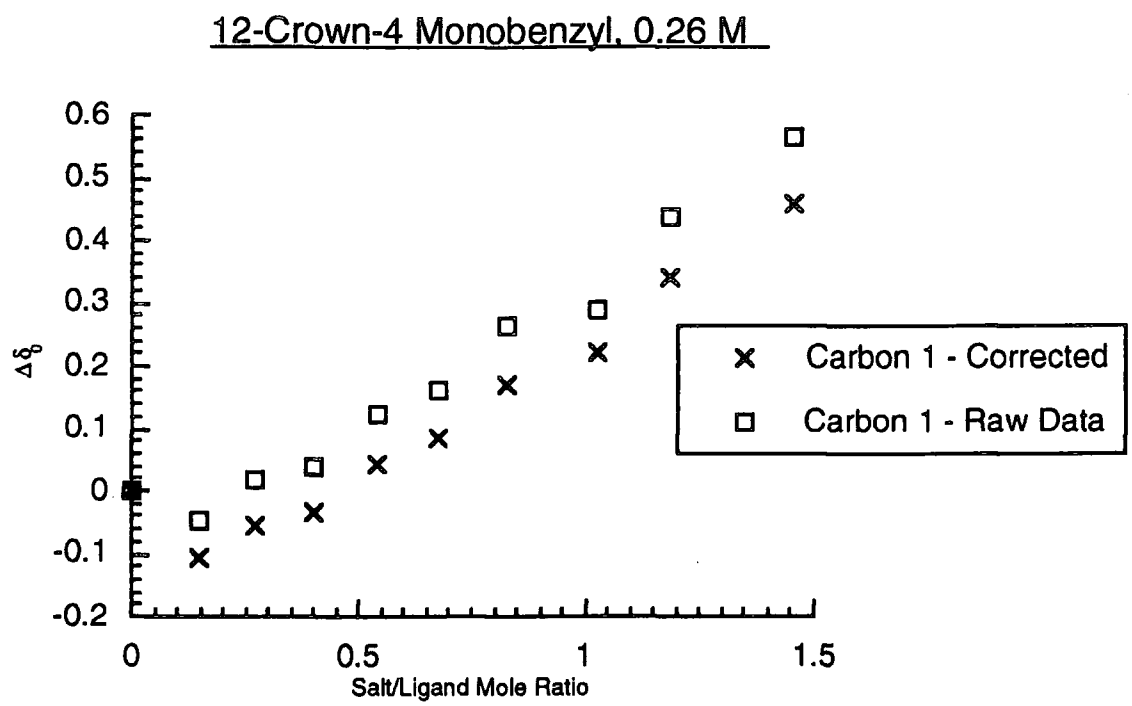

Figure 4.2 *Change in Carbon-13 Chemical shift of C-1 (raw data) and in the shift difference between C-1 and C-11 (corrected) on addition of $LiClO_4$*

Both the "raw data" and "corrected" plots show a significant deviation from the behaviour predicted by the simple 1:1 complexation model. This is almost certainly due to the formation of a 2:1 (ligand : lithium) sandwich complex in addition to the 1:1 complex. This will be discussed more fully in section 4.1.2.iii.

Any pair of lines may be used to produce a "corrected" plot, and a few of the resulting curves are shown in figure 4.3. All of them exhibit an increase in slope as more lithium is added, although the extent of this varies considerably. A simple 1:1 model requires that the slope of all the plots is a maximum at the origin, as shown in figure 4.1.

The formation of 2:1 "lithium sandwich" compounds is disfavoured at lower total concentrations, so $[L]_{int}$ was reduced from 0.26 to 0.16 M, and measurements made at increased salt/ligand ratios. Unfortunately, the plots still did not resemble the predicted curve. This indicates that the 1:1 complex is very weak, and is unable to compete well with either the 2:1 "sandwich" compound or solvation of the lithium ions by methanol. No quantitative value for K_1 was obtained.

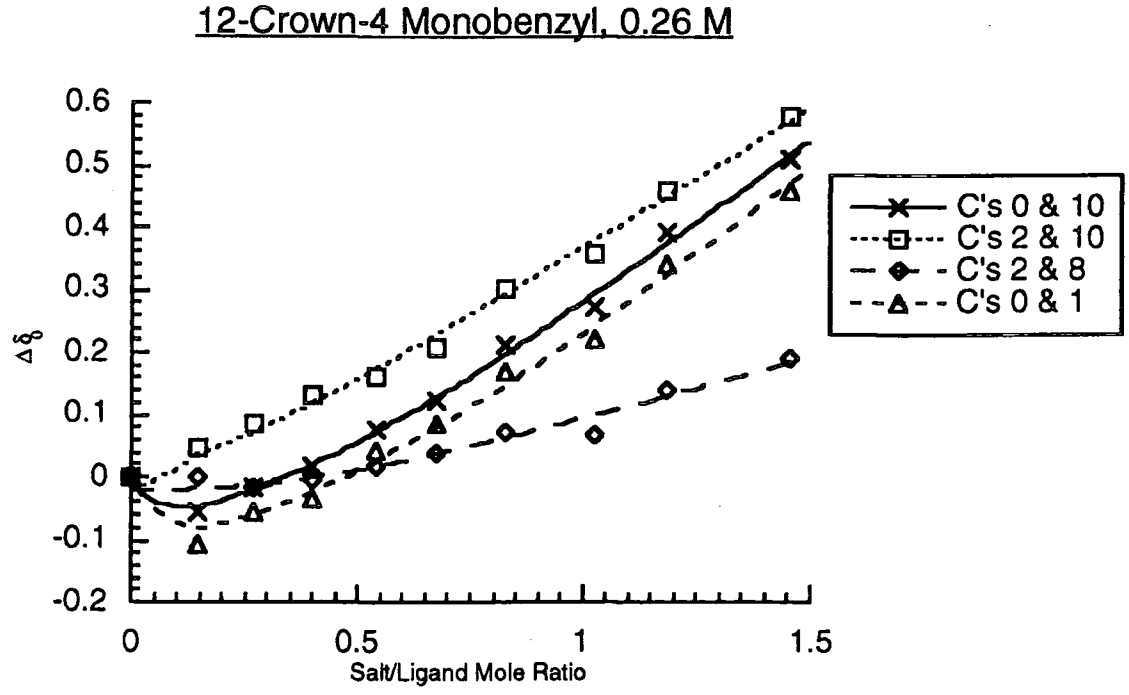

Figure 4.3 *Changes in Chemical Shift Difference for Several Pairs of Resonances. The fitted lines are empirical, as the 1:1 binding model does not apply*

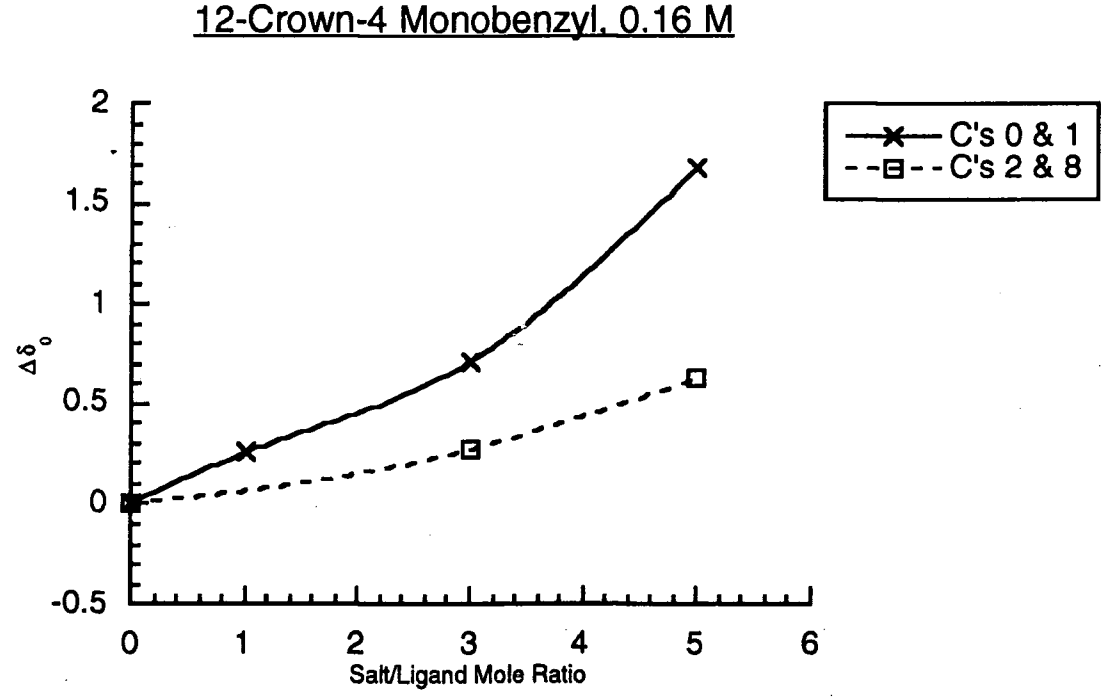

Figure 4.4 *Chemical Shift Change Measured at Reduced Ligand Concentration and Increased Salt Concentration. No "limiting shift" is detectable*

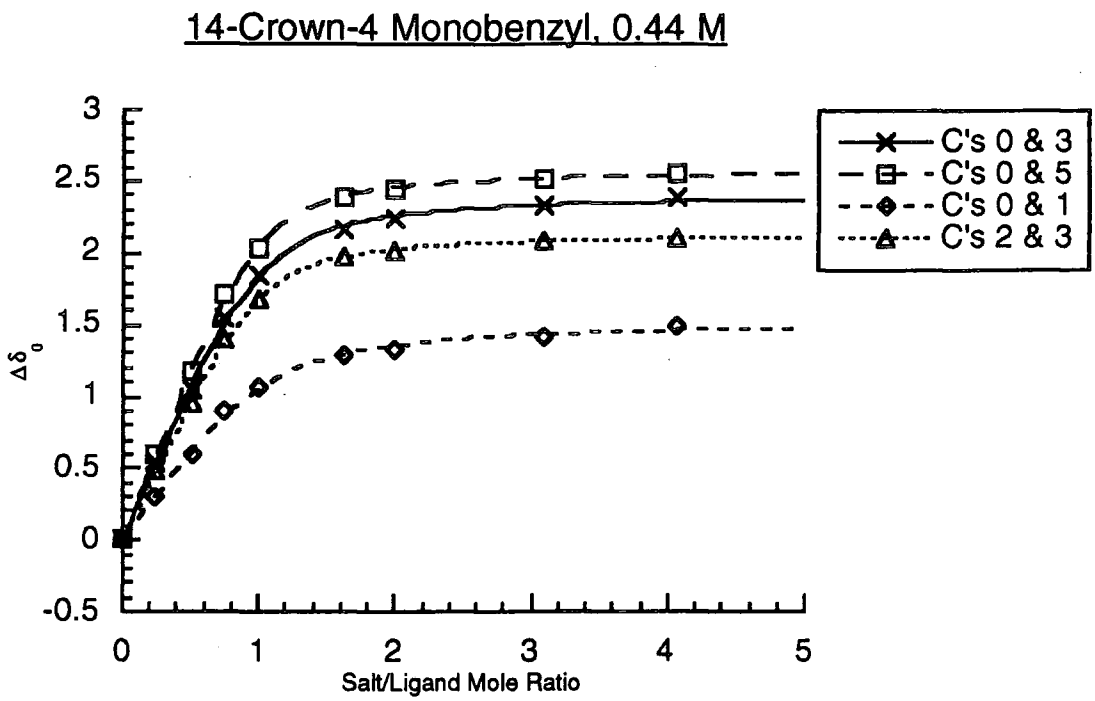

Figure 4.5 *Changes in Chemical Shift Difference for Several Pairs of Resonances. The points have been fitted to the 1:1 binding model .*

As can be seen from figure 4.5, the data obtained for the 14-monobenzyl ligand fit quite well to the 1:1 binding model derived in equations 4.1-4.7. A value for $\log(K_1)$ of 1.45 ± 0.25 was obtained from the numerical fit. The complex between the 14-monobenzyl ligand and lithium ions is therefore fairly weak, at least in methanol.

4.1.1.iii. Interpretation of NMR Titration Curves

It is instructive to compare the data obtained for the 12- and 14-monobenzyl crowns with similar work done on related compounds by others in this laboratory.[3,4]

The procedures and conditions used to titrate these ligands were identical to those used for the 12- and 14- monobenzyl systems. Figure 4.6 shows the compounds investigated, and the results obtained are shown in figure 4.7. In each case, the shift variation of the unique methylene carbon (C-1 in the convention used for figures 4.2-4.5) is plotted against the salt/ligand mole ratio.

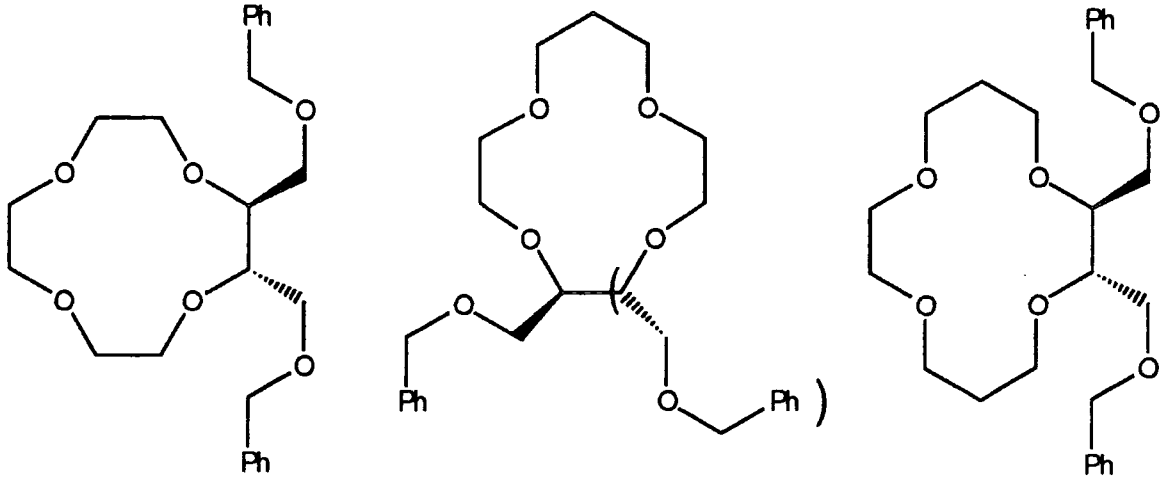

Figure 4.6 *The 12-dibenzyl, 13-monobenzyl (and dibenzyl) and 14-dibenzyl ligands.*

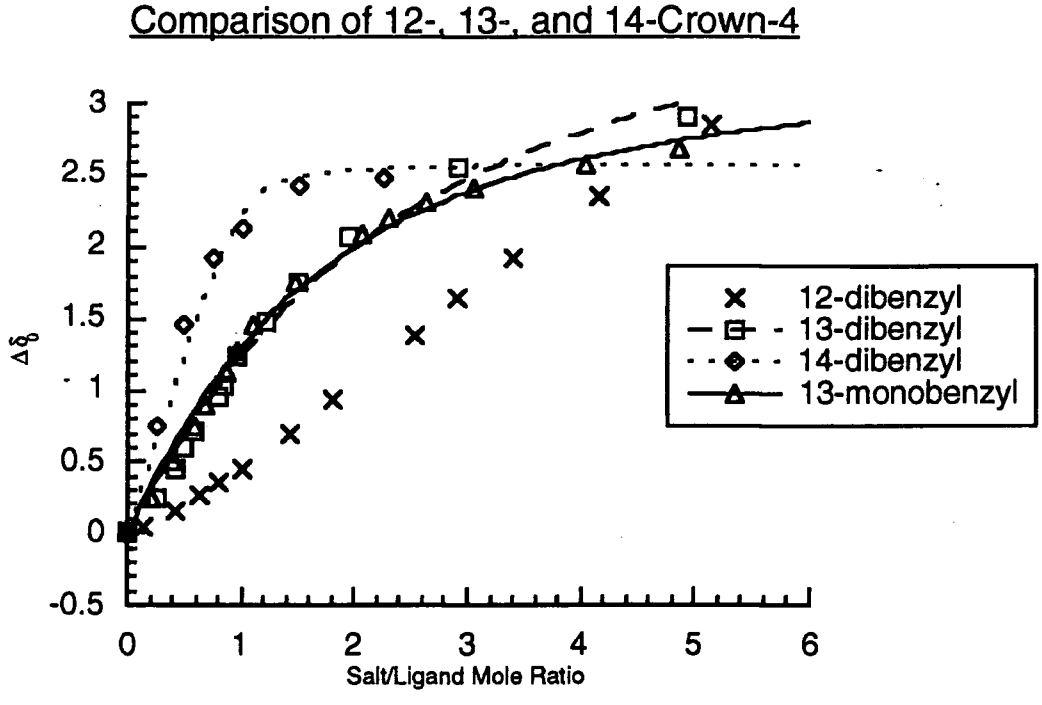

Figure 4.7 *Titration Plots for the 12-, 13-, and 14-Crown-4 Ligands shown in Figure 4.6. The Fitted Curves are for the 1:1 Binding Model.*

Clearly, the 14-dibenzyl ligand forms the strongest complex of those investigated. The 1:1 binding model could not be fitted to the plot obtained for the 12-dibenzyl complex, so no numerical estimate of the binding constant could be obtained. For the other compounds, the fitted curve is shown. The estimates of $\log(K_1)$ for all the ligands studied are given in table 4.1.

Ligand	$Log(K_1/M^{-1})$
12-Monobenzyl	(no fit, $K_1<1$)
12-Dibenzyl	(no fit, $K_1<1$)
13-Monobenzyl	0.19
13-Dibenzyl	0.08
14-Monobenzyl	1.45
14-Dibenzyl	2.50

Table 4.1 *$Log(K_1)$ values Estimated by fitting Equation 4.7 to the NMR Titration Data*

In comparing the mono and dibenzylated series the greatest differences are seen in the 14-membered ring compounds. For the twelve and thirteen membered rings, there is relatively little effect. Both mono- and dibenzyl twelve membered rings exhibit very weak 1:1 complexation and a good estimate for log K could not be made with confidence. The 12-mono system shows a strong tendency to 2:1 complexation which is less evident in the twelve dibenzyl ligand. For the thirteen membered ring ligands, both mono- and dibenzyl systems give weak complexes, with some indication of 2:1 complex formation.

The differing behaviour of the 12-, 13-, and 14-membered ring systems may be interpreted as relating simply to the cavity size of the three rings. The Li^+ ion cannot fit into the ring plane, (defined by the four ring oxygens) in the 12- and 13- membered rings. Only in the 14-membered ring ligands can the Li^+ be bound equally by both of the side-arms of the dibenzyl ligand. This is much the strongest complex, and also the most different from its monobenzyl analogue. For the 12- and 13-membered rings, the second side-arm is blocked from binding to the lithium ion by the CH_2 groups of the ring.

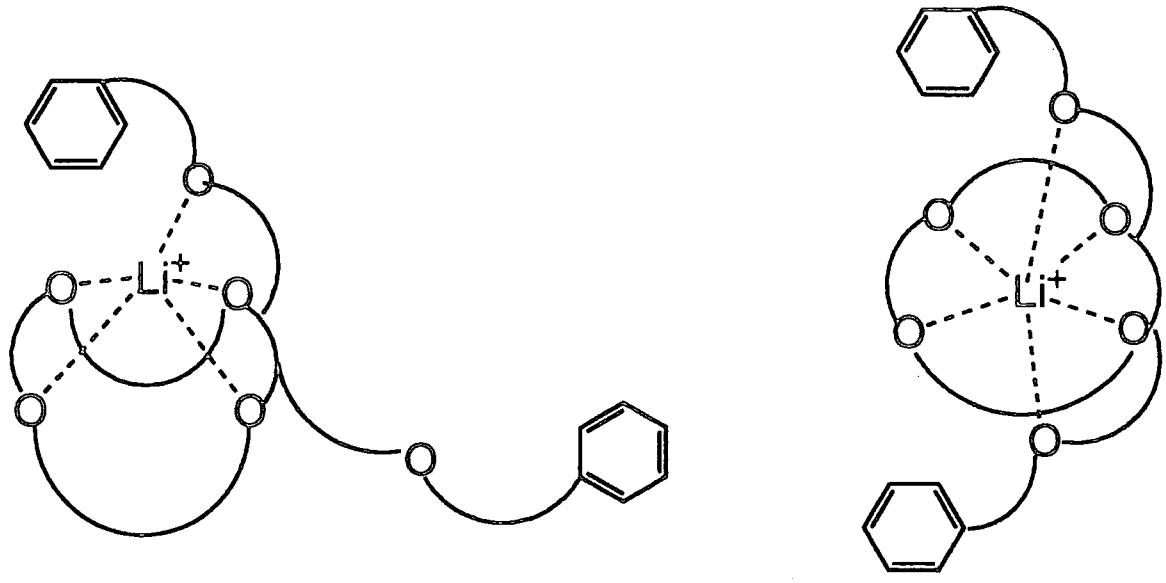

Fig. 4.8 *Schematic of the Lithium Complexes of Dibenzyl 12- and 14-Crown-4'*

The apparent difference in the strength of 2:1 complexation between the mono- and dibenzyl 12-membered rings may be due to the added bulk of the dibenzyl ligand. The formation of a tight "sandwich" compound will restrict the motion of the second side chain, even though it is not involved in binding to the lithium ion. This will lead to an additional reduction in the conformational entropy of the 2:1 complex compared to the free ligand, and so weaken it. Since this effect has no counterpart in the formation of complexes by the 12-monobenzyl ligand, it will bind more strongly.

Both the mono- and dibenzyl 13-membered rings exhibit only weak 1:1 complexation and very weak 2:1 complexation. Any differences between the mono- and dibenzyl ligands are not significant.

4.1.2. ^{7}Li NMR Studies

The lithium titration experiments discussed in section 4.1.1 give information only about the equilibrium constants of the various complexes studied. In the context of lithium ions within polymers, these equilibrium constants are relevant to the degree to which the added lithium is solvated, and effectively separated from its counter-ions. However, high ionic conductivity requires not only a high concentration of lithium ions, but also high ionic mobility. Ionic mobility is generally limited by the speed of polymer segment motion, as discussed in section 1.2.2, but if the rate of lithium exchange between neighbouring binding sites is very slow, this may degrade

the overall ionic mobility. Any attempt to relate the properties of a monomer ligand to the ionic conductivity of the corresponding polymer therefore requires some understanding of the kinetics of the exchange process, as well as its equilibrium states

The lithium exchange rate is related to $\Delta G_c^{\dagger}$, the free energy of activation for lithium complexation. This quantity is not derivable from equilibrium data such as the complexation constant, but may be obtained from variable temperature NMR if a line coalescence can be observed between the resonances of solvated and ligated Li^+. At the coalescence temperature, the exchange rate is related to the line separation by:–

$$\frac{1}{\tau_c} = 2\pi\delta\upsilon \qquad \ldots. (4.8)$$

where τ_c is the time for Li^+ complexation/decomplexation, and $\delta\upsilon$ is the shift difference between the resonances of solvated and ligated Li^+, in Hz. An estimate of the exchange rates for Li^+ between solvent and crown ether ligands in solution was made by using variable temperature ^7Li NMR.

Initially, methanol was used as the solvent, but no coalescence was observed, only a single line at all accessible temperatures. Methanol is too strong a solvent for Li^+ and competes effectively with the crown ether ligands. The much weaker solvent dichloromethane was found not to dissolve lithium perchlorate or triflate sufficiently to allow samples to be prepared for NMR. The least polar solvent that was found to dissolve Li^+ salts was nitromethane, and by using CD_3NO_2 as the NMR solvent a coalescence point was found for the 14-crown-4-monobenzyl/Li^+ system at a temperature of 283 K. Below 263 K, two distinct lines are seen, for solvated and ligated lithium, with a separation of 0.5 ppm. This corresponds to a free energy of activation for the complexation process, $\Delta G_c^{\dagger}$, of 65±2 KJ/mol. For the equivalent 12-crown-4-monobenzyl system no coalescence was observed, only a single time-averaged line down to a temperature of 233 K. This sets an upper limit to $\Delta G_c^{\dagger}$ of approximately 50 KJ/mol for this ligand.

The faster exchange found in the 12-crown-4 system is consistent with earlier work[5] and with the ^{13}C NMR results which show that the 12-crown-4-monobenzyl ligand binds Li^+ relatively weakly. The relatively slow exchange seen in the 14-crown-4 system suggests that polymers based on it may have reduced conductivities, even though ion pair separation is likely to be greater than in 12-crown-4 based systems.

4.1.3. ^{13}C NMR of Crown Ether Polymers

Carbon-13 NMR studies are frequently used to determine the microstructure (tacticity) of synthetic polymers, and the results obtained on the undoped crown ether bearing polymers were described in section 2.8. By adding a lithium salt to the polymer solution, the affinity of the polymers for Li^+ ions could in theory be determined as was done for the benzylated crowns. However, in an amorphous polymer, the atoms in any particular repeat unit are in slightly different environments from those in other units, so the lines in the NMR spectrum appear broadened compared to those in isolated small molecules. Additionally, polymer molecules move and rotate relatively slowly, leading to short T_1 and T_2 relaxation times, which further broadens the observed lines. Both broadening effects are strongest for the resonances of atoms closest to the polymer backbone, but all lines are effected to some degree. This prevents the quantitative measurement of complexation constants, as line positions cannot be determined with sufficient accuracy, but some qualitative information may still be obtained.

To provide a solution environment as close to the solid polymer as practicable, the solvent should be a poor solvator of Li^+ ions, but this makes it difficult to dissolve the lithium salt when preparing the sample, as in the ^7Li NMR experiments described in the previous section. This problem was solved by first dissolving the polymer and $LiCF_3SO_3$ in dry acetone, in which they are both freely soluble, and then removing the acetone under high vacuum and redissolving the doped polymer in either CD_2Cl_2 or $C_2D_2Cl_4$ (for measurements above ambient temperature). The removal of the acetone is confirmed by the absence of its resonances from the NMR spectrum.

The polymers studied were the unextended 14- and 12- methacrylates **(A)** and **(B)**. The clearest resonance line in the ^{13}C NMR spectra in both cases was that of the CHO carbon of the rings, at about 76 ppm, (denoted C-1 in the benzylated rings in section 4.1.1.ii), which is well separated from other resonances. At 293 K this resonance had a width at half height, $\omega_{1/2}$, of 25 Hz in the undoped polymers. For polymer **(B)**, the 12-crown-4 based material, addition of small amounts of Li^+ produced a large broadening of all the resonance lines, with the C-1 line broadening to $\omega_{1/2}$=70 Hz at a doping level of 0.2 Li^+/ring. Further addition of lithium did not produce any observable changes. Varying the temperature of the sample from 243 K (in CD_2Cl_2) to 373 K (in $C_2D_2Cl_4$) did not show any resolution/coalescence of resonances, though all the lines broadened at low temperatures and sharpened at high temperatures. This is probably due to variation in molecular mobility and

hence NMR relaxation times. For polymer **(A)**, the C-1 resonance was split into two peaks at 76.64 and 76.54 ppm in the undoped polymer, presumably due to interaction of the stereocentre at C-1 with that at the junction with the polymer backbone. On addition of lithium to a doping level of 0.2 Li^+ per ring, the diastereomers are not resolved, but the combined C-1 peak has $\omega_{1/2}$=30 Hz, (compared with 70 Hz for polymer **(B)** at the same dopant level), and the peak only broadens to $\omega_{1/2}$=50 Hz at a doing level of 0.33 Li^+/ring. Varying the temperature of the sample altered all the line widths, as with polymer **(B)**, but without revealing any coalescence points.

The differing behaviour of the two polymers may be explained by the greater tendency of 12-crown-4 to form 2:1 (ring : Li) complexes, compared to 14-crown-4. Within a polymer, 2:1 complexes will act as temporary cross-links, and their presence will greatly reduce polymer mobility, and consequently broaden all lines due to the shortening of NMR relaxation times. Even a small number of cross-links could have a large effect in this way, and further addition of Li^+ would not increase the broadening much further. In polymer **(A)**, with 14-crown-4 rings, there will be little tendency to form 2:1 complexes, and the observed line broadening on the addition of lithium is most likely to be due to the increase in the number of micro-environments for individual ligands, which may be binding to Li^+ or empty, and have filled or empty neighbours. The results of the earlier ^7Li NMR experiments on benzylated 14-crown-4, (6), suggest that the separate resonances for empty and filled rings should be resolvable at temperatures below about 260-270 K, but the increasing width of all the resonances at lower temperatures masks any such detail.

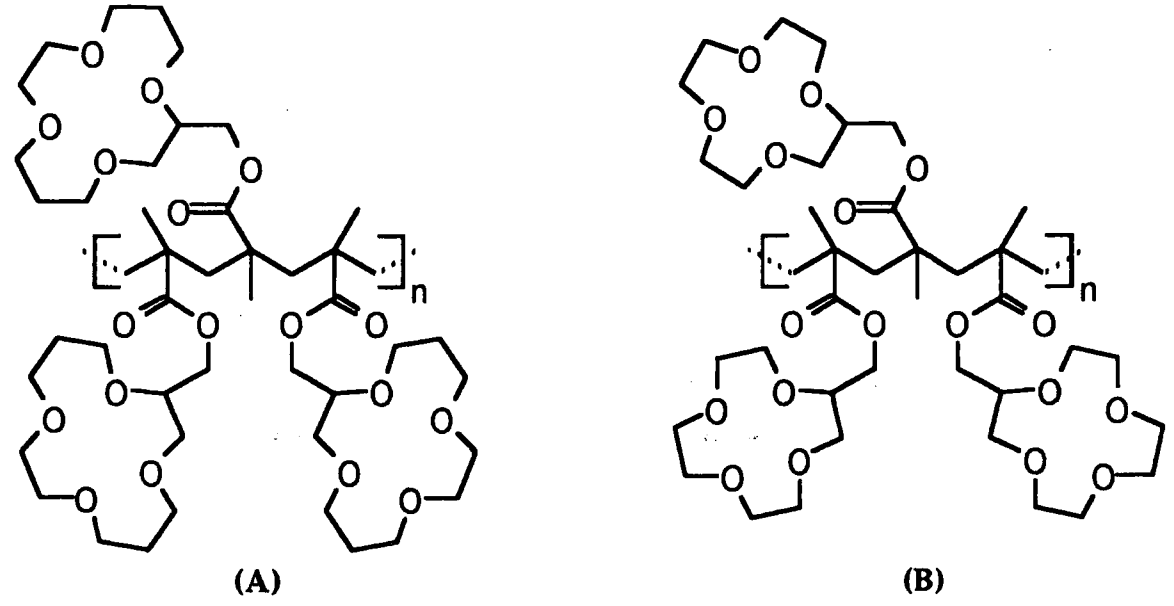

(A) **(B)**

Figure 4.9 Structures of polymers (A) and (B).

4.2. Conductivity and Glass Transition Temperature Studies

The principal influence on the measured conductivity of a non-crystalline polymer complex is the difference between the temperature at which the measurement is made, and the glass transition temperature, T_g of the polymer complex. The relationship was discussed in section 1.2.2.i, and leads to the **Vogel–Tamman–Fulcher (VTF)** equation, equation (1.8) :-

$$\sigma = AT^{-1/2} \exp\left\{\frac{-B}{T - T_0}\right\}$$

The pre-exponential factor A is proportional to the concentration of free mobile charge carriers, but is essentially an empirical constant. T_0, the temperature at which free volume vanishes, is related to T_g by $T_0 - T_g \approx 50K$. If the complex becomes crystalline, conductivity will fall rapidly, and the VTF equation will no longer apply.

Measurements of the conductivity of samples of the lithium doped polymers investigated in this work were made by our collaborators at the I.R.C. in Polymer Science at the University of Leeds, who have previously studied related materials containing acyclic ether side-chains. The purified polymer sample was dissolved in acetone, and the required quantity of lithium dopant added as lithium triflate, $LiCF_3SO_3$, which is also soluble in acetone. The solvent was then removed under reduced pressure, and the doped sample dried in a vacuum oven. The T_g of the sample was determined by differential scanning calorimetry (DSC), and the conductivity by AC impedance spectroscopy, using blocking electrodes.

4.2.1. Results

4.2.1.i. Effects of Lithium Doping Ratio

The first material prepared and investigated, polymer **(A1)** was the "unextended" methacrylate bearing 14-crown-4 ligands, derived from monomer **(14)** by the aqueous polymerisation method, which results in high molecular weight material. Polymer **(A2)**, which was prepared from the same monomer but using the solution polymerisation method, had similar characteristics. Figures 4.10(a) and (b) show the variation in the conductivity of samples of polymers **(A1)**, and **(A2)**, with temperature at a range of dopant levels. The T_g values for these samples are given in table 4.2.

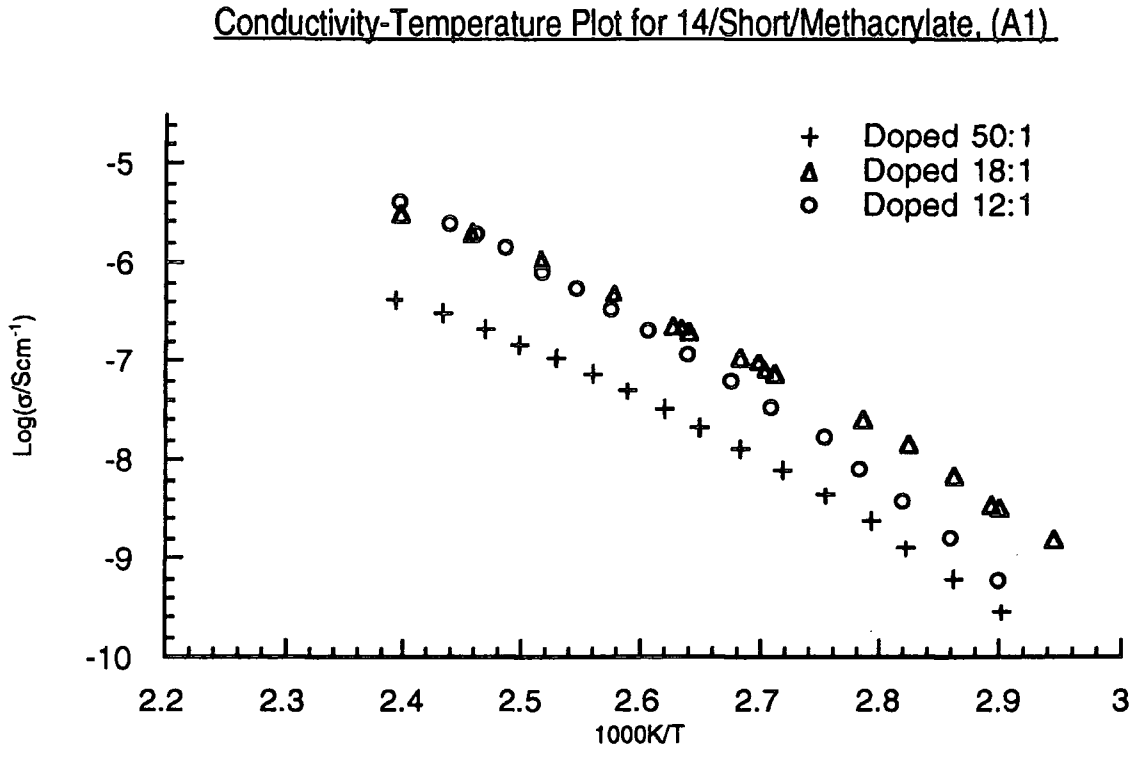

Figure 4.10(a) *Log (Conductivity) against Reciprocal temperature for Polymer (A1), 14-Crown-4 Unextended Methacrylate.*

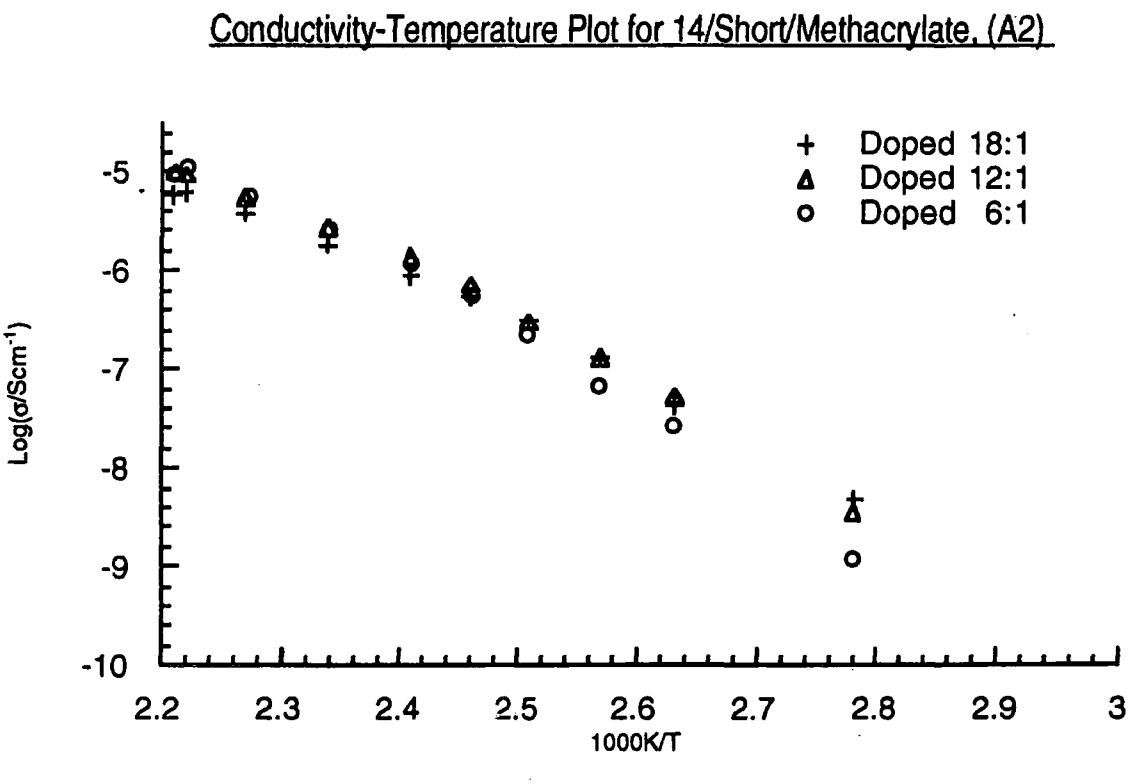

Figure 4.10(b) *Log (Conductivity) against Reciprocal temperature for Polymer (A2), 14-Crown-4 Unextended Methacrylate.*

Dopant Ratio	Glass Transition Temperature, T_g /°C	
	(A1)	**(A2)**
Unsalted	31	31
50:1	41	—
18:1	52	44
12:1	32	44
6:1	—	47

Table 4.2. Variation of Glass Transition Temperature, T_g with Dopant Ratio for Polymers (A1) and (A2).

The dopant level of the samples is expressed as a mole ratio of **ring** oxygens to lithium ions. A dopant level of 12:1 is therefore equivalent to one lithium ion for every three rings. The plots in figure 4.10 clearly show that the conductivity of doped polymer increases with increased doping level up to doping levels of about 18:1. Increasing the doping level beyond this point reduces the conductivity, especially at lower temperatures. This reduction in conductivity does not parallel the reduction of the T_g of sample **(A1)** at higher doping levels, as expected from the free volume model of ionic mobility. At high dopant levels, it is likely that crystals of [crowned-lithium] triflate precipitate out within the polymer at low temperatures, leading to a rapid fall in conductivity below the melting point of these salt complexes. This behaviour is commonly observed in conventional acyclic ether comb polymers,[6] and may explain the observation of low conductivity at low T_g.

Polymer **(A2)**, the lower molecular weight material ($M_n \approx 30{,}000$, compared to > 100,000 for **(A1)**) appears to be somewhat more conductive, and to be less sensitive to dopant level, but exact conductivity and T_g values are always strongly dependent on sample history, so this difference should not be over interpreted. Lower molecular weight polymers are always less viscous, and hence more conductive.

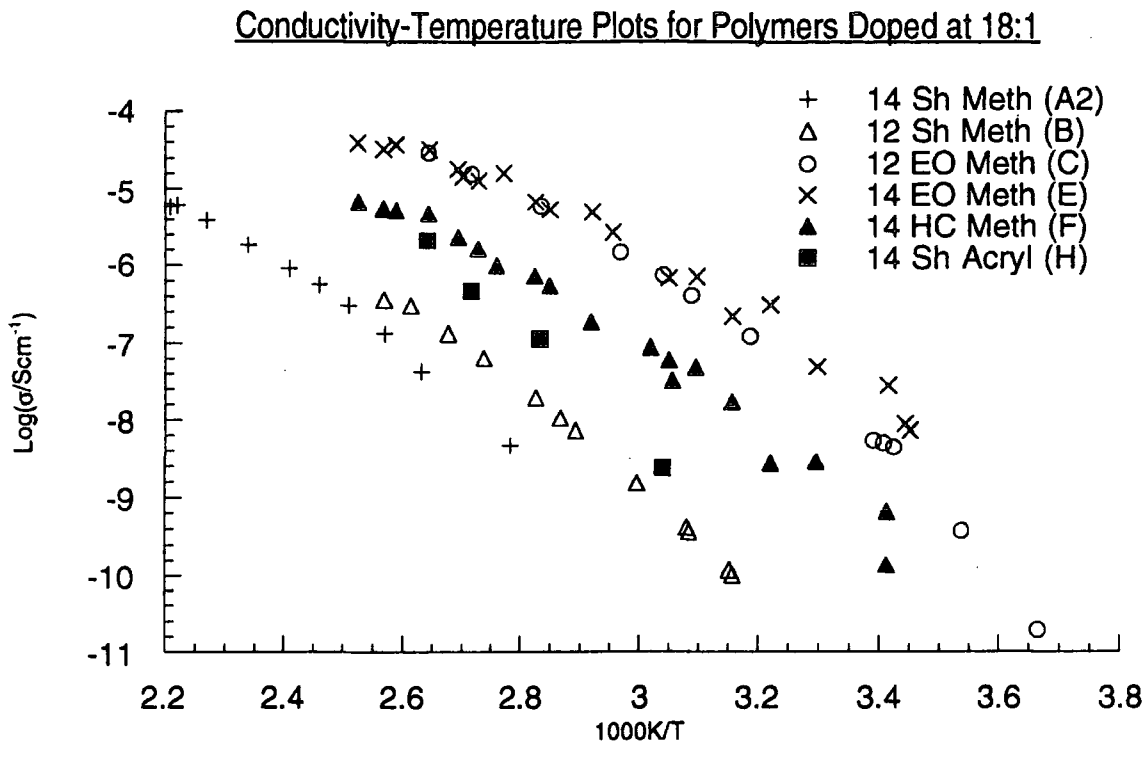

Figure 4.11 The Effect of Polymer Structure on the Conductivity - Temperature Relationship of Crown Ether Polymers

Polymer	Glass Transition Temperature, T_g /°C		
	Undoped	Doped 18:1	Doped 12:1
(A2) 14 Short Methacrylate	+31	+44	+44
(B) 12 Short Methacrylate	0	+17	+23
(C) 12 Ethoxy Methacrylate	-39	-23	-24
(E) 14 Ethoxy Methacrylate	-55	-55	-52
(F) 14 H-C Methacrylate	-20	-24	-20
(H) 14 Short Acrylate	-8	-1	—

Table 4.3 Glass Transition Temperatures of Lithium Doped Polymers .

4.2.1.ii. Effect of Spacer Groups and Polymer Backbone

Since the conductivity of a lithium-doped polymer is greatly influenced by the T_g of the doped sample, a series of crown ether polymers were synthesised, with varying structures to influence the T_g of the resultant polymer electrolytes. The attachment of the crown ether to the backbone was made either directly, or via a spacer group. Additionally, the polymer backbone was varied. These structural alterations have well-known effects on polymer T_g, which are qualitatively predictable. The addition of spacer groups lowers T_g since they act as internal plasticisers. The T_g values of polymers based on methacrylate, acrylate, and propylene oxide backbones can be expected to follow the trend of the "parent" polymers, i.e. poly(methyl methacrylate) > poly(propylene oxide) > poly(methyl acrylate) for T_g.

In addition to their effects on T_g, variations in polymer structure were expected to have an independent "direct" effect on lithium cation mobility, and to study these influences two different spacer groups were used: a C_6 hydrocarbon chain, and an ethoxyethylene group, $(CH_2CH_2)_20$. The oxygen atom in the latter spacer group may be able to bind to the LI^+ dopant ions. The T_g values and conductivity of 12- and 14-crown-4 bearing polymers, with methacrylate and acrylate backbones were investigated in this work. Later work by Dr. J. E. Denness et. al.[4] investigated poly(propylene oxide) backbones, and 13-crown-4.

The T_g values of the free and lithium doped polymers are given in table 4.3. It is clear that in general high conductivity at a given temperature correlates strongly with low T_g values, and that this effect dominates other influences, so that the most conductive polymers complexes are those with the lowest T_g. This observation is as expected from the form of the VTF equation, and previous studies[6,7,8,9,10]. High T_g values, and hence low conductivity, are associated with the unextended polymers, **(A)**, **(B)**, and **(H)**. The 14-crown-4 unextended methacrylate, **(A)**, has the highest T_g and lowest conductivity of any investigated.

The 12- and 14-crown-4 ethylene oxide-extended poly(methacrylates) have a T_g difference of over 30°C (see Table 4.3). Despite this, the conductivity of the two polymers is not significantly different above 25°C, though the higher T_g of the 12-crown-4 based material does cause its conductivity to fall off more rapidly at lower temperatures. This shows that lithium ions migrate between 12-crown-4 sites more easily than between 14-crown-4 sites, as had been indicated by the earlier solution NMR studies, described in section 4.1.

The difference between the 14-crown-4 acrylate and methacrylate polymers can be attributed entirely to the difference of 45 °C in their T_g values.

Although the overall trends in the data shown in figure 4.11 are reasonably clear, the data points are significantly scattered, especially those for polymers **(E)** and **(F)**. Once synthetic work on the other polymers of interest had been completed, new samples of some of the previous materials were prepared, and were subjected to more stringent drying conditions, being kept in a vacuum oven for periods of 8-12 weeks. The previous samples were also re-dried similarly, and the T_g and conductivity values re-measured. The results are shown in figure 4.12, and table 4.4.

The measured T_g values for polymers **(C2)** and **(E2)** were significantly higher than those of the previous samples **(C)** and **(E)**, by 14 and 53 °C respectively. The conductivity plot for **(C2)** is very similar to that for **(C)**, but **(E2)** was found to be less conductive than **(E)** by about a factor of four. Polymer sample **(F')**, which is from the same batch as **(F)**, was found to have the same T_g values, but substantially lower conductivity. It seems likely that in this case the first sample absorbed water from the atmosphere between its T_g and conductivity measurements. Polymer **(E)** probably retained significant amounts of water or other solvent at the time its T_g was measured, and was not completely dried for the conductivity measurements either. Polymer **(C)** also retained some solvent for its T_g measurements, though the conductivity results were not greatly effected.

The modified T_g and conductivity values do not alter the tentative conclusions drawn from the first set of data. The polymers **(C2)** and **(G)** (12-ethylene-oxide-extended methacrylate and 12-hydrocarbon-extended methacrylate) have similar T_g values of -10 and -7 °C when doped at 18--1 while **(C2)** is more conductive than **(G)** by nearly an order of magnitude at all temperatures. This is strong evidence for the involvement of the oxygen atom of the spacer group in Li^+ migration. Polymer **(I)**, the 13-ethylene-oxide-extended methacrylate[4] has a T_g of -3 °C at 18 : 1 doping, and a conductivity plot very similar to that of polymer **(G)**, while polymer **(F')** has a lower T_g (-24 °C at 18 : 1 doping) and also has a similar conductivity trace. Taken with the evidence that ethylene-oxide-extended systems are better conductors than hydrocarbon-extended ones, other factors being equal, this indicates that 12-membered rings produce more conductive systems than 13- and 14-membered ones.

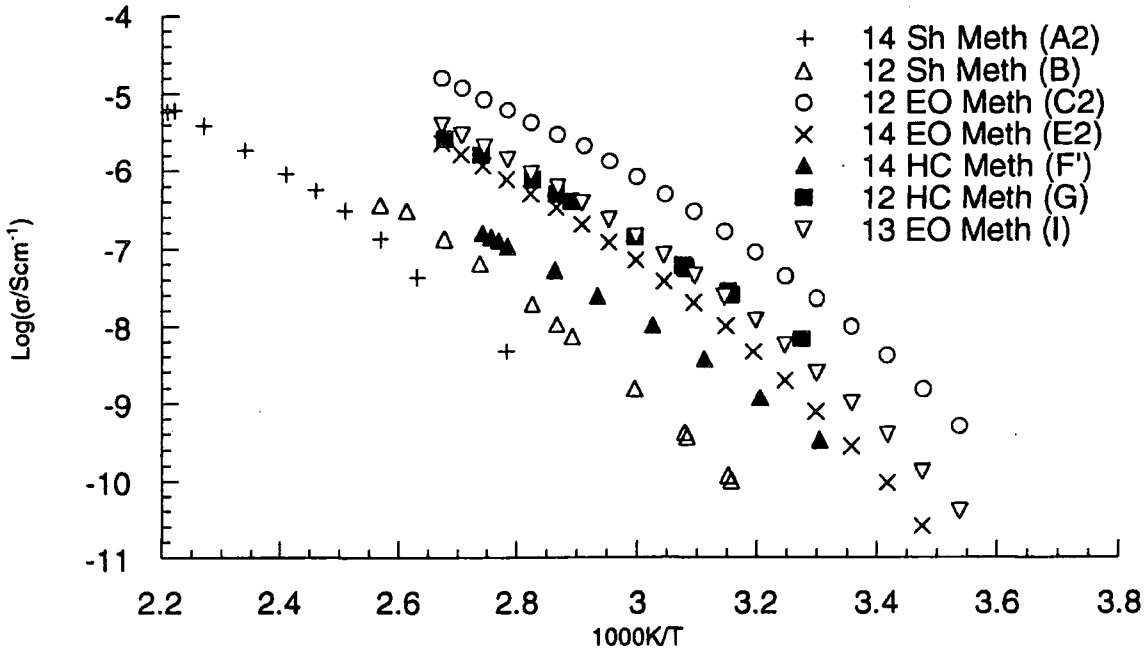

Figure 4.12 *Revised Data on the Conductivity - Temperature Relationship of Crown Ether Polymers*

Polymer	Glass Transition Temperature, T_g /°C		
	Undoped	Doped 18:1	Doped 12:1
(A2) 14 Short Methacrylate	+31	+44	+44
(B) 12 Short Methacrylate	0	+17	+23
(C2) 12 Ethoxy Methacrylate	-25	-10	0
(E2) 14 Ethoxy Methacrylate	-10.5	-1.5	+1.2
(F') 14 H-C Methacrylate	-20	-24	-20
(G) 12 H-C Methacrylate	-26	-7	-5
(I) 13 Ethoxy Methacrylate	-18	-3	+1

Table 4.4 *Revised Glass Transition Temperature Data for Lithium Doped Crown Ether Polymers .*

4.2.2. Analysis of Polymer Conductivities

In order to examine the direct effects of polymer structure on ion transport more quantitatively, the influence of T_g must be normalised out of the data. The **Vogel–Tamman–Fulcher (VTF)** equation, equation (1.8) :-

$$\sigma = AT^{-1/2} \exp\left\{\frac{-B}{T - T_0}\right\}$$

can be rearranged to :-

$$\sigma T^{1/2} = A \exp\left\{\frac{-B}{T - T_0}\right\} \qquad \text{.... (4.9)}$$

Hence :-

$$\log\left(\sigma T^{1/2}\right) = \ln(A) - \frac{B}{T - T_0} \qquad \text{.... (4.10)}$$

Any set of temperature and conductivity data can be re-plotted on a graph of log ($\sigma T^{1/2}$) against $1/(T-T_0)$, and should fit a straight line if the VTF equation applies. The data from two polymers differing *only* in their T_0 values would fall on the *same* line, as they would have identical $\sigma T^{1/2}$ values at equivalent temperatures above T_0.

The value of T_0 (the temperature at which free volume vanishes) can be determined in two distinct ways. For a series of related polymers, such as those studied here, T_g and T_0 are approximately related by a constant, which usually has a value in the range 50-70 K. Measurements of T_g may therefore be used to estimate T_0. Alternatively, a "best fit" curve may be computed through a plot of σ against $1/T$, with the constants A, B and T_0 left as free parameters. This derived T_0 can then be used to normalise the data. Normalised plots produced using these two methods on the first set of conductivity data (that used in figure 4.11) are shown in figure 4.13(a) and (b). Table 4.5 summarises the parameters determined from fitting the VTF equation to this data. Similar plots for the revised conductivity data used in figure 4.12 are shown in figures 4.14(a) and (b), and the derived parameters are given in table 4.6

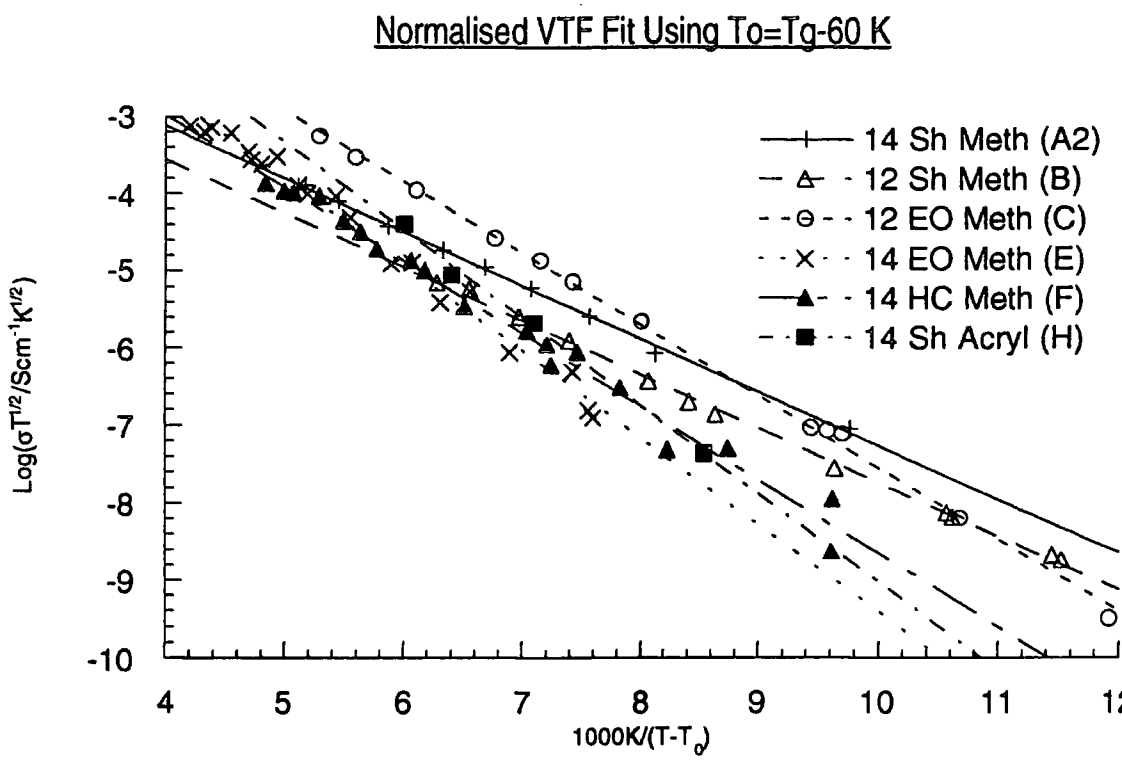

Figure 4.13(a) *Normalised VTF plot, constructed from the first set of polymer conductivity data using* $T_0 = T_g - 60K$

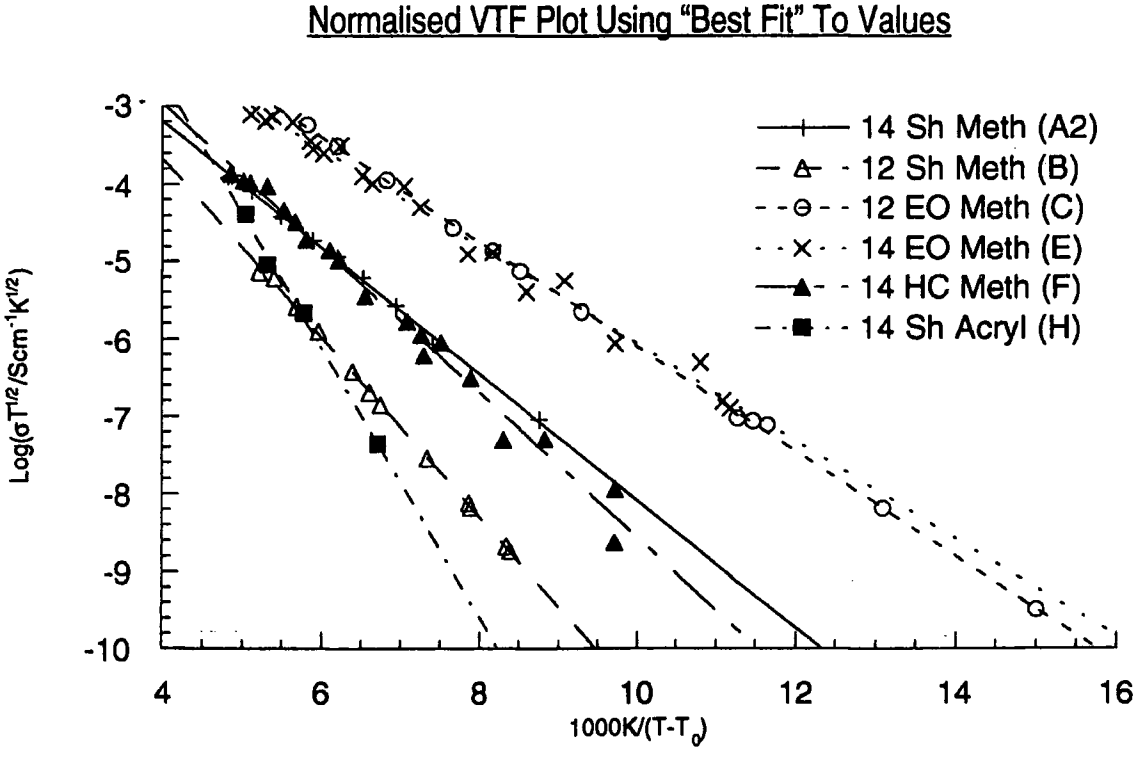

Figure 4.13(b) *Normalised VTF plot, constructed from the first set of polymer conductivity data using "Best Fit"* T_0 *values*

The T_0 values given in table 4.5 are those determined by fitting the conductivity plots in figures 11 and 13. While some of the conductivity curves are in reasonable agreement with the approximation T_g-T0 = 60K, the plots for polymer samples **(B)** and **(H)** imply T_0 values that are much lower than those expected from T_g measurements. Only four points were determined for polymer (H), and this is too few to provide an accurate fit. No consistent and repeatable results were ever obtained with this material, and it will not be considered further. Polymer **(B)** however was dried in a vacuum oven for several weeks before measurements were made, and its plot is almost scatter free.

Polymer sample **(E)** has a derived T_0 only 18 °C below its measured T_g and the plot shows considerable scatter. This confirms that this sample contained traces of water or other solvents at the time of its conductivity and (especially) T_g measurements. Polymer sample **(C)** also has a rather small gap between T_g and T_0.

Polymer	T_g/K	T_0/K	$\frac{T_g-T_0}{K}$	$\log\left(\frac{A}{Scm^{-1}K^{1/2}}\right)$		B/1000K	
				T_g-T_0=60K	"Best Fit"	T_g-T_0=60K	"Best Fit"
(A2) 14 Short Methacrylate	317	245	72	-0.3430	0.0699	1.59	1.88
(B) 12 Short Methacrylate	290	197	93	-0.7680	0.9691	1.61	2.67
(C) 12 Ethoxy Methacrylate	249	206	43	1.717	0.3031	2.13	1.49
(E) 14 Ethoxy Methacrylate	218	200	18	1.8096	0.2055	2.58	1.44
(F) 14 H-C Methacrylate	249	190	59	0.8097	0.7625	2.18	2.15
(H) 14 Short Acrylate	272	180	92	2.3669	4.287	2.62	4.00

Table 4.5 *T_0 values and other VTF Parameters derived from Fitting the VTF Equation to the Data shown in Figure 4.11*

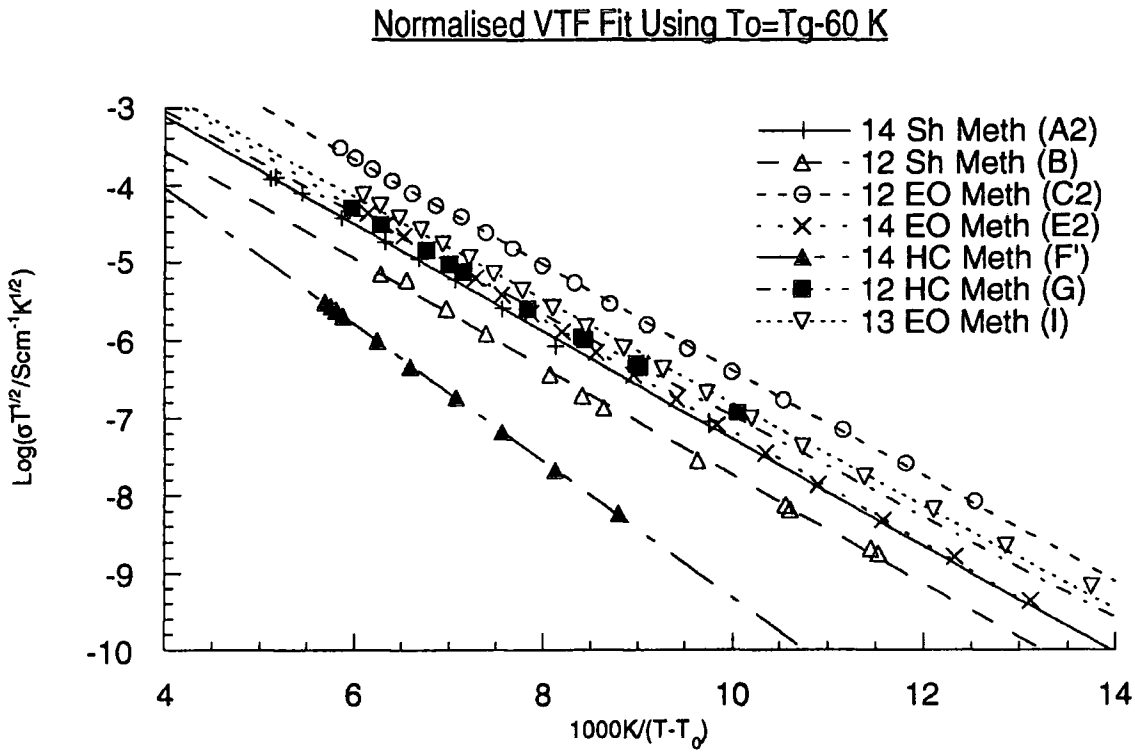

Figure 4.14a) *Normalised VTF plot, constructed from the revised set of polymer conductivity data using* $T_0 = T_g - 60K$

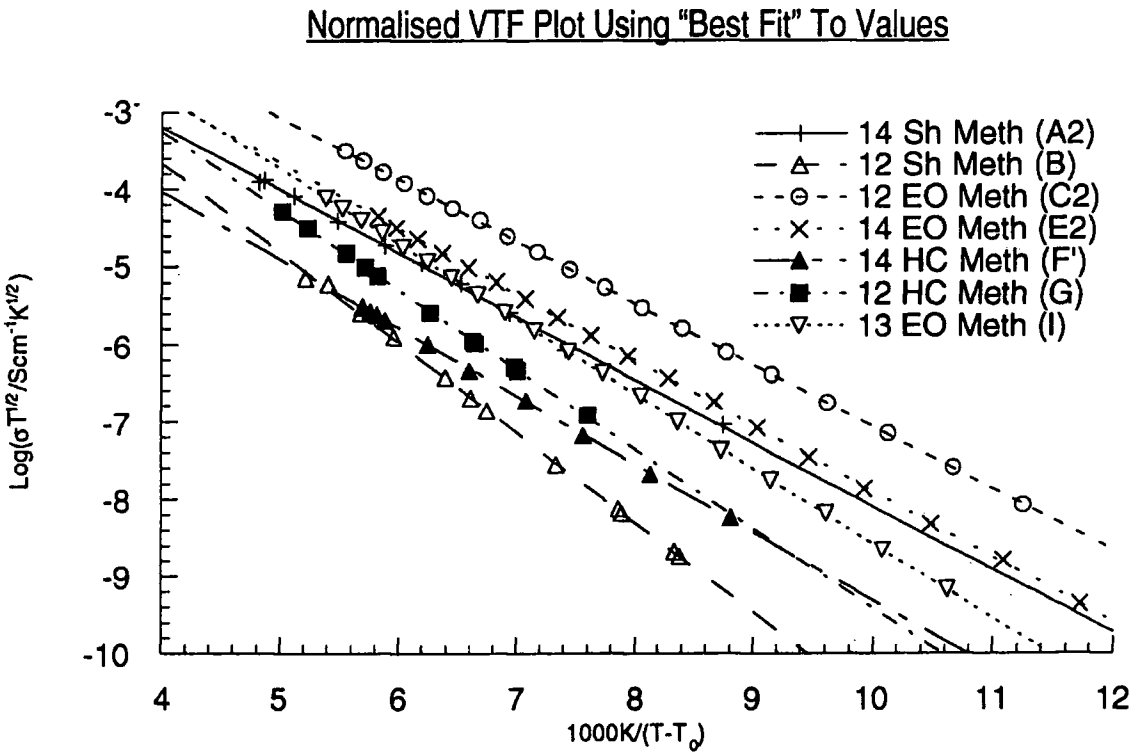

Figure 4.14b) *Normalised VTF plot, constructed from the revised set of polymer conductivity data using "Best Fit"* T_0 *values*

The revised polymer data used for figure 4.14 and table 4.6 gives plots that exhibit considerably less scatter than those derived from the earlier data, and the variation in T_g-T_0 is much reduced. Both effects may be attributed to a more complete removal of trace of water or solvent prior to making the measurements. However, polymer samples **(B)**, (unextended 12-crown-4 methacrylate), **(G)**, (hydrocarbon extended 12-crown-4 methacrylate), and to a lesser extent **(I)**, (ethylene oxide extended 13-crown-4 methacrylate) have a rather large T_g-T_0. While this may be due to solvent contamination or other errors, it is possible that the 12-crown-4 rings are forming 2:1 (ring : Li^+) complexes within the polymer, providing temporary cross-links. Cross-links are likely to raise T_g but are likely to help ionic transport, since they provide a low energy pathway for Li^+ to migrate from one site to another.

Polymer	T_g/K	T_0/K	$\frac{T_g-T_0}{K}$	$\log\left(\frac{A}{Scm^{-1}K^{1/2}}\right)$		B/1000K	
				T_g-T_0=60K	"Best Fit"	T_g-T_0=60K	"Best Fit"
(A2) 14 Short Methacrylate	317	245	72	-0.3430	0.0699	1.59	1.88
(B) 12 Short Methacrylate	290	197	93	-0.7680	0.9691	1.61	2.67
(C2) 12 Ethoxy Methacrylate	263	194	69	0.4247	0.8939	1.57	1.83
(E2) 14 Ethoxy Methacrylate	271	202	69	0.0280	0.570	1.66	1.95
(F') 14 H-C Methacrylate	249	189	60	-0.5150	-0.5205	2.03	2.02
(G) 12 H-C Methacrylate	266	175	91	-0.4254	0.8080	1.51	2.33
(I) 13 Ethoxy Methacrylate	270	189	81	-0.1493	1.0868	1.53	2.22

Table 4.6 *T_0 values and other VTF Parameters derived from Fitting the VTF Equation to the Data shown in Figure 4.12*

Some trends are clear from inspection of figures 4.13 and 4.14, and the associated tables 4.5 and 4.6.

Polymers based on 12-crown-4 are better conductors than those based on 14-crown-4, at equivalent temperatures above T_g. This is probably due to the lower activation energy for Li^+ desolvation from 12-crown-4

Polymers containing the ethylene oxide spacer group are better conductors than those without a spacer group or with the hydrocarbon spacer group. This may be due to the ability of the oxygen in the ethylene oxide spacer to continue to bind to a Li^+ ion when it is outside the crown ether ring, so it is never necessary to desolvate the Li^+ ion entirely, lowering the activation energy for Li^+ exchange.

Some further insights may be gained by considering the VTF parameters derived from the normalised conductivity plots. The parameters log(A) and B are the intercept and slope, respectively, of these plots. Due to the empirical nature of the VTF equation, it is important not to over interpret the numbers obtained from VTF fits. However, it is generally accepted that parameter A is related to the concentration of free ions, and parameter B to the availability of free volume within the polymer and how fast it varies with temperature (See section 1.2.2.i). The derivation of the VTF equation assumes that ion migration is not an activated process (i.e., there is no energy barrier to ion migration provided that sufficient free volume is available), but over restricted temperature ranges the presence of an activation energy for ion migration simply leads to an increase in the value determined for B, without distorting the form of the conductivity-temperature relation to an observable degree. While it is possible to add an activation energy term into the VTF equation, resulting in a relation of the form:–

$$\log\left(\sigma T^{1/2}\right) = \ln(A) - \frac{B}{T - T_0} - \frac{E_A}{kT} \qquad \text{.... (4.11)}$$

where E_A is the activation energy for ion migration and k is Boltzmann's constant, it is not possible to determine the activation energy term separately by fitting equation 4.11 to the data points, as a wide range of possible pairs of B and E_A values are consistent with the data. The activation energy for ion migration may therefore be considered as a component (probably a small component) of B.

The data shown in table 4.6 indicate that all the polymers studied have fairly similar values of both the A and B parameters, indicating that the major determinant of ionic mobility is polymer backbone structure, rather than the precise micro-environment of the migrating ions. The values of parameter A, derived from extrapolating the fitted lines back to "infinite temperature" are rather scattered, although there is some evidence from the fits based on $T_0 = T_g - 60K$ that the polymers containing the ethylene oxide spacer group have higher values of parameter A, perhaps indicating better ion pair separation in the more polar environment. T

All the values of B obtained from the $T_0 = T_g - 60K$ fit fall within a narrow range (around 1600K), with the exception of that for the 14 H-C Methacrylate polymer **E2**. A higher B value of 2000K was derived for this material, and since parameter B is influenced by the activation energy for lithium migration this may indicate that the combination of strong Li^+ binding in the 14-membered ring with the absence of exocyclic ether groups makes migration difficult.

The "best fit" VTF curves do not, unfortunately, reveal any significant trends in the derived A and B values. The temperature T_0 is not strongly constrained by data measured at temperatures 100-200K above it, and leaving it as a free parameter in a computational fit allows small amounts of random scatter in the data to strongly influence the derived A and B values. T_0 can be set to T_g-60K, T_g-70K or T_g-80K without visibly altering the quality of the fit, but the derived A and B values are changed significantly.

4.3. Conclusions.

The results found during this work indicate that polymer T_g dominates all other factors in its influence on the ionic conductivity of polymer-salt complexes. The effects of Li^+ solvation are discernible only after normalising for T_g as far as possible. Traces of trapped solvent cause significant scatter in the derived VTF parameters, since they increase polymer free volume and hence lower T_g and T_0, not necessarily by equal amounts.

This work has been concerned with Li^+ mobility, but it is generally accepted[11, 12] that anions carry at least 50% of the current in lithium salt/polymer systems, with t^- typically around 60-70%. Strong Li^+ binding, as is found with the 14-membered rings, reduces t^+ and is therefore undesirable.

Further support for these conclusions comes from analysis of the results obtained for crown-ether bearing polyphosphazene[13, 14] and polypropylene oxide[4] derivatives.

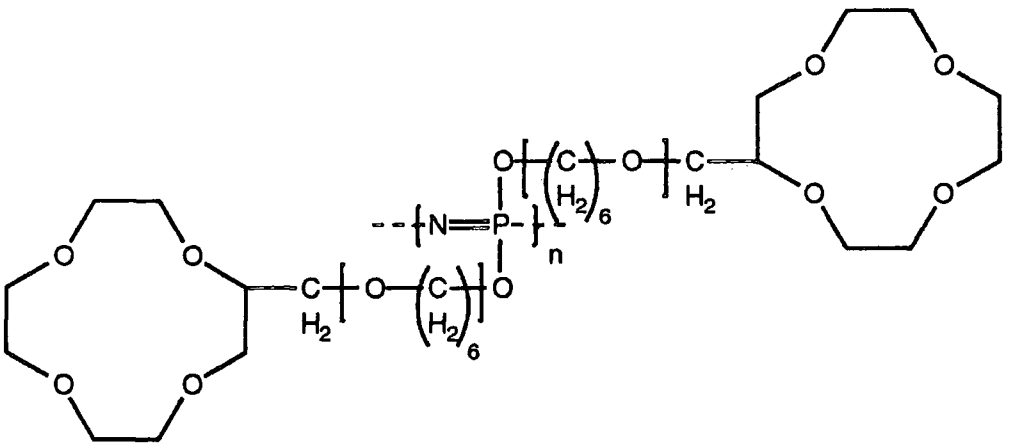

Figure 4.15 *Structures of the [Extended] and Unextended 12-Crown-4 Functionalised Polyphosphazenes Studied by Cowie.*[13, 14]

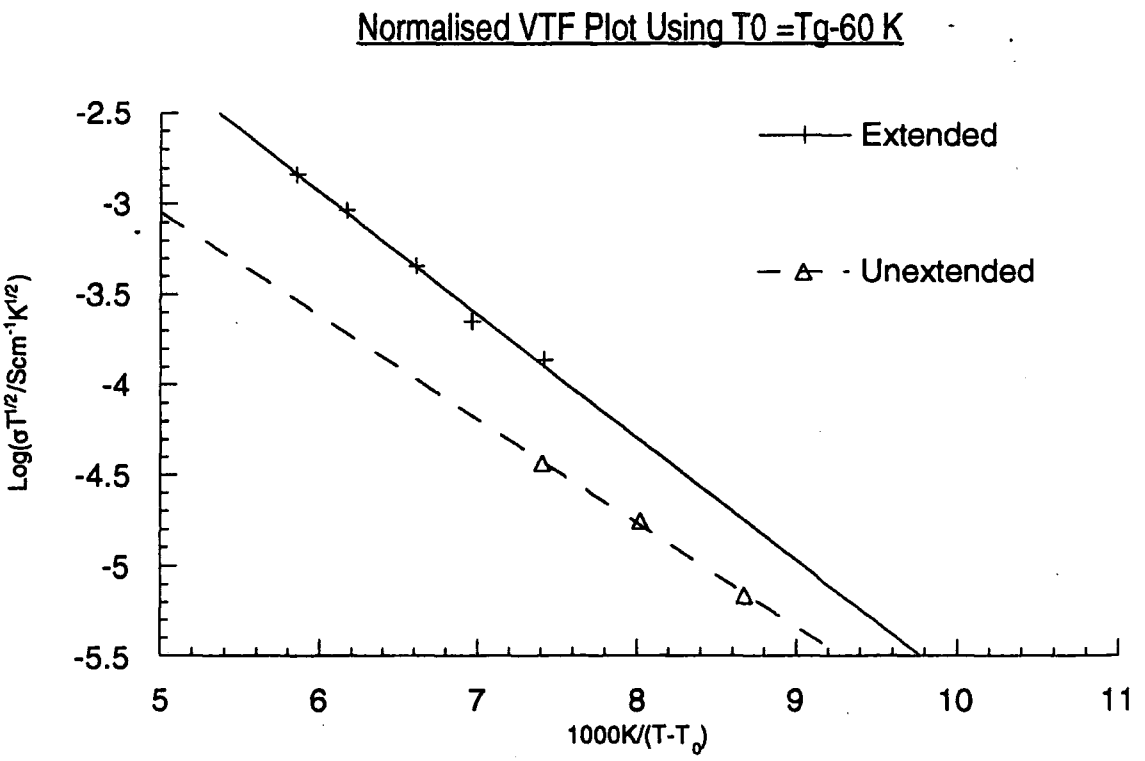

Figure 4.16 *Normalised VTF Plot Prepared from Data in Reference* [14]. *The Polymers were Doped to O/Li = 16 with* $LiBF_4$.

Polymer	T_g/K (Doped 16/1)	σ_{298}/Scm^{-1}	$\log\left(\frac{A}{Scm^{-1}K^{1/2}}\right)$	B/1000K
Unextended	258	2×10^{-7}	-0.18379	1.3186
Extended	221	1×10^{-5}	1.1347	1.5623

Table 4.7 Conductivity and VTF Parameters for Polyphosphazenes

The VTF B parameters for the polyphosphazenes are somewhat lower than those for the nearest equivalent methacrylates, polymers **(B)** and **(G)** (See table 4.6). The absolute conductivities of the polyphosphazenes are also much higher, which underlines once again the importance of T_g to polymer conductivity. The increase in the B parameter on addition of the hydrocarbon extension group may be attributable to its non-solvating nature, causing an increase in the activation energy for lithium ion migration.

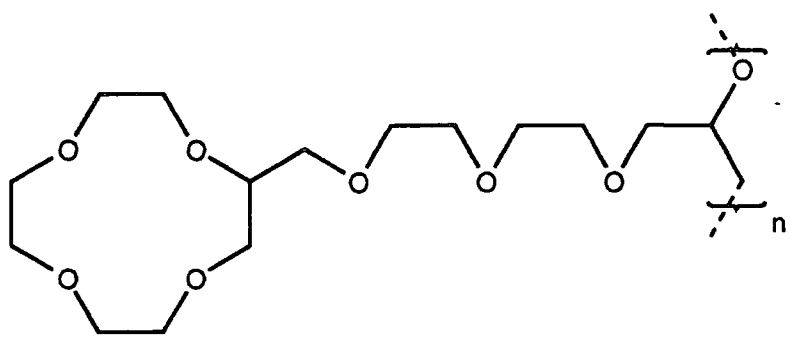

Figure 4.17 Structure of a 12-Crown-4 Bearing Polypropylene Oxide. An analogous Compound with a 13-Membered Ring was also Studied.[4]

Polymer	T_g/K (Doped 18/1)	σ_{298}/Scm^{-1}	$\log\left(\frac{A}{Scm^{-1}K^{1/2}}\right)$	B/1000K
12-Ring	239	2×10^{-7}	0.47	1.58
13-Ring	241	3×10^{-9}	-0.96	1.54

Table 4.8 Conductivity and VTF Parameters for Polypropylene Oxides

The VTF parameter B values for the 12- and 13-crown-4 containing polypropylene oxides are very close to those for the corresponding

methacrylate polymers **(C2)** and **(I)**, 1570 K and 1530 K, respectively. The A parameters of the 12-crown-4 containing polymers are also similar, but the 13-crown-4 containing polypropylene oxide has a very low A value compared to its methacrylate analogue (-0.96 $Scm^{-1}K^{1/2}$, against -0.15 $Scm^{-1}K^{1/2}$).

The absolute conductivities of the polypropylene oxides lie between those of the methacrylates and the polyphosphazenes. While this is partly explicable by T_g differences, the unextended polyphosphazene has a similar conductivity at room temperature to the 12-EO-extended polypropylene oxide, despite its higher T_g value (258 K compared to 239 K) and the advantages of a lithium solvating extension. This is reflected in the low value (1310 K) of the B parameter for this material.

The work of Denness et al.[4] confirms the superiority of polymers bearing 12-membered rings over equivalent materials with other ring sizes. However, it is clear that the dominant factor in determining lithium ion conductivity is the T_g of the polymer-salt mixture, which is largely determined by the nature of the polymer backbone and the degree of internal plasticisation present.

4.4. References

1. Cox, B. G. and Schneider, H., Coordination and Transport Properties of Macrocyclic Compounds in Solution, Edition, Elsevier, Amsterdam, 1992, p.

2. Lenkinski, R. E., Elgavish, G. A. and Reuben, J., J. Magn. Res., **32** 367 (1978).

3. Collie, L., Denness, J. E., Parker, D., O'Carroll, F. and Tachon, C., J. Chem. Soc., Perkin Trans. II, 1747-1758 (1993).

4. Denness, J. E., Parker, D. and Hubbard, H. S. V. A., J. Chem. Soc., Perkin Trans. II, 1445-53 (1994).

5. Bradshaw, J. S., Christensen, J. J., Izatt, R. M., Lamb, J. D. and Nielson, S. A., Chem. Rev., 271-339 (85).

6. Bannister, D. J., Davies, G. R., McIntyre, J. E. and Ward, I. M., Polymer, **25** 1600 (1984).

7. Armand, M. B., Gauthier, M. and Muller, D., in Electroresponsive Molecular and Polymeric Systems, ed. Skotheim, T. A., Marcel Dekker, New York, 1988, p. 41-97.

8. Cowie, J. M. G., in Polymer Electrolyte Reviews, ed. MacCallum, J. R. and Vincent, C. A., Elsevier, New York, 1987, vol. 1, p. 69-102.

9. Armand, M. B., Solid State Ionics, **(9/10)**, 745-754 (1983).

10. Ballard, D. G. H., Cheshire, P., Mann, T. S. and Przeworski, J. E., Macromolecules, **23** 1256-1264 (1990).

11. Cowie, J. M. G. and Cree, S. H., Annu. Rev. Phys. Chem., **40** 85-113 (1989).

12. Vincent, C., Prog. Solid State Chem., **17** 145-261 (1987).

13. Cowie, J. M. G., Makromol. Chem., Macromol. Symp., **53** 43-52 (1992).

14. Andrei, M., Cowie, J. M. G. and Prosper, P., Electrochimica Acta, **37 (9)**, 1545-1549 (1992).

Appendix

First Year Courses

Modern NMR Techniques

IRC Introductory Lecture Series

Colloquia, Lectures and Seminars given by Invited Speakers, 1st August 1989 To 31st July 1992

Events marked with their dates in **bold** were attended by the author

PALMER, Dr. F. (Nottingham University) — **17th October, 1989**
Thunder and Lightning.

FLORIANI, Prof. C. (University of Lausanne, Switzerland) — 25th October, 1989
Molecular Aggregates - A Bridge between homogeneous and Heterogeneous Systems.

BADYAL, Dr. J.P.S. (Durham University) — **1st November, 1989**
Breakthoughs in Heterogeneous Catalysis.

GREENWOOD, Prof. N.N. (University of Leeds) — 9th November, 1989
Novel Cluster Geometries in Metalloborane Chemistry.

BERCAW, Prof. J.E. (California Institute of Technology) — **10th November, 1989**
Synthetic and Mechanistic Approaches to Ziegler-Natta Polymerization of Olefins.

BECHER, Dr. J. (Odense University) — **13th November, 1989**
Synthesis of New Macrocylic Systems using Heterocyclic Building Blocks.

PARKER, Dr. D. (Durham University) — **16th November, 1989**
Macrocycles, Drugs and Rock 'n' roll.

COLE-HAMILTON, Prof. D.J. (St. Andrews University) — **29th November, 1989**
New Polymers from Homogeneous Catalysis.

HUGHES, Dr. M.N. (King's College, London) — **30th November, 1989**
A Bug's Eye View of the Periodic Table.

GRAHAM, Dr. D. (B.P. Reserch Centre) 4th December, 1989
How Proteins Absorb to Interfaces.

POWELL, Dr. R.L. (ICI) **6th December, 1989**
The Development of CFC Replacements.

BUTLER, Dr. A. (St. Andrews University) The **7th December, 1989**
Discovery of Penicillin: Facts and Fancies.

KLINOWSKI, Dr. J. (Cambridge University) 13th December 1989
Solid State NMR Studies of Zeolite Catalysts.

HUISGEN, Prof. R. (Universitat Munchen) 15th December, 1989
Recent Mechanistic Studies of [2+2] Additions.

PERUTZ, Dr. R.N. (York University) 24th January, 1990
Plotting the Course of C-H Activations with Organometallics.

DYER, Dr. U. (Glaxo) **31st January, 1990**
Synthesis and Conformation of C-Glycosides.

HOLLOWAY, Prof. J.H. (University of Leicester) **1st February, 1990**
Noble Gas Chemistry.

THOMPSON, Dr. D.P. (Newcastle University) 7th February, 1990
The role of Nitrogen in Extending Silicate Crystal Chemistry.

LANCASTER, Rev. R. (Kimbolton Fireworks) **8th February, 1990**
Fireworks - Principles and Practice.

LUNAZZI, Prof. L. (University of Bologna, Italy) **12th February, 1990**
Application of Dynamic NMR to the Study of Conformational Enantiomerism.

SUTTON, Prof. D. (Simon Fraser University, 14th February, 1990
Vancouver B.C.)
Synthesis and Applications of Dinitrogen and Diazo Compounds of Rhenium and Iridium.

CROMBIE, Prof. L. (Nottingham University) **15th February, 1990**
The Chemistry of Cannabis and Khat.

BLEASDALE, Dr. C. (Newcastle University) **21st February, 1990**
The Mode of Action of some Anti-tumour Agents.

CLARK, Prof. D.T. (ICI Wilton) **22nd February, 1990**
Spatially Resolved Chemistry (using Natures's Paradigm in the Advanced Materials Arena)

THOMAS, Dr. R.K. (Oxford University) 28th February, 1990
Neutron Reflectometry from Surfaces.

STODDART, Dr. J.F. (Sheffield University) **1st March, 1990**
Molecular Lego

CHEETHAM, Dr. A.K. (Oxford University) **8th March, 1990**
Chemistry of Zeolite Cages.

POWIS, Dr. I. (Nottingham University) **21st March. 1990**
Spinning off in a huff: Photodissociation of Methyl Iodide.

BOWMAN, Prof. J.M. (Emory University) 23rd March, 1990
Fitting Experiment with Theory in Ar-OH.

GERMAN, Prof. L.S. (USSR Academy of Sciences, Moscow) 9th July. 1990
New Syntheses in Fluoroaliphatic Chemistry: Recent Advances in the Chemistry of Fluorinated Oxiranes.

PLATONOV, Prof. V.E. (USSR Academy of Sciences, Novosibirsk) 9th July. 1990
Polyfluoroindanes: Synthesis and Transformation.

ROZHKOV, Prof. I.N. (USSR Academy of Sciences, Moscow) 9th July. 1990
Reactivity of Perfluoroalkyl Bromides.

MACDONALD, Dr. W.A. (ICI Wilton) **11th October, 1990**
Materials for the Space Age.

BOCHMANN,† Dr. M. (University of East Anglia) **24th October, 1990**
Synthesis, Reactions and Catalytic Activity of Cationic Titanium Alkyls.

SOULEN,† Prof. R. (South Western University, Texas) **26th October, 1990**
Preparation and Reactions of Bicycloalkenes.

JACKSON,† Dr. R. (Newcastle University) **31st October, 1990**
New Synthetic Methods:
a-Amino Acids and Small Rings.

LOGAN, Dr. N. (Nottingham University) **1st November, 1990**
Rocket Propellants.

KOCOVSKY,† Dr. P. (Uppsala University) **6th November, 1990**
Stereo-Controlled Reactions Mediated by
Transition and Non-Transition Metals.

GERRARD,† Dr. D. (British Petroleum) 7th November. 1990
Raman Spectroscopy for Industrial Analysis.

SCOTT, Dr. S.X. (Leeds University) **8th November, 1990**
Clocks. Oscillations and Chaos.

BELL,† Prof. T. (SUNY, Stoney Brook, U.S.A.) **14th November. 1990**
Functional Molecular Architecture and Molecular
Recognition.

PRITCHARD, Prof. J. (Queen Mary & Westfield 21st November, 1990
College, London University)
Copper Surfaces and Catalysts.

WHITAKER,† Dr. B.J. (Leeds University) 28th November, 1990
Two-Dimensional Velocity Imaging of
State-Selected Reaction Products.

CROUT, Prof. D. (Warwick University) **29th November, 1990**
Enzymes in Organic Synthesis.

PRINGLE,† Dr. P.G. (Bristol University) **5th December, 1990**
Metal Complexes with Functionalised Phosphines.

COWLEY, Prof. A.H. (University of Texas) **13th December. 1990**
New Organometallic Routes to Electronic Materials.

ALDER, Dr. B.J. (Lawrence Livermore Labs, California) **15th January, 1991**
Hydrogen in all its Glory.

SARRE, Dr. P. (Nottingham University) **17th January, 1991**
Comet Chemistry.

SADLER, Dr. P.J. (Birkbeck College London) **24th January, 1991**
Design of Inorganic Drugs:
Precious Metals, Hypertension + HIV.

SINN,† Prof. E. (Hull University) **30th January, 1991**
Coupling of Little Electrons in Big Molecules.
Implications for the Active Sites of (Metalloproteins
and other) Macromolecules.

LACEY, Dr. D. (Hull University) **31st January, 1991**
Liquid Crystals.

BUSHBY,† Dr. R. (Leeds University) **6th February, 1991**
Biradicals and Organic Magnets.

PETTY, Dr. M.C. (Durham University) **14th February, 1991**
Molecular Electronics.

SHAW,† Prof. B.L. (Leeds University) **20th February, 1991**
Syntheses with Coordinated,
Unsaturated Phosphine Ligands.

BROWN, Dr. J. (Oxford University) **28th February, 1991**
Can Chemistry Provide Catalysts
Superior to Enzymes?

DOBSON†, Dr. C.M. (Oxford University) 6th March, 1991
NMR Studies of Dynamics in Molecular Crystals.

MARKAM, Dr. J. (ICI Pharmaceuticals) **7th March, 1991**
DNA Fingerprinting.

SCHROCK, Prof.R.R. (Massachusetts Institute of Technology) **24th April, 1991**
Metal-ligand Multiple Bonds
and Metathesis Initiators.

HUDLICKY, Prof. T. (Virginia Polytechnic Institute) 25th April, 1991
Biocatalysis and Symmetry Based Approaches to the
Efficient Synthesis of Complex Natural Products.

BROOKHART, Prof. M.S. (University of N. Carolina) 20th June, 1991
Olefin Polymerizations, Oligomerizations
and Dimerizations Using Electrophilic
Late Transition Metal Catalysts.

BRIMBLE, Dr. M.A. (Massey University, New Zealand) **29th July 1991**
Synthetic Studies Towards the Antibiotic Griseusin-A.

SALTHOUSE, Dr. J.A. (Manchester University) **17th October 1991**
Son et Lumiere - a demonstration lecture.

KEELEY, Dr. R. (Metropolitan Police Forensic Science) **31st October 1991**
Modern forensic science.

JOHNSON,† Prof. B.F.G. (Edinburgh University) 6th November 1991
Cluster-surface analogies.

BUTLER, Dr. A.R. (St. Andrews University) 7th November 1991
Traditional Chinese herbal drugs:
a different way of treating disease.

GANI,† Prof. D. (St. Andrews University) **13th November 1991**
The chemistry of PLP-dependent enzymes

O'FERRALL,† Dr. R. More (University College, Dublin) **20th November 1991**
Some acid-catalysed rearrangements
in organic chemistry.

WARD, Prof. I.M (IRC in Polymer Science, University of Leeds) **28th November 1991**
The SCI lecture:
The Science and Technology of Orientated Polymers.

GRIGG,† Prof. R. (Leeds University) **4th December 1991**
Palladium-catalysed cyclisation
and ion-capture processes.

SMITH, Prof. A.L. (ex Unilever) 5th December 1991
Soap, detergents and black puddings.

COOPER,† Dr. W.D. (Shell Research) 11 December 1991
Colloid science: theory and practice.

HARRIS,† Dr. K.D.M. (St. Andrews University) **22nd January 1992**
Understanding the properties of
solid inclusion compounds.

HOLMES,† Dr. A. (Cambridge University) **29th January 1992**
Cycloaddition reactions in the service of the synthesis
of piperidine and indolizidine natural products.

ANDERSON, Dr. M. (Sittingbourne Research Centre, Shell Research) — **30th January 1992**

Recent Advances in the Safe and Selective Chemical Control of Insect Pests.

FENTON,† Prof. D.E. (Sheffield University) — **12th February 1992**

Polynuclear complexes of molecular clefts as models for copper biosites.

SAUNDERS, Dr. J. (Glaxo Group Research Limited) — 13th February 1992

Molecular Modelling in Drug Discovery.

THOMAS,† Prof. E.J. (Manchester University) — **19th February 1992**

Applications of organostannanes to organic synthesis.

VOGEL, Prof. E. (University of Cologne) — **20th February 1992**

The Musgrave Lecture

Porphyrins: Molecules of Interdisciplinary Interest.

NIXON, Prof. J.F. (Sussex University) — 25th February 1992

The Tilden Lecture

Phosphaalkynes: new building blocks in inorganic and organometallic chemistry.

HITCHMAN,† Prof. M.L. (Strathclyde University) — 26th February 1992

Chemical vapour deposition.

BILLINGHAM, Dr. N.C. (Sussex University) — **5th March 1992**

Degradable Plastics - Myth or Magic?

THOMAS,† Dr. S . E . (Imperial College) — **11th March 1992**

Recent advances in Organoiron chemistry.

HANN, Dr. R.A. (ICI Imagedata) — **12th March 1992**

Electronic Photography - An Image of the Future.

MASKILL,† Dr. H. (Newcastle University) — 18th March 1992

Concerted or stepwise fragmentation in a deamination-type reaction.

KNIGHT, Prof. D.M. (Philosophy Department, University of Durham) — **7th April 1992**

Interpreting experiments: the beginning of electrochemistry.

GEHRET, Dr. J-C (Ciba Geigy, Basel) 13th May 1992
Some aspects of industrial agrochemical research.

† Invited specially for the postgraduate training programme.

I. R. C. Seminar Series

Prof. H. Cherdon,
Research Director
Hoechst-Aktiengesellschaft 25th March 1992
Centrale Polymerforschung University of Durham
Frankfurt am Main, Germany

"Structural Concepts and Synthetic Methods
in Industrial Polymer Science"

Prof. Walther Burchard, 11th May 1992,
University of Freiburg, Germany. University of Durham

"New Insights into the Global Dynamics of Polymers
by Light Scattering"

Prof. E. N. Thomas, 21st September 1992
MIT, Cambridge, Massachusetts. University of Leeds

"Interface Structures in
Copolymer-Homopolymer Blends"

Conferences

Modern Aspects of Stereochemistry
Sheffield
18th December 1991

Polymer Ionics 1992
Gothenburg, Sweden.
August 19-21, 1992

Publications

Luke Collie, David Parker, Christine Tachon,
H. V. St. A. Hubbard, G. R. Davies, I. M. Ward and S. C. Wellings,

Polym. Commun., **34**, p 1541 (1993)

"Synthesis of Functionalised 12-, 13-, and 14-Membered Crown Ethers Bearing Exocyclic Polymerisable Groups and the Binding Properties and Conductivities of their Lithium Doped Polymers"

Luke Collie, James E. Denness, David Parker,
Fiona O'Carroll and Christine Tachon

J. Chem. Soc, Perkin Trans. 2, p 1747 (1993)